University of Rhode Island

DigitalCommons@URI

2014

A PAPER-BASED LATERAL FLOW DEVICE FOR THE DETECTION OF IαIP VIA ELISA

Hanno Teiwes
University of Rhode Island, hanno.teiwes@gmail.com

Recommended Citation

A PAPER-BASED LATERAL FLOW DEVICE

FOR THE DETECTION OF IαIP VIA ELISA

BY

HANNO TEIWES

A THESIS SUBMITTED IN PARTIAL FULFILLMENT OF THE

REQUIREMENTS FOR THE DEGREE OF

MASTER OF SCIENCE

IN

MECHANICAL ENGINEERING AND APPLIED MECHANICS

UNIVERSITY OF RHODE ISLAND

2014

MASTER OF SCIENCE IN MECHANICAL ENGINEERING

OF

HANNO TEIWES

APPROVED:

Thesis Committee:

Major Professor   Mohammad Faghri

                    Constantine Anagnostopoulos

                    Jason R. Dwyer

                    Nasser H. Zawia
                    DEAN OF THE GRADUATE SCHOOL

UNIVERSITY OF RHODE ISLAND

2014

ABSTRACT

This study focuses on the development of a new paper-based microfluidic device for the detection of IαIP via ELISA. Recent studies proved that the concentration of IαIP is related to the mortality rate of patients who suffer from sepsis. The developed device is able to determine the concentration of IαIP in a buffer solution where a low concentration is an indicator for sepsis. Using a microfluidic valve, the reagents needed to perform the ELISA can be loaded sequentially. The microfluidic device consists of paper on which the channel geometry is printed with wax ink. Different layers of the device are stacked together with double sided tape where paper is biodegradable. After applying the reagents, the device produces the results autonomously in form of a colored dot. The intensity of the dot is linked to the concentration of the target analyte IαIP. Two methods to distinguish the concentration of IαIP were conducted to decide which method is more appropriate for this experiment. After optimizing the reagents with regards to reproducibility, optimal signal to noise ratio and sensitivity a standard curve is produced that links the intensity of a color dot to a concentration of IαIP. Compared to other methods like a blood test which needs 48 hours to deliver a result or microtiter-plates which need large fluid volumes, the microfluidic paper device is able to obtain a result within minutes as well as it uses smaller fluid volumes.

ACKNOWLEDGMENTS

Last but not least I would like to thank my girlfriend Franziska Ruholl who means a lot to me because she was the one who was always there in good times as in bad.

TABLE OF CONTENTS

LIST OF TABLES

LIST OF FIGURES

LIST OF ABBREVIATIONS

μPads   Microfluidic Paper-Based Analytical Devices

A3CS   Allyltrichlorosilane

AB   Antibody

ALP   Alkaline Phosphatase

BAPNA   Nα-Benzoyl-DL-Arginine 4-Nitroanilide Hydrochloride

BCIP/NBT   5-Bromo-4-Chloro-3-Indolyl Phosphate Nitroblue Tetrazolium

BPTI   Basic Pancreatic Trypsin Inhibitor

BSA   Bovine Serum Albumin

CL-ELISA   Chemiluminescence ELISA

DAB   3,3'-Diaminobenzidine

DMSO   Dimethylsulfoxide

ELISA   Enzyme-Linked-Immunoassay

FC-72   Perfluro-Compound

FITC   Fluorescein

GSA   Global Sepsis Alliance

HA   Hyaluronan

HC   Heavy Chain

HRP   Horseradish Peroxidase

IαIP   Inter-A-Inhibitor-Protein

LFD   Lateral Flow Devices

LFT	Later Flow Test
LOD	Limit-Of-Detection
LT	Lethal Toxin
Mab 69.31	Monoclonal Antibody 69.31
NYP	Neuropeptide Y
PAA	Poly-Acrylic Acid
PAH	Poly-Allylamine Hydrochloride
PBD	Paper Based Point Of Care Devices
PDMS	Polydimethylsiloxane
PEM	Polyelectrolyte Multilayers
PIRO	Predisposition, Infection, Response And Organ Dysfunction
POC	Point-Of-Care Devices
PP	Polypropylene
PROGRESS	Promoting Global Research Excellence in Severe Sepsis
PROWESS	Recombinant Human Activated Protein C Worldwide Evaluation in Severe Sepsis
RGB	Red-Green-Blue
SHAP-HA	Serum-Derived Hyaluronan-Associated-Protein
TEA	Triethanolamine
TMB	3,3',5,5'-tetramethylbenzidine
TSG-6	Tumor necrosis factor-inducible gene 6 protein

LIST OF SYMBOLS

Latin Symbols

A	Area Of The Channel	m²
D	Pore Diameter	μm
L	Length	cm
Q	Volumetric Flow Rate	m³/s
t	Time	s
ΔP	Total Pressure Drop	N/m²
V	Volume	m³

Greek Symbols

μ	Viscosity of the Fluid	Ns/m²
γ	Surface Tension	N/m
η	Dynamic Viscosity	Pa·s
κ	Permeability Of The Paper	m²

1   CHAPTER 1 - Introduction

This chapter provides background knowledge for the reader on various Paper Based point of care Devices (PBD) like Lateral Flow Devices (LFD), µPads and Enzyme-Linked-Immunoassays (ELISA's). Also, the principles of general immunoassay tests are explained. Furthermore, the importance of sepsis detection and the role of Inter-alpha inhibitor protein is discussed.

1.1   Sepsis an Introduction

The word sepsis has its origin in the Greek language with Sepsis (greek. σῆψις) meaning putrefaction and decay. It is a health problem in developing countries as well as in the industrialized world [1]. Sepsis is listed 13th in the top 15 International Classification of Disease with a 39.6% -hospital mortality rate with 1.8% of all in-hospital deaths resulting from sepsis [2]. Septicemia therefore is a serious disease and cause for lower life expectancy. Konrad Reinhart the chairman of the Global Sepsis Alliance (GSA) said *"Tens of millions of people die from sepsis each year, making it the likely leading cause of death worldwide. Sepsis kills regardless of age, ethnicity, location and access to care."*

In many cases it is not trivial to recognize that a patient suffers from Sepsis, but it is difficult to differentiate inflammation symptoms of the flu or other afflictions [1]. One method for characterization is to define the various stages of sepsis in the **PIRO**-scheme (**P**redisposition, **I**nfection, **R**esponse and **O**rgan dysfunction), which was introduced in 1991. Each category is evaluated with 0 to 4 points with each point

representing an increase in the risk for mortality by 30%-50% [3]. Many other characterization schemes have also been established (e.g. Recombinant Human Activated Protein C Worldwide Evaluation in Severe Sepsis (**PROWESS**) and Promoting Global Research Excellence in Severe Sepsis (**PROGRESS**)). Unfortunately, the existence of competing definitions makes it difficult to compare several conditions or stages of sepsis [1].

In 2005 the international sepsis forum categorized the six most common infections which can cause sepsis. These included pneumonia, blood-stream infections, intra-abdominal infections, urological infection and surgical wound infection [4]. One new understanding is that bacteria release certain toxins (e.g. endotoxin) in case of cases of gram-negative sepsis, which attack certain organs and several immune cells which then release mediators. Mediators can kill bacteria and inactivate toxins but an inflammation is created as well [5].

The evolution from infection to a septic shock occurs quickly (couple of hours), therefore, early detection and characterization is detrimental to reduce chances of mortality. Therefore there is a need for a device that may rapidly detect sepsis [1].

1.2 The course of sepsis

An infection is called septic when a nidus which is a place in which bacteria have multiplied, is formed in the body. It releases periodically pathogenic bacteria into the human bloodstream. The pathogen causes subjective and objective complaints. Subjective complaints are only noticeable by the affected person whereas objective

complaints are visible to other people as well [6]. Sepsis can be caused by many different types of bacteria. Table 1-1 is a summary of sepsis nidi and pathogens.

Table 1-1: Nidi and pathogens of sepsis [7]		
Organ	**Infection**	**Typical pathogen**
ear, nose and throat area	Tonsillitis, sinusitis, otitis	Streptococci, pneumococci and meningococci, Bacillus fusiformis
Lung	pneumonia	Pneumococci, Haemophilus influenzae
intestine	Peritonitis	Salmonella, E. coli, enterococci
Biliary tract	Cholangitis	E. coli, Enterobacteriaceae, anaerobes
gynecological area	Postpartum sepsis or arbortum	Streptococci, Clostridium perfringens
Genitourinary system	urinary infection	E. coli, enterococci, Klebsiellen, Proteus, Pseudomonas
Skin	Wound infection, burned skin	Staphylococci, streptococci, gram-negative bacteria (Pseudomonas)

Many organs could become a nidus of septic infection when several pathogens are present. However, not all infectious nidi lead to sepsis. Although the issue is not fully understood, one possible source might be from people who have a weakened immune system as a result of recent surgery. The proportion of and aggressiveness of a pathogen to the body's defense also seems to be important in determining whether a patient will develop sepsis or not [5].

Possible symptoms of sepsis are a body temperature more than 38 °C or less than 36 °C, a cardiac frequency over 90 beats/min, a respiratory frequency over 20 breaths/min and a leucocytes level higher than 12000/µg (leukocytosis) or less than 4000/µg (leucopenia). A patient is said to be septic when they have at least two out

of four symptoms. Due to the expansion of the peripheral vessels, blood pressure decreases and a higher cardiac frequency may incur a septic shock. Therefore, if the disease is not trated correctly, mortality will be imminent [5].

1.3   The role of Inter-α-Inhibitor proteins

Within the realm of paper-based-microfluidic device a possible target is Inter-α-inhibitor-proteins (IαIP). The IαIP belongs to the family of protein-glycosaminoglycan-protein complexes (PGP). It was first discovered in the 1960's and isolated from human plasma. The IαIP is located in plasma also in urine [8]. It is named after the α-region through where it passed when an electrophoresis is performed [9]. In a healthy organism the concentration in human plasma is 400-800 mg/liter [10]. The structure of IαIP is shown in Figure 1-1.
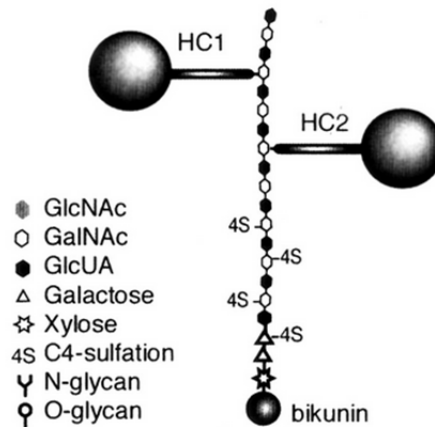
Figure 1-1: Inter-α-inhibitor proteins [8]

It consists out of two heavy chains. One is called heavy chain 1 and the other is called heavy chain2 (HC1 and HC2). Additionally, a light chain (bikunin) linked with a glycosaminoglycan chain (black and white chain) is present [8]. Many physiological

and pathological processes in the body are performed with the help of IαIP's. Inflammation, wound healing and stabilization of the extracellular matrix occur with the mediation of IαIP's [11].

IαIP's are synthesized mainly in hepatocytes in the liver. The IαIP is needed later on to form for example the Serum-Derived Hyaluronan-Associated-Protein-complex (SHAP-HA-complex), which is present can be found in the synovial fluid in inflamed knee joints. During an illness synthesis rate in the liver decreases by 20-90% from its original rate [12]. The synthesis of IαIP's and the SHAP-HA-complex is shown in Figure 1-2.
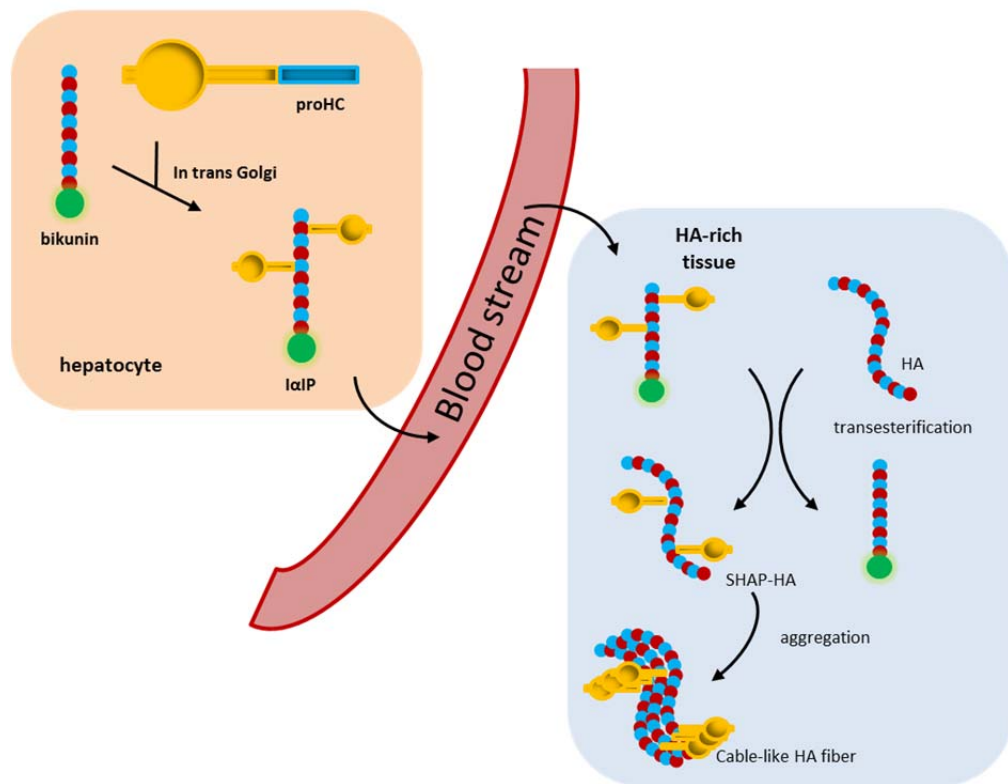
Figure 1-2: Synthesis of IαIP and the SHAP-HA complex [8]

Therefore bikunin and the two HC's are linked together in the Golgi apparatus. The three components of the IαIP have different tasks whereas the task of the heavy chains is currently not fully understood [13]. Bikunin is responsible for the serine protease inhibitory activity. Bikunin is inactive as long as it is bound in the protein complex between the two heavy chains. In a proteolytic degradation the IαIP is split into smaller polypeptides (HC1, HC2 and bikunin) and amino acids (glycosaminoglycan chain) [11]

As explained earlier, the IαIP can fight inflammation. Hyaluronan is the main glycosaminoglycan in synovial fluid. In a recent study, several probes were taken from knee joints of patients who suffer from active rheumatoid arthritis, ie. people who have a constant onset of inflammation. In comparison to normal synovial fluid the rheumatoid fluid contained a higher amount of bound IαIP's. The IαIP's are linked to Hyaluronan (HA) in a trans-esterification to a SHAP-HA-complex [8]. This study shows that the amount of IαIP's decreases during an inflammation [14]. Several studies were performed by Chaaban et. al. [12], Lim et. al. [14] and Opal et. al. [15] to find a correlation of the concentration of IαIP in the plasma and the mortality rate of a person who suffers from sepsis.

Opal et. al. [15] exposed lipopolysaccharide (LPS) activated peritoneal macrophages to lethal toxin (LT) and varying concentrations of IαIP. The results of the test are shown in Figure 1-3.

6
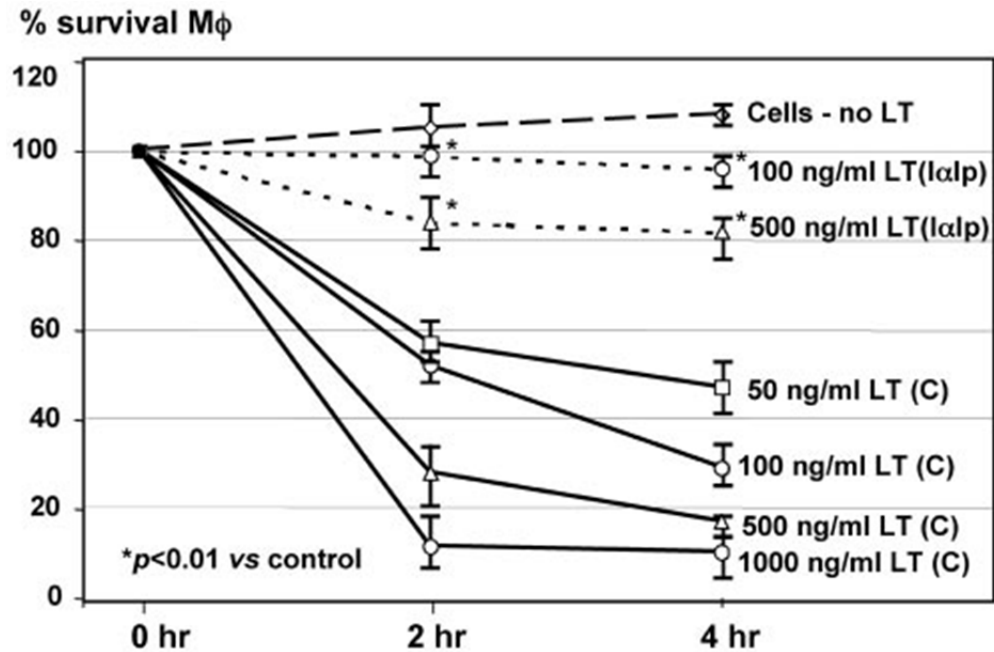
Figure 1-3: Correlation between mortality rate and c(IαIP) in mice [15]

The survival percentage is plotted over the time. It can be seen that the mortality rate is proportional to the level of lethal toxin. When IαIP is added to the sample the mortality rate decreased. IαIP is proposed to affect the activity of furin an enzyme which is important for the formation of lethal toxin. Furthermore the presence of the monoclonal antibody 69.31 (MAb 69.31), which is used by Lim et. al. [14] to immobilize IαIP increases the mortality rate again. The MAb 69.31 interacts with bikunin the active site of the IαIP which possesses the protease inhibitor function [15].

In the previous section experiments were performed on mice. Lim et. al. [14] conducted experiments on blood samples from patients with sepsis. The IαIP was immobilized with MAb 69.31 on a 96 well plate. Next a horseradish peroxidase (HRP)

7

labeled AB was attached to the protein and the absorbance of light at 405 nm was measured on an ELISA plate reader. Figure 1-4 illustrates the correlation between the concentration of IαIPs and the mortality rate.
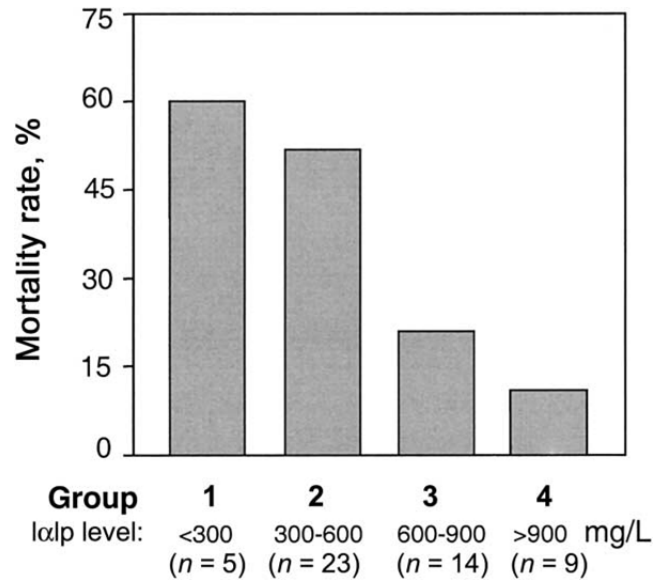
Figure 1-4: Correlation between mortality rate and c(IαIP) in humans [14]

The mortality rate decreases when the concentration of IαIP increases. During severe sepsis the synthesis of many other proteins is disturbed. In addition systemic proteolysis induces the degradation of IαIPs during sepsis. In contrast, patients with a high level of IαIP in their blood are less likely to develop septic shock. These findings show that IαIP's are needed to effectively treat a septic patient [14].

Kaczmarczyk et. al. [9] points out the roles of IαIP during an inflammation. Tumor necrosis factor-inducible gene 6 protein (TSG-6) in combination with IαIP builds an extracellular matrix containing Hyaluronan. The reaction is illustrated in Figure 1-5.

8
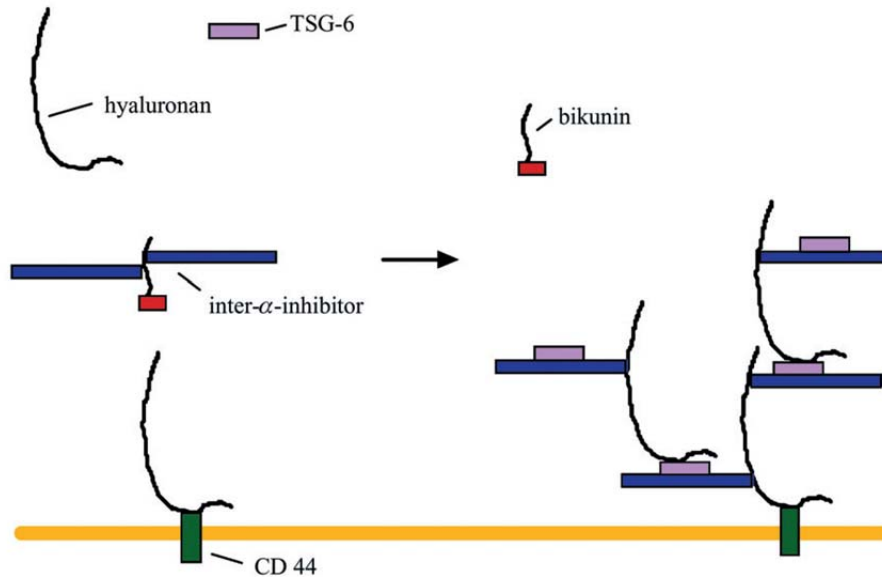
Figure 1-5: Coating of extracellular matrix with Hyaluronan [9]

Hyaluronan usually binds to the cell surface receptor (CD44). From the split IαIP the HC1 and the HC2 connect to hyaluronan. Bikunin is not involved in the reaction. After the TSG-6 molecule sticks to the HC's and makes it possible that more hyaluronan to bind to the cell surface. Crosslinking of hyaluronan molecules ends in a stable structure [9]. This hyaluronan coat on the cell surface facilitates the cell migration for leucocytes which improve the cure of inflamed tissues [16].

1.4   Enzymatic reactions on the chip

So far two different procedures have been proposed. These methods are detection via ELISA or via immunosorbent assay. Of these, the assay which is more promising for determining IαIP in a sample will be used. Both methods are explained and discussed in the next section

9

1.4.1 Enzymatic or Inhibitory assay

On an immunosorbent surface, enzymes are immobilized which are able to capture certain proteins. When a sample flows over this surface, some of the proteins, for which the enzymes have an affinity, will be immobilized [17]. In the proposed chip, trypsin enzymes are immobilized on the filter nitrocellulose to capture the previously discussed IαIP. Those enzymes that have captured the proteins are deactivated. Thus when the substrate flows over the test spot area, only those enzymes which have not been deactivate by IαIP will produce the color product. BAPNA is the substrate typically used for trypsin enzymes.

1.4.2 ELISA

An alternative method is by Enzyme Linked Immunosorbent Assay (ELISA). An ELISA uses antibodies and a substrate, which causes a color change, to identify a certain target analyte. The scheme of a common ELISA Test is displayed in Figure 1-6.
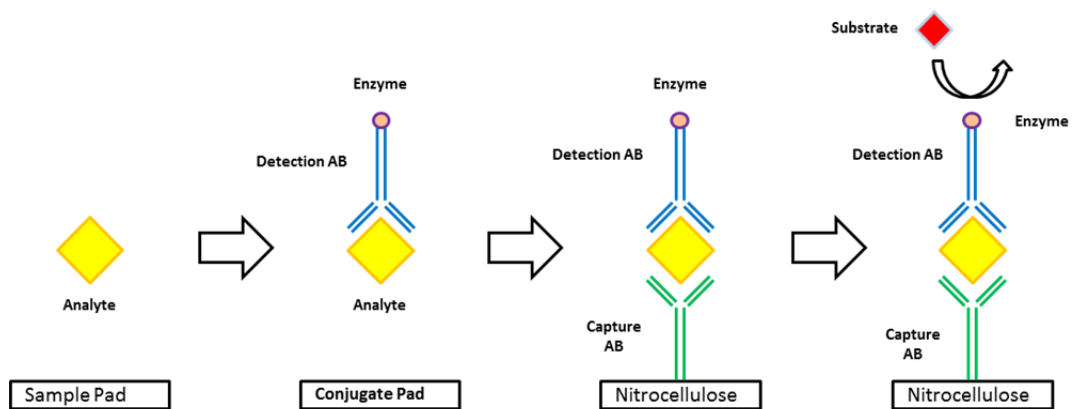
Figure 1-6: Scheme of an ELISA-Test

Capture antibodies are immobilized onto a surface such as the bottom of a plastic well or a nitrocellulose membrane in case of a PBD. The in-sample target substance should bind to the capture antibody. In the next step, a detection antibody which is tagged with an enzyme (Horseradish Peroxidase (HRP) or Alkaline Phosphatase (ALP)), binds to the substance to form a complex that includes a capture antibody-target substance-detection antibody sandwich. In the last step, a substrate like 5-Bromo-4-chloro-3-indolyl phosphate nitroblue tetrazolium (BCIP/NBT) for ALP or 3,3',5,5'-tetramethylbenzidine (TMB) for HRP is added to induce a color change.

The ELISA sandwich assay is applicable to all types of antigens or proteins which can be captured with a certain antibody. Following this step, a colored signal can be produced using a substrate and a detection antibody tagged with an enzyme to indicate the presence of a target substance. Föllscher et. al. [18] and Gerbers et. al. [19] showed that their developed circuit is able to determine certain concentrations of Rabbit IgG via a paper-based ELISA. The example of Murdock et. al [20] shows that many other target analytes can be detected using ELISA on paper. In their case they detected various concentrations of neuropeptide Y (NYP).

1.5 Point of Care devices

In recent years there has been a growing interest in the field of paper-based devices. These devices are less complex and less expensive than previous gadgets used for detection (e.g. an immunoassay test) [21]. The aim of this field of research is to develop devices that satisfy the criteria of Point-of-Care devices (POC) and can be

used in developing countries where no medical infrastructure is present [22]. POC devices have to be "ASSURED: **a**ffordable, **s**ensitive, **s**pecific, **u**ser-friendly, **r**apid, **r**obust, **e**quipment free and **d**eliverable for the end user [23]. An appropriate POC device meets all of these requirements. One example is the device which is introduced by Föllscher et. al. [18] and Gerbers et. al. [19].

The most common example for a POC-device is the Lateral Flow Test (LFT). LFT's are an appropriate method to establish POC-devices in developing countries because e.g. they are cheaper than complex tests which need a lot of expensive instrumentation [22]. Currently there are several lateral-flow-devices (LFD) on the market. The most familiar LFD's to the public are pregnancy tests, HIV tests and drug tests [24]. As discussed before, all "ASSURED" criteria's need to be fulfilled. A pape-based LFT is therefore a suitable choice because it meets these requirements.

Paper is available everywhere in the world. It is inexpensive compared to other materials and furthermore it is biodegradable [23]. Also, it is biocompatible with all of the reagents tested so far [25]. Most of the tests require expensive equipment to read out the results of a specific test or a pump to maintain the fluid flow inside the device. PBD do not need mechanical equipment such as a pump due to the capillary flow; this further reduces the need for expensive additional equipment to run test [26].

1.6 Justification

A bacterial infection has to be treated with an antibiotic which is specific to the infection present in the human body [27]. As explained earlier treatment of sepsis has to be done as rapidly as possible. In order to detect the specific pathogen, a diagnostic result that produces a result faster than the current tests (24-48hrs) is needed [28]. Unfortunately, according to Engel et. al. [29] the specific pathogen which causes illness is correctly detected in only 57% of all cases. Almost every other patient cannot be treated with a specific antibiotic. Therefore most of the patients can be treated only with broad spectrum of non-specific antibiotics, regardless if they are certain to combat an infection or not. Due to the possible use of ineffective antibiotics, the pathogen may develop a resistance against the antibiotics [30].

As one can see, the need for a faster detection method than offered by the microbiological blood analysis has to be developed. This is especially necessary in half the cases where the pathogen can be identified correctly.

T2 Biosystems, Inc. has understood the implications of the aforementioned problem and has focused on the development of the T2Candida®, which is able to detect five species of the fungal infection candida. Candida is a fungal infection which may also cause Sepsis. Previous tests took anywhere between two to five days to return results, whereas the T2Candida® provides a result in approximately 3 hours. The reduction of time decreases the mortality rate from 40% to 11% as well as the hospitalization time of patients. The identification of the correct pathogen eliminates

the need for treating the patient with broad spectrum antibiotics. The potential savings are estimated to be $4.3 billion only in the U.S: healthcare system [31].

POC devices are therefore suitable to provide results faster than as many other methods currently on the market. Föllscher et. al. [18] and Gerbers et. al. [19] show that in case of PBD not only a qualitative results can be measured with these devices but quantitative results as well.

The goal is to develop a fluidic circuit which makes it able to determine the concentration of IαIP by conducting ELISA on a paper based platform by measuring the color intensity on the detection spot. The color is measured using the program ImageJ®.

1.7   Objective and Outline of the Thesis

The structure of the thesis is as follows:

Chapter 1 – Introduction – gives a brief introduction covering the illness sepsis and introduces the function and advantages of Point-of-Care devices. Furthermore, two methods to detect IαIP are discussed.

Chapter 2 – Literature Review – discusses the current state of the art. Several fields of application, production methods of POC devices and a detailed review of immunoassay test are shown. Furthermore different types of fluid flows are reviewed.

Chapter 3 – Methodology – illustrates the experiments which were done during the thesis. Biological spot test, development of a fluidic circuit and assay development are found in this chapter.

Chapter 4 – Findings – shows and discusses the results of the experiments mentioned in chapter 3.

Chapter 5 – Conclusion – summarizes the findings and proposes future directions of this research.

2   CHAPTER 2 - REVIEW OF LITERATURE

This chapter is about the state of art in the development of paper based microfluidic devices. First of all, the elements of a fluidic circuit are discussed and different techniques to modify the paper surface to make it suitable for biological reagents are explained. Furthermore, the performed ELISA test is illustrated. Finally, the fluidic system research is summarized along with different methods to fabricate a PBD.

2.1   Elements of a fluidic circuit

The most commonly known point of care device is the lateral flow strip; Pregnancy tests or simple drug test are examples of LFS. In Figure 2-1 a typical lateral flow device is displayed.
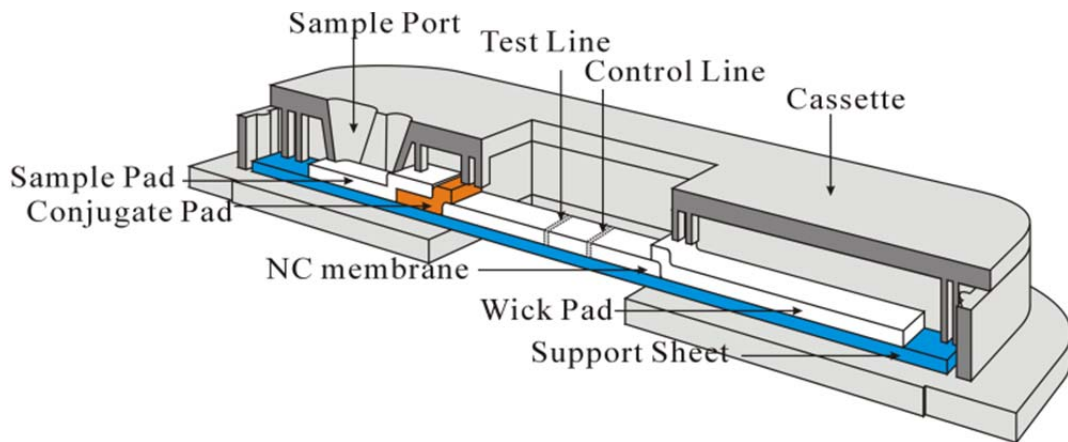
Figure 2-1: Typical lateral flow device [32]

A lateral flow test is mostly surrounded by a plastic housing. This housing stores the complex paper strip. It also prevents the fluid from evaporation and contamination. Furthermore, applying a sample is facilitated through the sample port. A cutout in the housing allows users to view the test and control line. When the

fluid is applied to the sample port it wicks through the sample pad to the wick or absorbent pad. By flowing down the strip, the sample interacts with the labeled ABs which were previously dried onto the conjugate pad. The test and control lines are located on the nitrocellulose membrane. Nitrocellulose paper has a high affinity for proteins because of the potentials for electrostatic charge. Every time the test is completed successfully the control line should be visible or change color regardless of the outcome of the test line. The test line only changes color or becomes visible when the analyte is present in the sample, otherwise no color should be present [32].

2.1.1 Nitrocellulose

Nitrocellulose is formed by exposing cellulose fibers to nitric acid. It is commonly used in the antigen-antibody in pregnancy tests as a detection area. The detection areas are key functional units in a lateral flow device [33]. The antibodies usually remain bound to the nitrocellulose through electrostatic binding forces. These forces act between the nitrocellulose fiber (left) and the protein (right). The forces are illustrated in Figure 2-2.

Figure 2-2: Electrostatic binding on nitrocellulose [33]

A nitrocellulose fiber is a cellulose fiber with nitrate ester. Nitrogen and oxygen form strong dipoles which interact with the peptide bonds of the protein. These electrostatic forces are not influenced by altering the pH-value.

Fluid runs over the membrane and the analyte which has to be detected e.g. IαIP binds to the immobilized AB. The correlation between the capillary flow rate and the sensitivity of the lateral flow test is inversely proportional; meaning the faster fluid flow over that spot will result in a decreased sensitivity. Furthermore, a strong signal compared to the background noise is required; otherwise a satisfactory result may not be determined [33].

2.1.2 Conjugate Pad

The conjugate pad is a storage area for the detection antibodies, which are labeled with colored nanoparticles or an enzyme like alkaline phosphatase or horseradish peroxidase (HRP). An ELISA test uses detection AB. These ABs are usually dried onto this pad and are released during interaction with the sample. The sample solution contains the analyte e.g. an antigen which binds to the labeled AB. An immuno-complex of analyte and AB is formed. According to Healthcare [33] an ideal conjugate pad has to fulfill the following attributes:

(1) Low non-specific binding

The dried detection reagent has to be re-mobilized easily when the sample runs over the pad. If it cannot be re-mobilized, there will be no immunocomplex at the test line.

(2) consistent flow characteristics,

The reagent needs to be solubilized steadily to have a uniform signal development. Streaks on the membrane are indications of a non-uniform flow.

(3) consistent bed volume

The amount of detection fluid which is loaded in sample the pad needs to be the same every time the test is performed, if quantitative results are desired.

(4) low extractables

There must not be any other particles which might bind to the analyte or the detection antibodies.

(5) Good web handling characteristics and consistent compressibility

These two characteristics facilitate high yield manufacturing and ensure an overall good connection between and the various membranes.

2.1.3 Absorbent Pad

The absorbent pad is important to ensure a sufficient and continuous flow. It needs to have a sufficient size with a big absorption volume to ensure a continuous capillary fluid flow.

2.2 Biology Research

As discussed earlier the PBD's consist mostly of paper. The involvement of dipolar forces in paper can cause problems regarding biological reaction. The goal is to minimize unwanted interactions which affect biological processes on the chip. The following abstract presents ways how the reagent paper interactions can be minimized.

2.2.1 Paper Surface Treatment

Paper provides certain advantages in comparison to the 96-well plates which are commonly used for ELISA. On the one hand ELISA can be conducted on paper in less than an hour with far less fluid (for example 20µl). The incubation time is shorter compared to plastic wells because the surface to volume ratio is much higher, which allows the reaction to take place faster. The overall time can be reduced to a couple of minutes. With the help of certain color enhancer, the result is readable by eye or can be evaluated using a desktop scanner. No expensive plate reader is needed. On the other side, the reaction conducted on paper is opened to the air which makes the result highly dependent on temperature and humidity. These are reasons why the

LOD of PBD's is not as low as with 96-well plates. Nowadays, the order of magnitude with respect to LOD is three times higher than with 96-well plates [34].

The use of a paper-based materials changes the way an ELISA test is conducted. This change is challenging because paper has a different surface structure than that of a well in a microtiter plate. Many reagents are used in the area of biological testing, like proteins and enzymes [35]. In general when paper is used its surface needs to be modified in a certain way to counteract certain effects which can influence biological processes. Proteins interact with paper fibers due to e.g. Van-der-Waals forces and the resulting dipole moments. Consequentially, non-specific binding can occur [33].

It is very important to minimize these interactions on the nitrocellulose to obtain a high quality result in the form of a clearly visible concentrated spot. Many groups have been researching methods to minimize non-specific binding. So far the approaches fit into two main strategies: surface modification or adsorption of a secondary protein [36].

The first strategy is to graft the surface or adsorb hydrophilic molecules on possible binding areas. The modified surface interacts only weakly with the detection antibodies [37]. The other method is to treat the paper with a secondary protein e.g. bovine serum albumin (BSA). This step prevents the non-specific binding of proteins to areas other than the already immobilized proteins [38]. One explanation is that

BSA blocks vacant binding sites on the nitrocellulose membrane so that antigens and antibodies can be react more uniformly so that more "sandwiches" are formed [39].

A third approach is to treat the paper with amino (NH_3) and carboxyl (COOH) altered silicon dioxide (SiO_2). Figure 2-3 shows the influence of NH_3, and COOH-SiO_2 blocking.
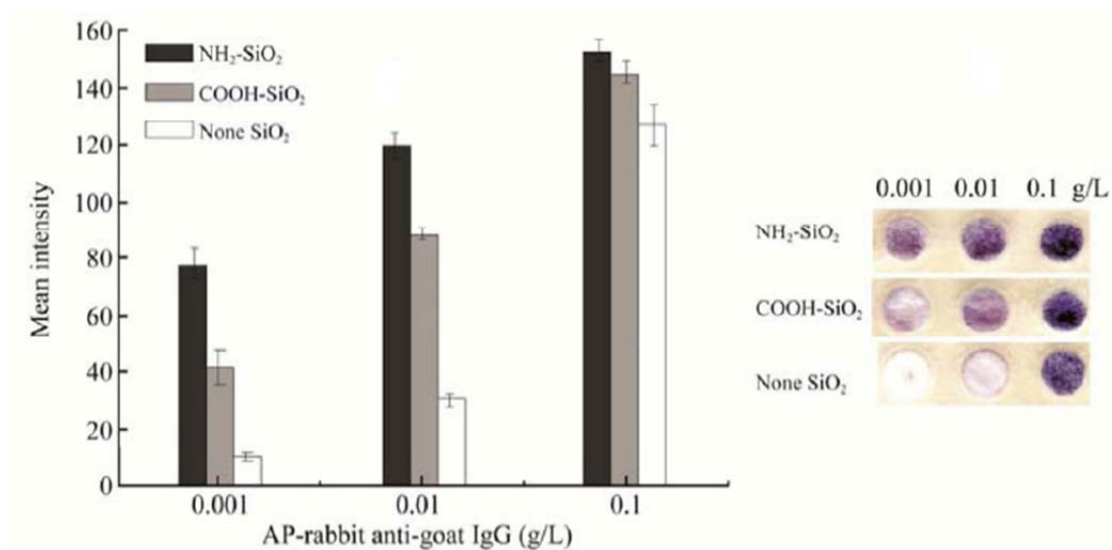
Figure 2-3: Effect of SiO2 blocking [40]

With the antibody concentration is increased, the mean intensity increases because more sandwich structures are formed. The signal on the SiO_2 treated paper is seven times higher than on untreated paper, whereas the effect of NH_3-SiO_2 is higher than the COOH-SiO_2. With increasing concentration of ABs the mean intensity variation vanishes between treated or untreated paper. However, the concentrations should always be kept as low as possible to increase the LOD later on.

Wang et. al. [41] reports on a chemiluminescence ELISA (CL-ELISA) on Chitosan modified paper. Using Chitosan wet-strength and the ability to bind

22

antibodies onto paper is improved. Chitosan and cellulose are structurally closely related and therefore more compatible [42]. Furthermore the mechanical strength is improved [43]. Wet-strength means that when the material gets wet it maintains its shape whereas mechanical strength might be affected by chemical reagents which make it brittle. In chemiluminescence reactions visible or ultraviolet light is emitted during the chemical reaction. Larsson et. al. [36] shows that viruses (M13 bacteriophage) can be detected on paper. To adsorb viruses electrostatically onto paper polyelectrolyte multilayers (PEM) are used in combination with anionic poly-acrylic acid (PAA) and cationic poly-allylamine hydrochloride (PAH).

2.2.2 Signal Enhancement

ELISA tests are commonly performed using a 96-well microtiter plates. The bottom surface is coated with a protein or antibody. Afterwards reagents are added and incubated at a certain temperature. Finally the plate is inserted into a microplate reader and illuminated with appropriate wavelength light. The reflected light is then measured. The wavelength indicates which kind of light is absorbed and the intensity of the color spot correlates to the concentration of the target substance.

Experiments conducted in microtiter plates have been expanded for use on paper-based devices. ELISA on paper was first conducted by a group from Harvard University, Cheng et. al. [34]. In general POC must not rely on expensive equipment. Therefore, a visible, readable detection scheme that does not rely on expensive equipment is most preferred. At the least, this may come in the form of a color

gradient to evaluate different concentrations. So far the limit-of-detection (LOD) for Rabbit IgG, for examples, is about 5 ng/mL which is demonstrated by Gerbers et. al. [19] and Föllscher et. al. [18]. There is still a difference of one to two orders of magnitude between paper and microtiter plate. At the very low levels of concentration, the color spot on the detection membrane cannot be read with the naked eye. In the following section, the use of color enhancer and rinse steps are illustrated

Evaluation methods performed by Chaaban et. al. [12] do not need an amplified signal because variations in the wavelength of a couple nanometers can easily be observed using a 96-well plate reader. But the use of signal amplification and rinse steps are necessary to develop a Point-of-Care device from which results can be evaluated without any extra instrumentation.

Fu et. al. [44] searches for new method to enhance the color signal on the detection spot. She proposes a rinse step and a chemical amplification step to get a stronger and clearer signal. A rinse step is needed to remove unbound proteins, which could interfere with the results. If these unbound proteins are not removed, the substrate will have more opportunities to bind to an AB and will result in an unclear color spot is slightly all over the detection area. The rinse step washes all unbound antibodies away to which a colored AB can bind which reduce the area where a color change is induced and the signal is more concentrated on one spot.

Another opportunity to strengthen the signal is the use of color particles. The enhancement of a detection spot with gold particles is adapted by [45] . In Figure 2-4 the influence of an amplification step is illustrated and in Figure 2-5 the signal strength is plotted over the analyte concentration with and without a rinse step.
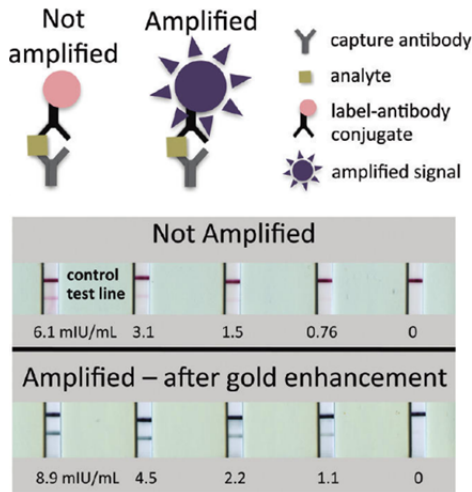
Figure 2-4: Signal amplification using gold particles [44]
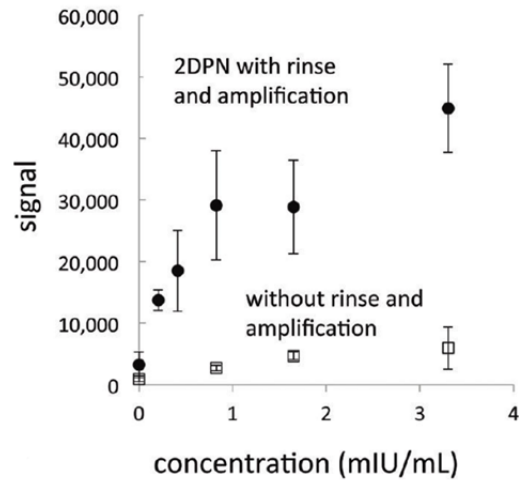
Figure 2-5: Effect of a rinse and amplification step [44]

The sandwich structure of analyte and antibodies illustrate how the signal is amplified. Below it can be seen that the gold enhancement facilitates the visual detection whether there is a positive reaction or not. The signal of the spot which is not washed and amplified with gold particles has a lower signal than the rinsed and amplified spot. The magnitude of the signal with a rinse step is up to four times higher than without a rinse [44].

An alternative method to enhance the colored spot onto the detection area is performed by Murdock et. al. [20]. They use different substrates in their ELISA-test in order to detect less concentrations of NYP. The use of different substrates which

25

induce a color change at the AP-labeled detection antibodies is varied. In Figure 2-6 the difference between two different substrates is illustrated.
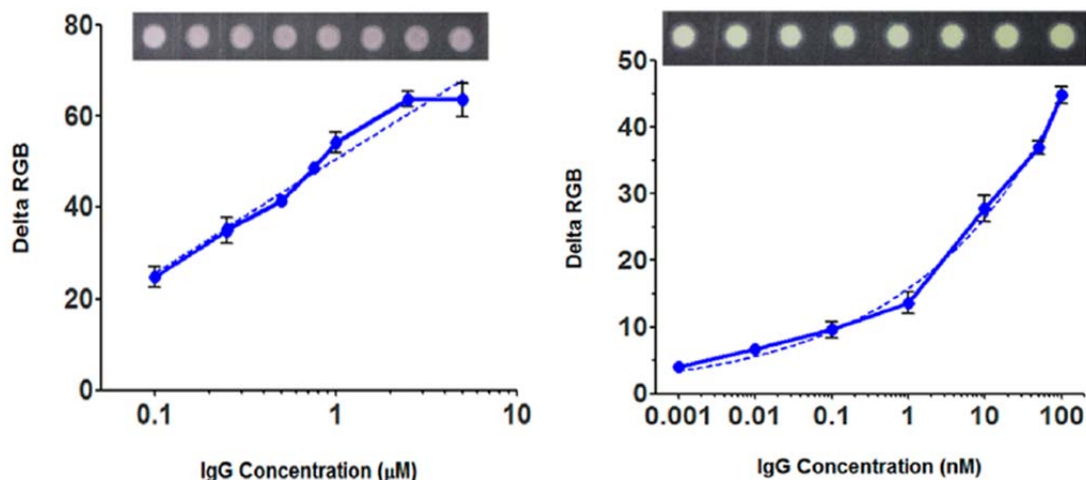
Figure 2-6: Rabbit IgG detection using BCIP/NBT (left) pNPP (right) [20]

The Red-Green-Blue (RGB) intensity is plotted over the concentration of Rabbit IgG. It can be seen that the LOD for the *p*NPP is much lower than that of BCIP/NBT. Murdock et. al refer to the fact that the alteration of BCIP/NBT is a two-step process where BCIP is immediately hydrolyzed by AP. Then it transforms NBT to the final product NBT–formazan indigo colored dye final whereas *p*NPP is directly hydrolyzed to form the yellow end-product, p-nitrophenol. The paper matrix might cause problems regarding the diffusion of the formed NBT-formazan. Another explanation is that AP creates different rates of hydrolysis using different substrates which increase the intensity of the detection spot.

2.2.3 ELISA-Test to determine IαIPs

The ELISA-test to determine the concentration of IαIP uses antibodies, which only bind to IαIP, and a subsequent color generation by induced by the use of

26

horseradish peroxidase (HRP) enzyme and the 3,3'-diaminobenzidine (DAB) substrate. The color spot's intensity, in relation to the background on the nitrocellulose membrane, corresponds to the concentration IαIP within the sample. In Figure 2-7 the schematic of the ELISA test is illustrated.
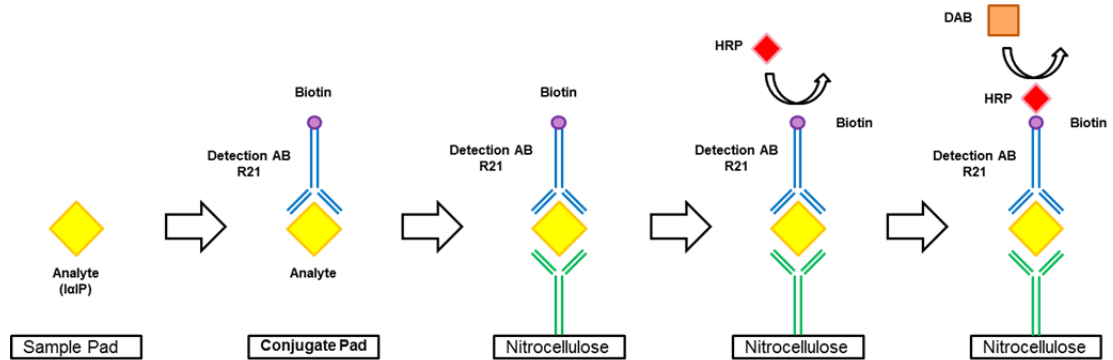
Figure 2-7: ELISA for detecting IαIP

The first step is to immobilize monoclonal antibodies 69.31 (MAb 69.31) on the nitrocellulose membrane. Afterwards the detection area is blocked. This can be done with Superblocker (Föllscher et. al. [18] and Gerbers et. al. [19]) or with non-fat milk powder diluted in PBS Lim et. al. [14]. Then the sample containing a certain concentration of IαIP flows down the main channel and binds to the biotin labeled polyclonal detection antibodies R21, which are dried in the conjugate pad. The IαIP/R21 conjugate then flows over the test spot where the IαIP portion of this conjugate is captured by the immobilized monoclonal antibody 69.31 at the test spot. A portion of the sample fluid, through a different channel, triggers the flow of the solution containing HRP enzymes tagged with streptavidin and which is stored at one of the reagent pads. This solution flows over the test spot and the HRP enzymes are

captured by the immobilized R21 antibodies via the streptavidin/biotin bond. Yet another portion of the sample fluid via a different channel triggers the flow of the DAB substrate which is stored in another of the reagent input pads. This solution containing the DAB substrate then flows over the test spot where it reacts with the immobilized HRP enzymes and produces a brown colored product that precipitates at or near the test spot, thus making it visible. By measuring the darkness or color intensity of this spot for various known IαIP concentrations in the sample, a calibration or standard curve or a color chart can be produced so that the concentration of IαIP can be inferred in samples where the concentration is unknown.

2.3 Fluidic Research

Besides the biological reaction on the chip the fluidic system which is necessary for the success of the enzymatic or enzyme linked test has to work properly and reliable in every environmental condition. This chapter illustrates the state of art and shows different approaches how to influence the fluid flow.

2.3.1 Channel geometry

Designing a fluidic paper chip is a long procedure because of the large number of variables that one has to be aware of during the procedure. For this reason, calculations have to be made to predict the flow characteristics to avoid additional testing after fabrication. In general there are two equations which can be used to estimate the capillary fluid flow, the Washburn equation and Darcy's law. Equation

(1) is the Washburn equation. It is used to calculate the time for a fluid to flow on and in a dry porous material of a certain length L over a time t.

$$L = \sqrt{\frac{\gamma D t}{4\eta}}$$ (1)

The time t is directly dependent on length L, the surface tension γ, the dynamic viscosity η and the pore diameter D. The experiments are performed at room temperature (25 degrees C). The surface tension γ of water is estimated to $0.0728\ \frac{N}{m}$ and the dynamic viscosity η is about $1.002 * 10^{-3}\ \frac{Ns}{m^2}$ [46]. Darcy's law also describes fluid flow but it is used when the fluid flows on and in materials which have been already wetted.

$$Q = -\frac{\kappa A}{\mu}\frac{(P_b - P_a)}{L} = -\frac{\kappa A}{\mu}\frac{\Delta P}{L}$$ (2)

Q is the volumetric flow rate, A is the area of the channel which is perpendicular to the flow, κ is the permeability of the paper, μ is the viscosity of the fluid, ΔP is the total pressure drop along the travelled path and L is the length of the channel. The value for ΔP at room temperature is $4,560\frac{N}{m^2}$ [47]. Rearranging Equation (2) with respect to the time provides Equation (3).

$$t = \frac{V}{Q} = \frac{\mu}{\kappa\Delta P}L^2$$ (3)

Where V is the Volume transported with a flow Q over time t. Regarding these two equations the flow of a fluid depends on geometrical variables such as length or

width of a channel as well as the atmosphere parameters within which the paper and the fluid are used.

2.3.2 Expansion and contraction

Fu et. al. [21] has conducted studies about how the width of the channels affects the fluid flow. Therefore, paper strips with different widths and different combinations of contraction or expansion were studied.

In Figure 2-8 the effect of an expansion on the movement of the wave front is pictured. Channels A-E have different geometries, whereas Channel A-C are similar except for the beginning of the expansion. The other two channels are different with respect to their widths.
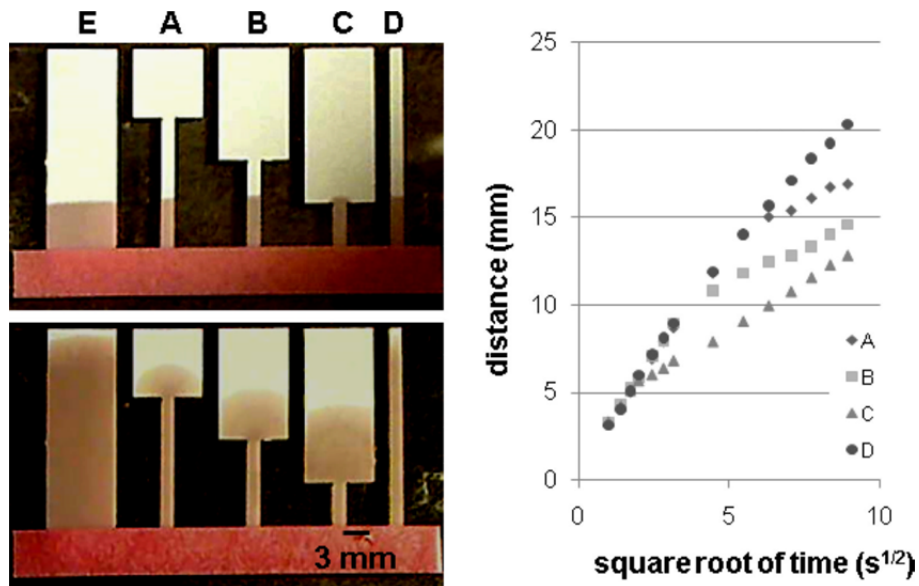
Figure 2-8: Effect of an Expansion [21]

The diagram on the right illustrates the distance in mm over the square root of time, $\sqrt{t}$. It can be seen that the distance travelled in design A-C decreases depending on the location of the expansion. The reason for this is that the smaller

30

width channel restricts the amount of fluid that may travel beyond. The fluid slows down but in design D and E the velocity is maintained. According to equation (3) the velocity of the fluid flow is the same when the width is constant irrespective of how wide the strip is.

The counterpart of an expansion of width is a contraction. Fu et. al. [21] set up the same strips but a strip design is inverted. The experiment is pictured in Figure 2-9.
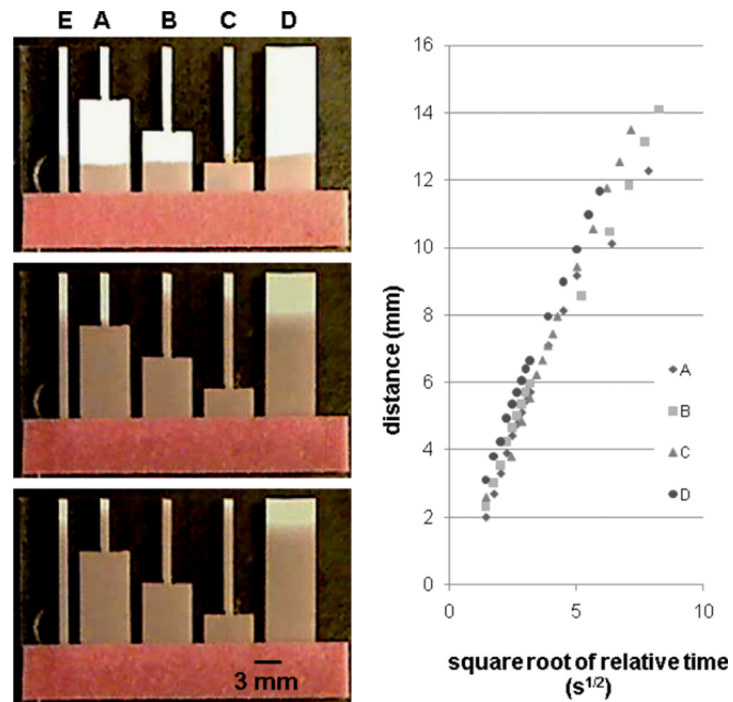
Figure 2-9: Effect of a Contraction [21]

Again the distance is plotted over the square root of time. In comparison to the expansion there, is rather no difference between the channels A-E. The fluid is not restricted by the wider part of the channel as it provides an unlimited source of fluid. These experiments show that the flow of a fluid can be slowed by including a narrower channel.

31

2.3.3 Reagents storage

Enzymatic reagents are stored in dry form to be released later when fluid runs over that area. Typically, proteins are dried on the conjugate pad. To facilitate the protein re-mobilization, mixtures of trehalose, sucrose and BSA are used. Otherwise, it is not possible to redissolve the proteins again after they are dried onto the pad. The use of sugar provides not only a better release of pre-dried proteins but can also delay the flow of fluids. Fridley et. al. [24] uses sugar as a barrier to slow down fluid flow. First the focus is on the storage and release of reagents. Figure 2-10 and Figure 2-11 illustrate how sugar solutions can facilitate the re-mobilization of proteins.
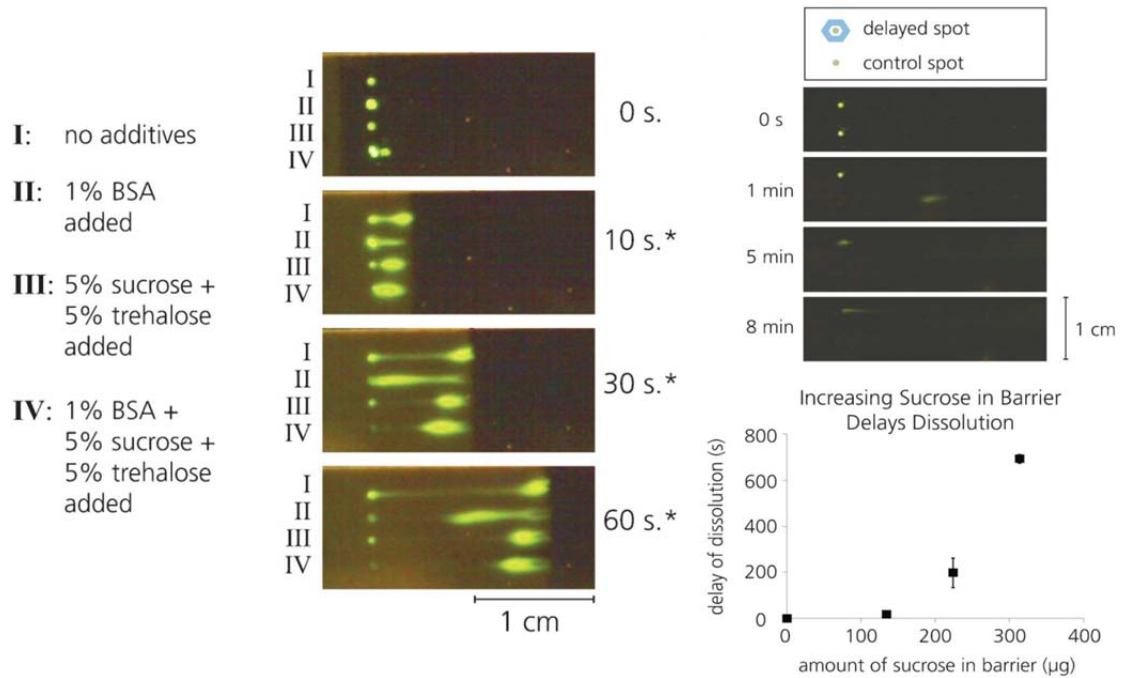
Figure 2-10: Sugar solution facilitates Protein release [24]   Figure 2-11: Sugar Barriers [24]

Different types of solutions were tested. The detailed composition of the fluids can be obtained from Figure 2-10. Stevens et. al. [48] discusses how trehalose

and sucrose molecules substitute for the water hydroxyl groups which are lost after drying. When fluid runs over the dried proteins hydroxyl group re-substitute for the sugar. The release is therefore easier in comparison to the glucose. The left image in Figure 2-10 shows that in composition IV no protein remains on the original spot of immobilization. Furthermore, trehalose has the ability to protect the protein from physical and chemical damage.

Aside from the release facilitation, sugar can be used to delay the fluid flow. The right image of Figure 2-10 shows that the higher the amount of sucrose, it delays the fluid flow longer. Sucrose barriers are therefore an additional method to control and delay the fluid flow.

2.3.4   New elements for a Fluidic Circuit

Instead of using geometrical changes to control the flow of the fluid, circuit components were invented. These components like a switch or a valve provide better fluidic control. The following summaries provide a better understanding of the manually activated mechanical switch, developed by Martinez et. al. [49] and the autonomous fluid actuated valve technology developed by Chen et al. [49].

2.3.4.1   Mechanical Switch

Martinez et. al. [49] developed microfluidic paper-based analytical devices (µPADs). They introduced a mechanical switch which is illustrated in Figure 2-12. The switch consists of multiple layers of wax-treated paper channels which are adhered with layers of tape. The hydrophilic inlets vertically match with the counterpart, but

the space in between these two layers has no material to bridge the fluid flow, leaving an air gap. This gap can be manually manipulated as soon as the fluid reaches the switch to continue the flow, in essence, by eliminating the air gap. The use of a switch further extends the possibilities for fluid flow control. Using multiple switches in one device can allow for the inclusion of multiple assays. The fluid can therefore be deliverable when needed through a physical manipulation of the switch.
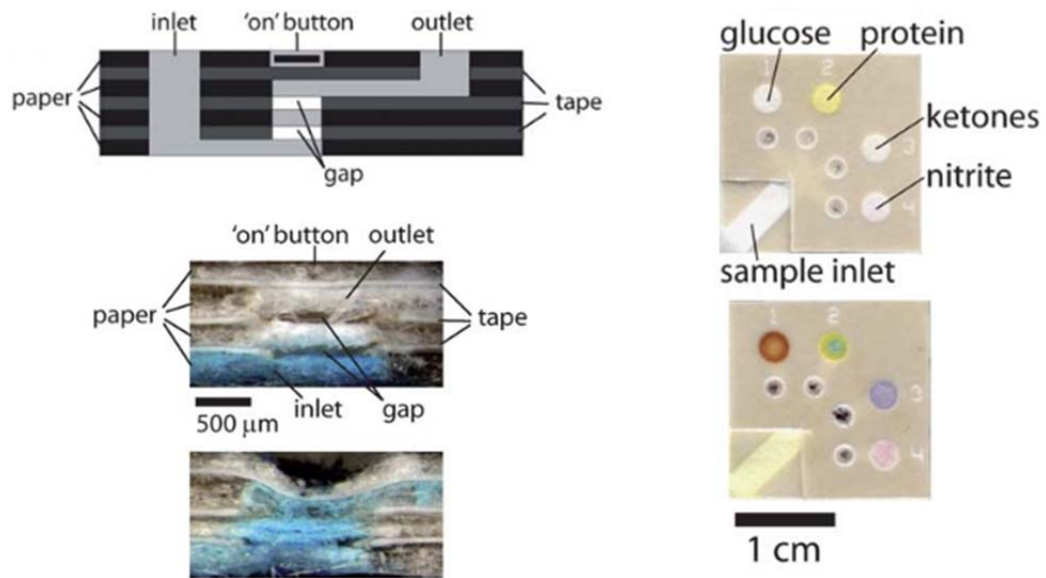
Figure 2-12: Mechanical Switch and examples of application [49]

The major disadvantage of this method is that user interaction is necessary. A trained person still has to activate every switch. The person who has to work with these devices needs to have basic knowledge of the procedure. This, however, is not the intention of the field of POC-devices. Little to no interaction is preferred and that rules out the potential for incorporating a mechanical switch.

2.3.4.2 Fluidic Valve

A new technology, which acts like a switch but does not require a user intervention, was developed by Chen et. al. [50]. The valve technology makes it possible to sequentially load fluids without any action by the user during the operation of the PBD. The principal of operation of this valve is illustrated in Figure 2-13.

The fluidic valve is similar to an electric diode (Figure 2-13a). An electric diode consists of an anode and a cathode. In this particular case, the current may not pass from cathode to anode, but the reverse is possible. The direction of the electrical flow is dictated by this electrical part. In his dissertation, Chen et. al. [50] transfers this principle onto a paper valve which is able to control fluid flow with the help of chemically treated components. The anode still represents the conductive part and the cathode the non-conductive part.
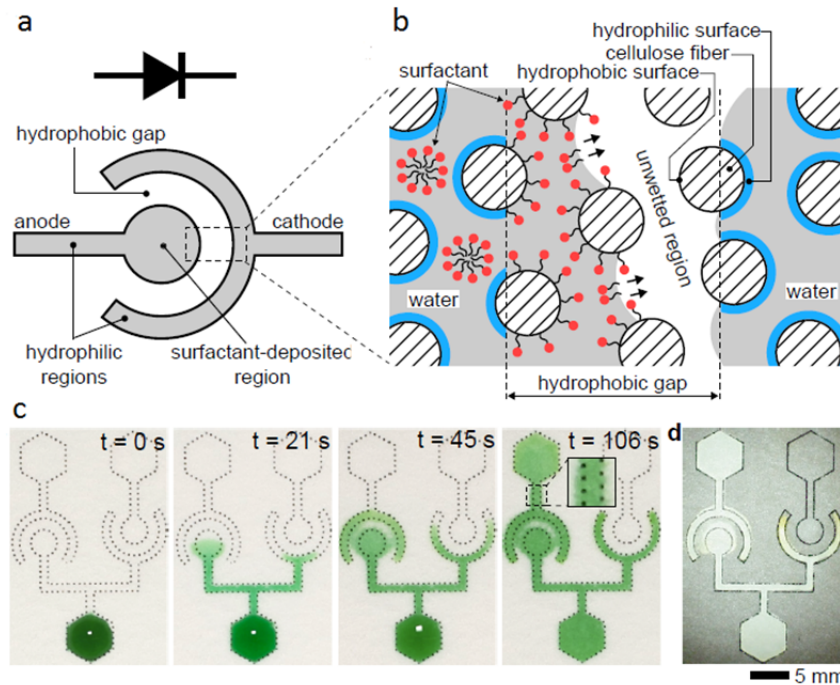
Figure 2-13: Principle of a Fluidic Valve [50]

In a fluidic context, this means one side of the paper-valve is hydrophobic, to block fluids, while the other side is hydrophilic, allowing for fluids to pass by. The hydrophobic side of the valve is treated with Allyltrichlorosilane (A3CS). The hydrophilic side is not treated with a solution but rather a surfactant which is placed in between hydrophobic and hydrophilic sides. When it is dissolved in water, surfactant materials are able to bridge hydrophobic areas (Figure 2-13b). The valve is then opened and fluid can flow in both directions whereas an electrical diode always blocks one direction of the flow.

With this new technology, advanced control of fluid flow is achieved. In Figure 2-13c the ability of the valve to block fluids is illustrated. On the left side the surfactant is dissolved and the hydrophobic area is bridged. Finally the colored water can flow to the end of the channel. On the right side the hydrophobic area cannot be

36

bridged due to the lack of dissolved surfactant which breaks down the hydrophobic area. The fluid is not able to continue its flow.

POC devices must not have a lot of user interaction like applying reagents on the paper chip in a certain order because these user interactions offer possibilities for failure. Reagents may be applied on the wrong area, too early, too late or may be forgotten. Therefore, it is necessary to reduce user interventions as much as possible to meet the requirements of a POC device [51]. The valve presented by Chen et. al. [50] is an approach in the right direction to reduce user interaction and make POC-devices suitable for more and more fields of application

2.3.4.3   Delay Channel and Sequential Loading

The fluidic paper valve as discussed in section 2.1 is able to stop the flow of a fluid because when the valve is aligned in a certain way it blocks fluid flow along one direction. A delay channel is combined with another fluid to reach the valve from the opposite side. The valve is opened from the delayed channel. The so called "trigger" fluid opens the valve. Another possibility is that the blocked fluid can open the valve on its own by flowing along a second path to the surfactant region of the valve. The principle of a delay channels is illustrated in Figure 2-14.
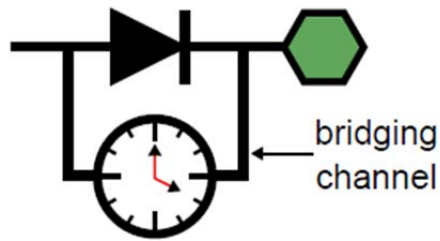
Figure 2-14: Delay Channel [50]

Lutz et. al. [26] proposed a method to load fluids sequentially with no user interaction. A chip is designed with channels on which reagents are dried. All channels have a different length because when the fluid level of the source drops the connection to the fluid is no longer maintained. The experimental set up and results are shown in Figure 2-15.
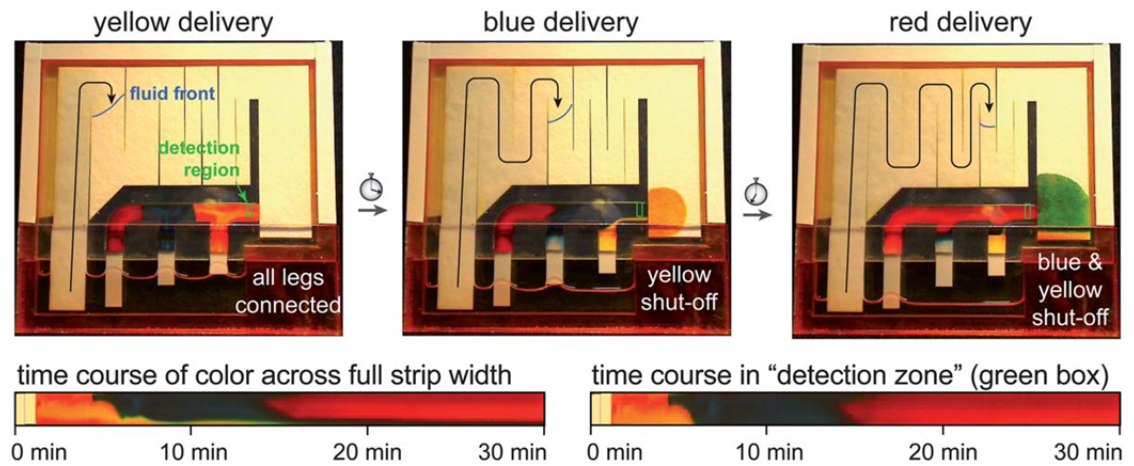
Figure 2-15: Sequentially loading of dried reagents [26]

At first all channels are connected to the fluid. Sequentially, the channels disconnect from the fluid as the source fluid level decreases. The displayed color trend shows a sequentially loaded fluid. The color of the detection strip changes from yellow to blue then to to red which demonstrates the principle of sequential loading.

38

Fu et. al. [52] run a similar experiment but pH-paper is used instead of filter paper. In this case the color change is based on a different pH-value caused by different buffers.

Another method is shown by Dr. Hong Chen using a paper valve in combination with a delay channel. This makes it possible to load fluids sequentially without any user interaction after loading the chip with fluids. The principle is shown in Figure 2-16.
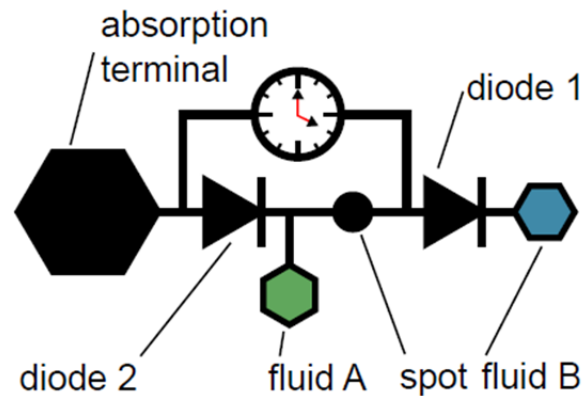
Figure 2-16: Sequentially Loading of a Fluid [50]

Two different fluids (A and B) are applied on the circuit. Fluid B stays on its spot because it cannot pass the valve. Fluid A can flow only in the right direction because a valve on the left side blocks its flow. It first opens diode 1 Fluid B, however, cannot flow to the test spot because diode 2 is still closed. Fluid A along with some of Fluid B is flowing over the delay channel to the diode 2. This opens this valve and now allows fluid B to flow in the horizontal direction towards the left and over the test spot. Both fluids end their flow in the absorption terminal.

2.3.5   FEM modeling of fluid flow

The production and testing of PBD is time consuming. A way to minimize effort through fabrication and to improve the yield is to simulate the fluid flow in a finite element model. Zimmermann et. al. [53] conducted an analytical simulation on the optimization of sensitivity, sample volume and on the time to complete a test. Their numerical results coincide with the analytical results which prove that a mathematical model is valid method for estimating fluid flow. This proves that PBD can be tested without actually fabricating one. Fu et. al. [54] developed a model regarding convection, binding and diffusion inside the fluidic channel. With a simple 2D finite element method it is possible to predict assay results when input parameters vary. By using a computer model, resources can be saved and the amount of testing can be reduced. Of course, results need to be validated with a physical model of the PBD but the amount of chips needed to be fabricated is reduced.

2.4   Fabrication Research

2.4.1   Different fabrication techniques

Paper-based POC devices may incorporate paper that is treated and manufactured in many different ways. An overview of several different manufacturing techniques is summarized in Table 2-1.

Table 2-1: Fabrication Methods an Overview [55]		
Fabrication Method	*Advantages*	*Drawbacks*
Photolithography	200µm barriers Sharp resolution	Organic solvents Less flexibility Expensive and complicated steps
PDMS plotting	Preserves flexibility	Special treatment of PDMS needed
Inkjet printing	Patterning directly on paper	Whole paper has to be treated Exposure to solvents and polymers
Cutting	Easy to fabricate	Need additional tape to stabilize structure Limited geometry
Plasma etching	Patterning directly on paper	Whole paper has to be treated Exposure to solvents and polymers
Wax printing	Fast and easy to produce Preserving native chemistry Cheap instrumentation	High resolution not possible because wax spreads out Careful determination before wax printing
Paper and toner Laminating	Results available as a snapshot	High temperature used in lamenting process
Wax screen printing [41]	Very fast to fabricate Faster than printing	contours are not very sharp screen stencil needed to fabricate

Photolithography is one of the first production methods which involve hydrophobic and hydrophilic reagents to produce channel geometry. UV light is used to bake hydrophobic barriers into the paper. This method has a high resolution with 200µm barriers which slow down the fluid flow. Unfortunately, many complicated steps with organic solvents render the paper less flexible and harder to handle [56]. In the case of PDMS plotting, the hydrophobic layer is created with a desktop plotter and the hydrophobic polymer Polydimethylsiloxane (PDMS). The chemical treatment with PDMS preserves the flexibility of the paper when compared to photolithography [57]. In the case of the inkjet printing, a solvent is directly printed onto desired regions of a hydrophobic paper. This procedure is good for high mass production because not many steps are involved. Plasma etching is a similar manufacturing method which uses a small amount of plasma. A side effect of both methods is the use of hazardous chemicals and polymers [58]. Cutting filter paper is the simplest fabrication method. In addition to the filter paper tape or another stiff material needs to be incorporated to maintain the rigidity of the cut pattern [59].

Nowadays, wax printing is the most common method to manufacture paper-based POC. Printing wax on paper is easy and affordable because a standard low cost wax printer can be used. The resolution is not as good as other processes because by melting the wax hydrophilic areas shrink and undesired spreading of wax might occur Carrilho et. al. [60]. For our conditions we found that the line geometries shrink by about 0.5mm in each direction which need to be considered in the fabrication

procedure. Another method called wax-screen printing is presented by [41]. In this

procedure, wax is rubbed through a stencil and melted afterwards into the paper. No

extra gadgets except for an oven are necessary to produce paper chips [41].

2.4.2   From 2D to 3D

The circuits discussed in the previous chapter are only in 2D. POCs, however,

have to be capable of running more complex tests involving multiple fluids.

Producing paper based devices in 3D has a number of benefits [61], [62]. They are:

Smaller chip size; smaller volumes of reagents; and faster assay times. Our new 3D

Delay circuit and the 3D Sequential Loading circuit are shown in Figure 2-17 and

Figure 2-18.
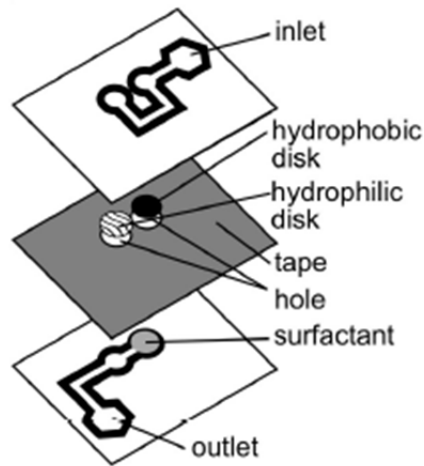
Figure 2-17: Delay Circuit in 3D [50]   **Figure 2-18: Sequential Loading in 3D [50]**
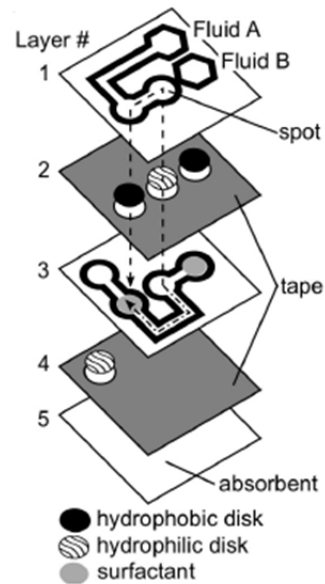
43

As illustrated above the valve can be vertically aligned in several layers to transfer the principal of sequential loading into a 3D format. In Figure 2-17 the 3D-Delay Circuit is shown. It consists of two layer of paper connected by a layer of double sided tape. In the tape, in both figures, are made holes. One is filled with a hydrophilic disc, which essentially forms a fluidic short between the top and bottom layers of paper. The other holes are each filled with a hydrophobic disc. In the bottom layer and aligned with the hydrophobic discs is deposited surfactant to complete the fluidic diode or valve. Figure 2-18 demonstrates sequentially loading of two fluids past the test spot. To be completed the 3D delay circuit requires two more layers. One is a thick absorbent paper sheet and a second layer of double sided tape to attaché this sheet to the whole device. The thick paper layer serves to ensure a sufficient capillary flow rate. The completed chip now consists of five layers. The capillary flow action of the 2D format works in just the same methods. In total two fluids are applied on the chip (A and B). Fluid B stays above the hydrophobic disc unable to flow any further until Fluid A flows to the second layer and dissolves the surfactant underneath bridging the gap to fluid B. This chip shows that it is possible to sequentially load multiple fluids using the developed 3D paper circuit without any user interaction [50]. Additional control of the fluid flow can be achieved by designed delay channels with a different length, width or porosity [61].

Since the fabrication process takes a lot of time, Lewis et. al. [62] proposes a high throughput method for fabricating paper-based microfluidic chips. Instead of

44

putting double sided tape in between two layers spray adhesive is used. Spraying adhesive in between two layers the number of layers in one chip can be reduced. In total this means 40% less paper and 50% less time to complete a test. Furthermore, the tedious assembly steps, which affect the reproducibility of the chips, are eliminated. By reducing the number of layers the time needed for a fluid to travel through all layers is reduced. According to Lewis et. al. [62] interactions of the adhesive with reagents used in the chip, which might influence the quality of the results or alter the wicking rate of the paper, were not observed.

3 CHAPTER 3 - METHODOLOGY

This chapter describes the fabrication processes for a paper based microfluidics chip for the detection of IαIP, a biomarker for sepsis. Several optimization steps and the assay protocol are also discussed.

3.1 Chip Fabrication

All paper chips are fabricated according to the fabrication methods which were previously introduced by Wilke Föllscher and Roman Gerbers. Six identical chips are fabricated at once in a single batch. A basic chip consists of at least three layers and blotting paper at the bottom to absorb fluids. Two layers of filter paper are printed with wax printed fluidic channels and a layer of double sided tape holds the layers together. The connection of the two layers is satisfied by spreading hydrophilic material in the holes of the tape layer. To form a more complex chip which can handle more than two fluids, additional layers with wax printed fluid channels are necessary.

3.1.1 Different types of paper

Fluids can only flow in the hydrophilic areas of the paper. To control the fluid flow, wax patterns are printed onto the filter paper. The black areas with wax form hydrophobic areas and white blank areas are hydrophilic. In these the fluids may flow. The black and white printing patterns are created using software Corel Draw® (Corel®). The channels are printed on a 8x10 inches filter paper (Grade 41, 20 μm) from Whatman® using a solid ink printer (Xerox® ColorQube® 8570) with solid ink

(Xerox® Genuine Solid Ink Black). Afterwards, the paper is cut with a CO_2 laser cutter (Epilog® Mini 24) to maintain accuracy and proper alignment during assembly. The printed wax channels are only printed on one side of the paper but the black hydrophobic wax areas have to be melted all the way through the paper to prevent the fluid flow in undesired regions. Therefore the printed filter paper is placed with the blank side up in a vacuum oven (Isotemp® Model 280A, Fisher Scientific) for 30s-40s with a temperature 130°C-140°C. The wax is allowed to melt through the entirety of the filter paper leaving a blank printed pattern which carries through to the opposite side of the paper. Depending on where the paper components are placed within the oven, the melting time can vary due to the varying temperature gradient, which makes it necessary to place the chips in the middle of the oven. Figure 3-1 shows what wax-treated and untreated paper looks like.
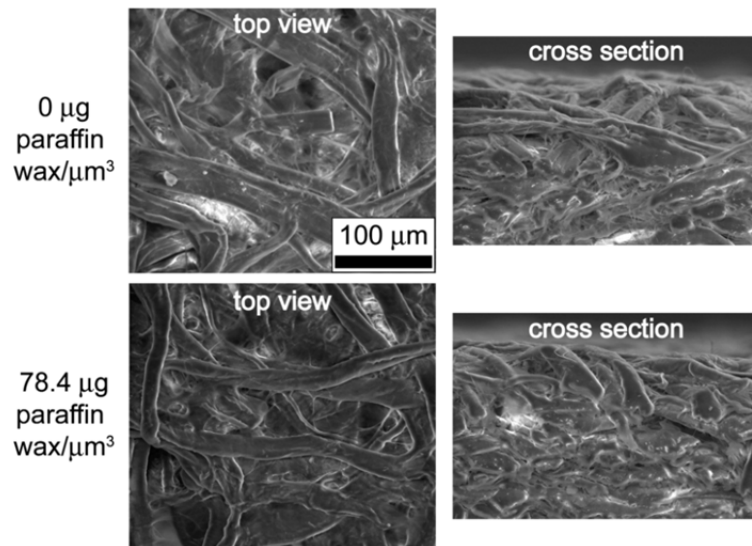
Figure 3-1: Wax on Paper [61]

Paper treated with wax is more compressed than paper without a wax treatment. The wax coating prevents liquids from traveling in undesired areas on the paper because it fills in the pores thus forming solid hydrophobic walls. In addition to filter paper two other types of paper are used, which are the blotting paper and an absorbent paper. These types of paper are used to maintain a steady fluid flow throughout the chip. Gel blot paper (GB003) from Whatman® and glass fiber membrane filters (GA-55) from Sterlitech® were purchased. The blotting paper forms the foundation of the chip providing a rigid support.

3.1.2   Double Sided Tape

The tape layer in another important component, it is used to hold adjacent layers of filter paper together. Double sided tape from Ace Hardware (Item No. 50106) is taped onto wax paper for handling and cutting purposes (Parchment Paper, Reynolds®). Later on the top coating of the tape and the parchment paper are removed leaving only the two adhesive sides. In total, three different types of double sided tape are cut. The tape between first and second layer has holes cut out, also cutouts for the absorption pads and small strip cutouts for the nitrocellulose filter and detection areas are included. These cutouts are helpful to align the small filter and detection spots on the tape. The second type of tape is similar to the first tape layer except of the cutout stripes because there are no filters etc. which need to be aligned properly. The last layer has only cutouts for the absorption squares. The cutting patterns are designed in Corel Draw® as well and cut with the CO_2 laser. The

aforementioned holes in the tape are cut with the CO_2 laser. The settings of the Laser cutter vary depending on what will be cut. A summary of all laser settings is displayed in Table 3-1.

Table 3-1: Printer Settings				
Material	Laser Power	Vector Speed	Vector Power	Frequency
Backing Paper	40 %	40 %	17 %	5000
Double-sided tape	40 %	50 %	25 %	5000
Filter paper	40 %	55 %	15 %	5000
Glass fiber (absorption area)	40 %	45 %	13 %	5000
Glass fiber (conjugate pads)	40 %	85 %	7 %	3025
Nitrocellulose	40 %	40 %	2 %	4250
Plastic PP-Layer 1.5mm	40 %	10 %	30 %	5000

3.1.3 Hydrophobic Layer and Surfactant/Hydrophilic Paste

The hydrophobic layer has the most important role in the fabrication of an autonomous immunoassay circuit, after the surfactant paste. It ensures that certain fluids cannot pass through a specific way unless a trigger fluid bridges the hydrophobic area of the paper. This is the principle of a delay channel introduced in section 2.3.4.3. Therefore, the surfactant enriched paste, which is placed and dried underneath the valve, needs to be dissolved in order to open the valve and release the stored fluid.

To create a hydrophobic disc, the 3mm wide spots have to be treated as specified by Föllscher et. al. [18] and Gerbers et. al. [19]. 8µl of the hydrophobic solution has to be pipetted but in 4x2µl drops on one spot otherwise the solution

49

evaporates too fast and cannot soak into the paper. The hydrophobic layer is illustrated in Figure 3-2 where only the four bottom spots in the center of the drawing are treated with the hydrophobic solution.

Figure 3-2: Hydrophobic Layer

The hydrophobic solution is a mixture of 4.76 Vol.-% Allyltrichlorosilane (ALS) in Perfluro-compound (FC-72). After the treatment the sheets of the paper have to be stored in a covered petri-dish overnight to fully develop their hydrophobic characteristics.

The surfactant paste is placed in the other side of the hydrophobic paper. Together they form the paper based valve. The surfactant solution is a 35 wt.% dilution of Tween 20 in Ethanol. The next step is to dilute 0.25mL/mL surfactant solution in ultra-pure water. The final step is to mix the water-ethanol-surfactant solution with the cellulose powder (0.5 g/mL). Holes without a hydrophobic spot are filled with hydrophilic paste to bridge the layers of filter paper. The hydrophilic paste is a mixture of cellulose powder in ultra-pure water (0.5 g/mL).

In addition to the different types of paste in combination with a hydrophobic layer paper, discs are used to build up a valve. In total there are three paper discs (hydrophobic, hydrophilic and surfactant). One hydrophobic and one surfactant disc are placed on the tape whereas the hydrophobic disc overlaps the hole to block it. Unfortunately, after treating paper with hydrophobic solution it becomes brittle, so many of the discs may crack when they are placed over the hole. This may cause premature release of the fluid.

3.2 Chip Fabrication

As mentioned before, the chip consists of three single wax paper layers which are attached to each other with double sided tape. Our paper chip is a hybrid of Roman Gerbers and Wilke Föllscher design. Föllscher's design is chosen because the fluid storage area is much bigger compared to Gerber's design. A higher amount of fluid can be stored without the help of wells made out of a 1.5mm thick Polypropylene plate. The second layer is chosen from Gerbers because in Föllscher's design the opening channels are not connected which means that they can be triggered independently from another. In Figure 3-3 the selection of layers is displayed. The first layer is from Wilke Föllscher and the second layer is from Roman Gerbers whereas the hydrophobic layer is used in both their designs.

Figure 3-3: Different Layers of the Microfluidic Chip (First Layer, Hydrophobic Layer, Second Layer)

The use of the alignment tool is necessary to ensure perfect alignment between each layer of the chip. The first step is to place the blotting paper onto the alignment tool and attach double sided tape. The double sided tape without any cutout for holes is used. After the tape is properly aligned on the blotting paper, the other side of the double sided tape is peeled off. Before attaching the second layer of the tape the absorbent pads need to be placed in the quadratic cutouts of the double sided tape, which connect every layer to the blotting paper at the bottom of the chip. Now the second layer is attached to the double sided tape followed by another layer of tape. This time the tape with cutouts for paste but without the alignment stripes for the nitrocellulose and the conjugate pad is needed. Before placing the absorbent pads the holes in the tape need to be filled with paste, a small metal spatula may be used. The mixture of hydrophilic and surfactant paste is discussed in section 3.1.3. The bottom four holes are spread out using surfactant paste because the holes are under the hydrophobic treated spots. The top hole is filled with hydrophilic paste.

After spreading the paste the assembled part of the chip, it needs to dry for around 20 min. Meanwhile the conjugate pad and the nitrocellulose membrane may be placed onto the remaining tape layer which includes cutouts for the holes and the alignment stripes. Attach the first layer onto this tape layer. Now all holes of the tape layer need to be filled with hydrophilic paste and subsequently need to dry for 20 min. After that time, the absorbent pads are put into the tape layer and the hydrophobic layer is attached. The next step is to combine the second layer with the top layer which includes first and hydrophobic layer. Finally clear tape is put on the first layer. To be able to place a certain amount of fluid volume onto the chip Polypropylene (PP)-wells are placed on the chip. After the assembly is completed the chip needs to be constrained to ensure sufficient contact at all connection points in the chip. A summary of all materials (Figure 3-4) needed and a more detailed assembly is illustrated in the photographic sequence.
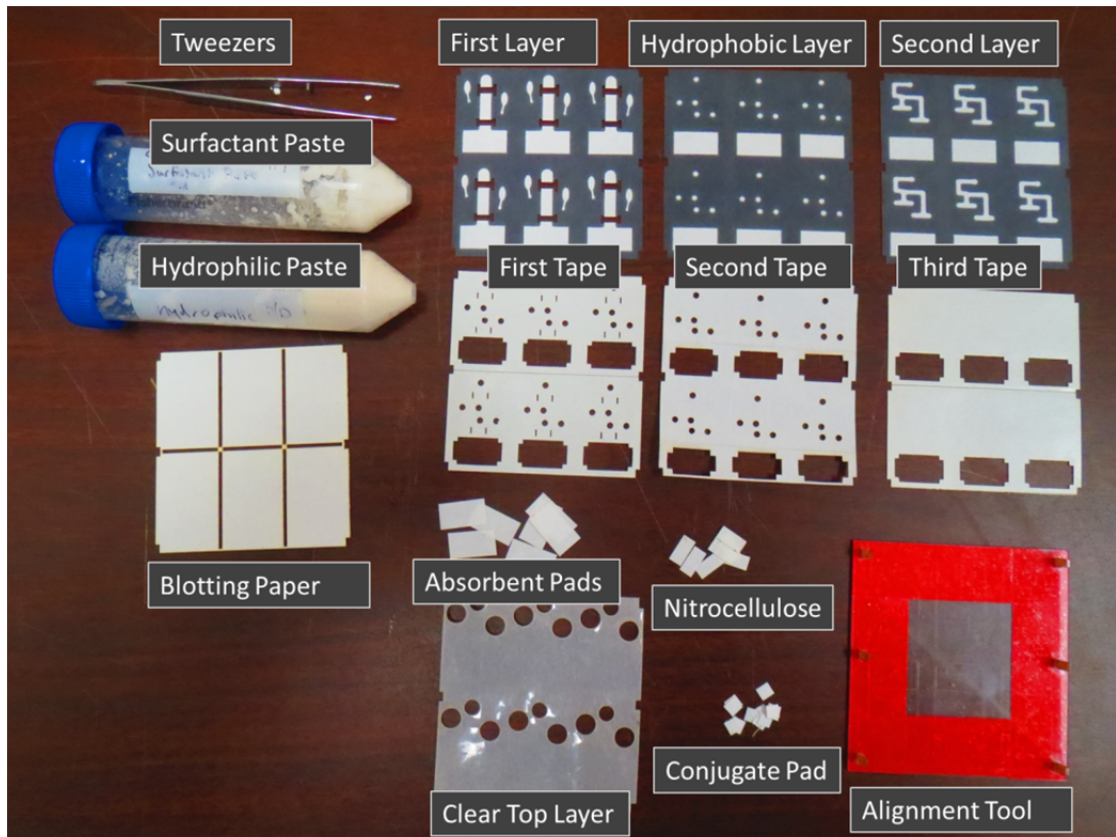
Figure 3-4: Materials for One Chip

As previously discussed in section 2.3.4.3, fluids which are used in the fluidic circuit need to be triggered in the correct sequence. Therefore all length and positions of the delay channels and amount of fluids have to be adapted for desired sequential loading. Figure 3-5 displays how the sequential loading works
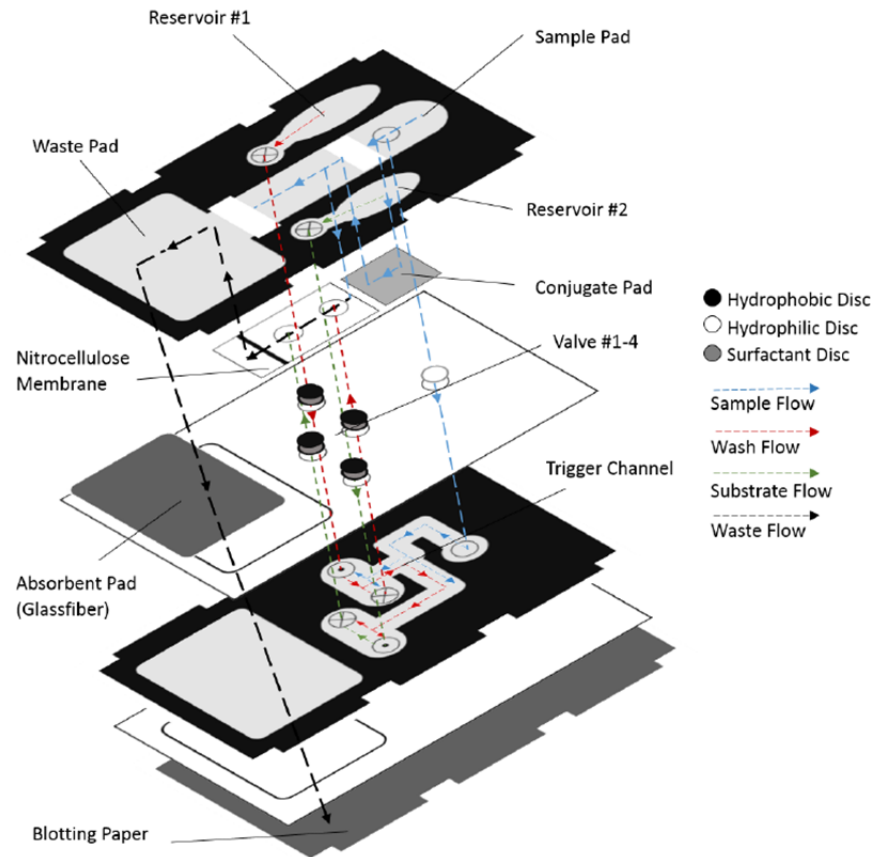
Figure 3-5: Fluid Flow in the PBD by [19]

There are three fluids which can be applied to the device. In the case of Gerbers et. al. [19] these fluids are a Sample-, Substrate-, and a Wash-fluid. The sample runs down the main channel over the conjugate pad and the nitrocellulose membrane. The conjugate pad stores dried detection reagents which are dissolved by the sample-fluid. Meanwhile, the fluid flow was divided into two streams with one traveling along a second layer. The second stream triggers the valves by dissolving the surfactant. Then the wash flow removes any unbound capture antibodies from the nitrocellulose membrane. Finally, the substrate runs down to the waste pad. If there are the desired antigens present in the sample, the indicator antibodies will

bind to the antigen-antibody complex to create a sandwich structure. This structure becomes visible when the substrate changes the color of the enzyme. A colored dot can be found on the nitrocellulose which would then indicate the presence of an antigen.

Our chip has IαIP in buffer as Sample; the second fluid is HRP in buffer which is not the wash fluid but rather the enzyme. This enzyme attaches to the detection antibody. In the end the substrate (DAB) introduces a brown color.

3.3 Influence of viscosity of the opening times

The first experiments are conducted with water and food coloring as a proof of concept for the lateral flow chip and to show that the sequential loading is possible using the valve technology of Dr. Hong Chen. Later on, IαIP diluted in buffer shall be used as reagent. The reagents have a different viscosity than water. Therefore the influence of viscosity has to be evaluated to determine its effects on the time required to open a valve. With water the time for water to dissolve the surfactant and open the valve is less than a minute.

Therefore a test with two test chips is developed with 108 valves in total. Six different concentrations of blood-plasma in TBS-buffer are tested: 100 vol.-% plasma with no buffer and different dilutions (75%/ 50%/ 25%/ 10%/ 1%-plasma in buffer). Each concentration is tested by pipetting 4µl drops on the surfactant side of the valve. In total, 18 spots per concentration are tested. The dissolve time of the surfactant to bridge the hydrophobic area is measured. To facilitate the time

measurement food color is mixed with the fluid because the plasma itself is clear which making it hard to determine the exact moment when the fluid bridges the valve. The time is recorded when moment when a colored spot is noticeable by eye coming through the paper valve.

3.4 Assay Development

To run a complete ELISA it is necessary to optimize all parameters of the biological assay (Reagent concentrations, amount of fluids needed for the enzymatic reaction etc.). Therefore it is helpful to split up the complete ELISA to concentrate on individual parts. After obtaining the desired results one can recombine them to perform the complete ELISA with each individual optimized component. Furthermore, this procedure helps to recognize in which part of the experiment an error occurs. In the following sections the split parts of the ELISA are illustrated.

First, a simple vertical test is performed using two different pairs of reagents which are both suitable to detect IαIP later on. One reactive pair is BAPNA and trypsin and the other reaction is conducted using HRP and DAB. The first reaction results with a yellow color spot and the second reaction results in a brown colored spot following the enzymatic reaction. Both reactions are evaluated if they are suitable for further experiments.

3.4.1 ELISA Pre-Testing

As explained earlier, IαIP should connect to the immobilized trypsin. Before a complete ELISA is conducted, trypsin and BAPNA are mixed in a small vial to confirm the expected color change from clear to a light yellow.

To produce the trypsin solution, 0.01g trypsin needs to be mixed according to the SOP from *ProThera Biologics©* with 50µl of 1M hydrochloric acid (HCl) in 50mL ultra-pure water. The HCl is needed otherwise trypsin would digest itself. 0.021g BAPNA powder is mixed with 1mL Dimethylsulfoxide (DMSO). These reagents are stored in Triethanolamine-buffer (TEA-buffer) at a pH-value of 7.8. The TEA-buffer is produced by putting 3.714g TEA-powder into 90mL deionized distilled water (dH$_2$O). Afterwards, small amounts of Sodium hydroxide bring the pH-value to 7.8. Add dH$_2$O until 100mL of solution is produced.

Afterwards, the possibility to immobilize trypsin on nitrocellulose and blotting paper is tested and compared to results that were previously conducted in 96-well plate. Different amounts of trypsin (1µl/1.5µl/2µl) are pipetted on nitrocellulose and (10 µl/15 µl/20 µl) on the blotting paper. The amounts of fluid are chosen regarding the absorption capacity of the paper. To see whether the trypsin immobilization is successful the same amount of BAPNA is pipetted on the paper to induce a color change. When a yellow color shows up the immobilization of trypsin is successful. The vertical enzymatic test is illustrated in Figure 3-6.

1	2	3	0	0	Trypsin[μl]
1	2	3	2	0	BAPNA[μl]

10	20	30	0	0	Trypsin[μl]
10	20	30	20	0	BAPNA[μl]
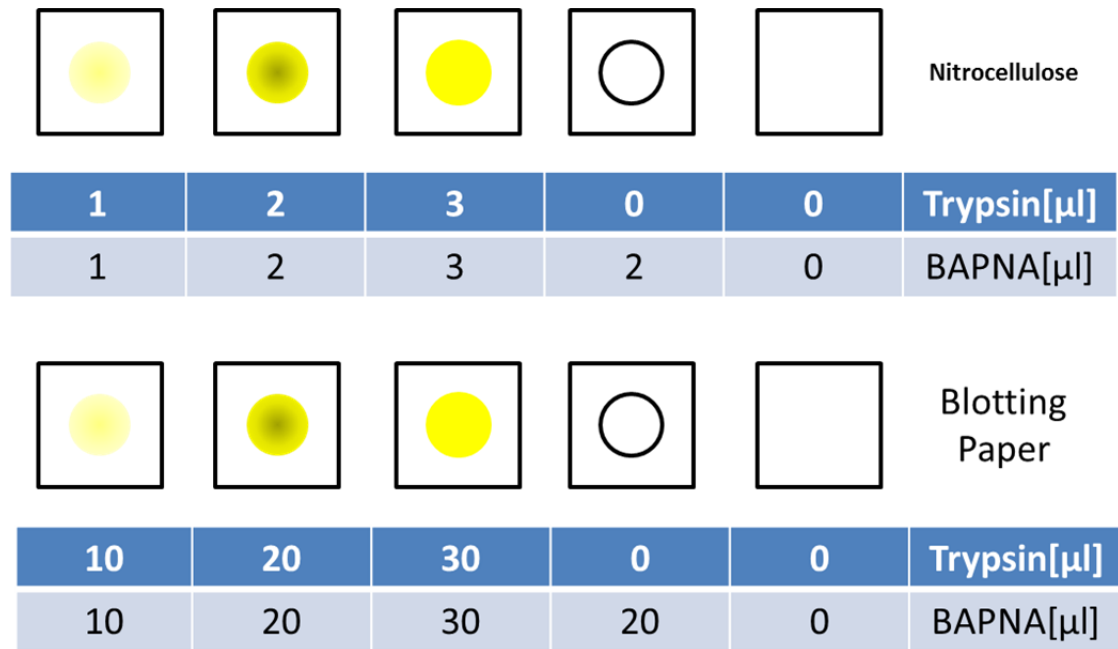
Figure 3-6: Vertical Test Trypsin and BAPNA

Besides nitrocellulose and blotting paper Glass Fiber Membrane Filters are tested to determine how well they immobilize trypsin. Two different types of Membrane Filters are tested: One Glass Fiber Membrane filter is treated with a binder and another is not treated with binder. Varying amounts of trypsin from 2μl-10μl in 2μl steps are pipetted onto the filter. Afterwards the color change is induced using a constant volume of BAPNA (12μl). The experiment is illustrated in Figure 3-7.

2	4	6	8	10	Trypsin[µl]
12	12	12	12	12	BAPNA[µl]

With Binder

2	4	6	8	10	Trypsin[µl]
12	12	12	12	12	BAPNA[µl]
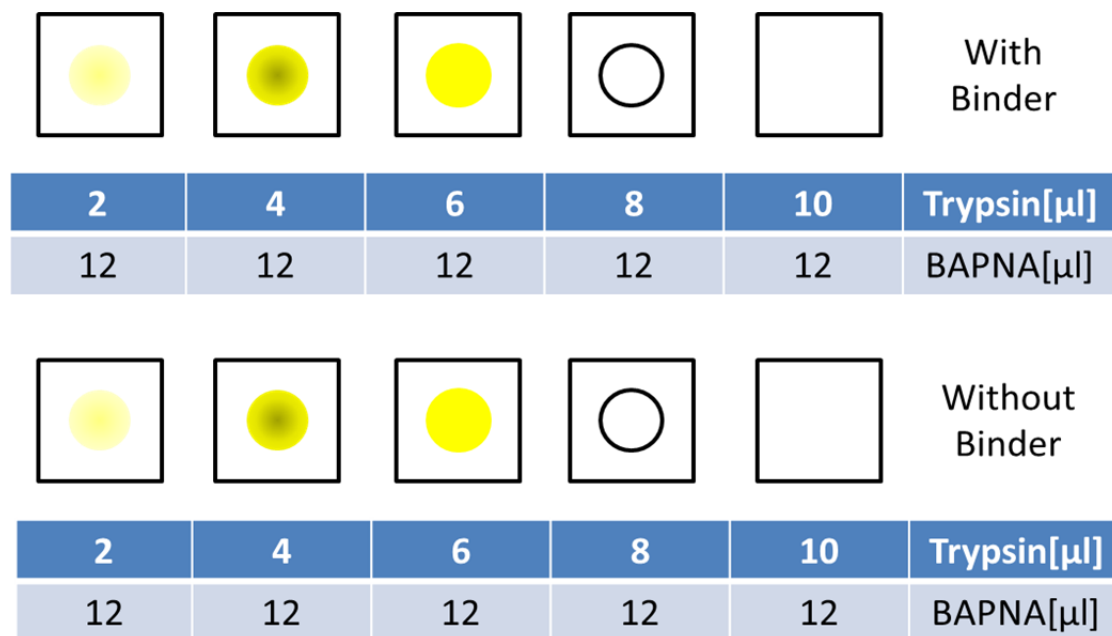
Without Binder

Figure 3-7: Vertical Test on Glass Fiber with and without binder

3.4.2 Vertical Test DAB

The different substrate DAB is used for further experiments. Trypsin and BAPNA which produce a yellow color change are replaced by 3,3'-Diaminobenzidine (DAB) and Horseradish peroxidase (HRP). DAB and HRP together produce a brown color at the place the reaction takes place. Since Murdock et. al. [20], Peng et. al. [40] and many more use a vertical test for their ELISA. To make sure that DAB and HRP like trypsin and BAPNA work together on paper further testing needs to be done.

Therefore a 96-wax-well plate can be printed onto paper using a wax printer (Xerox® ColorQube® 8570) and Whatman® Filter Paper 41. The Streptavidin Poly-HRP is purchased from Pierce Antibody (Cat. No. 21140) as well as the DAB Powder (Cat. No. 34001).

To produce a liquid DAB substrate from powder, instructions from IHC World [63] are used. The substrate solution has two components with a DAB part and a H_2O_2 part. For the DAB part (<u>1% DAB (20x) in Distilled Water</u>) 0.1g DAB are mixed with 10mL distilled water. Afterwards add 250µl of 10N HCl. The solution should turn light brown/dark purple.

The H_2O_2 (<u>0.3% H2O2 (20x) in distilled water</u>) is produced by mixing 100µl H_2O_2 in 10mL distilled water. Both solutions should be aliquot into small vial and stored at -20°C when they are not used. Finally, the substrate is produced by putting 250µl of both reagents in 5mL PBS X1.

The Streptavidin Poly-HRP is used in three concentrations (1:3000, 1:6000, 1:8000). Therefore pipette 0.75/1/2µl of Streptavidin Poly-HRP into 6mL of PBS X1.

The vertical test is performed on blotting Paper with HRP and DAB according to Figure 3-8.

| 10 | 20 | 30 | 0 | 0 | HRP [µl] |
| 10 | 20 | 30 | 20 | 0 | DAB [µl] |
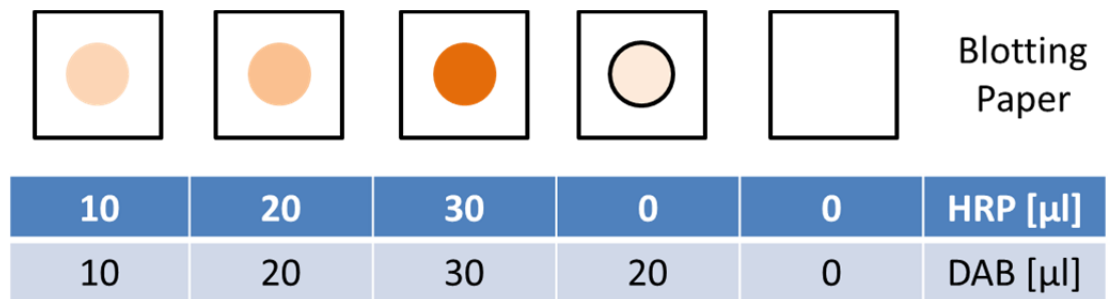
Figure 3-8: Vertical Spot Test DAB and HRP

In total, there are five test spots with varying amounts of HRP and DAB. The first three spots have an increasing amount of both reagents applied on the blotting paper. The fourth spot is a reference spot where only DAB is used to see if the color is different to a test spot with both reagents. This is done to prove that an enzymatic

reaction changed the color, rather than the substrate which gets darker itself as time elapses. The spot without no reagents serves as a reference with which the color intensity of the other spots may be compared. The program which is used to measure the color spots is ImageJ.

3.5   Enzymatic Lateral Flow Test

The results in section 4.3 show that the use of HRP and DAB is more promising because of the more intense color on the white background. The next step in the procedure is to develop a complete ELISA to detect IαIPs which means to transfer the vertical enzymatic test to a lateral flow test.

Vertical tests often need higher concentrations of all reagents; this test was developed by Elain Fu et al. They offer the possibility to Lower concentrations to measure the target analyte.

Therefore a lateral flow test, where 0.6 µl HRP with concentrations of 1/5/10/20/40 µg/mL are immobilized onto nitrocellulose with the pore size of 1.2 µm, is performed. Afterwards 70 µl of the DAB run over the nitrocellulose to create a color change due to the enzymatic reaction. To reduce non-specific binding the channels and the nitrocellulose are blocked with a non-fat milk solution.

After immobilizing HRP onto nitrocellulose the next step is to use the detection AB R21 labeled with biotin instead of HRP. The R21 with biotin is supposed to produce a darker brown color as compared to that of HRP with DAB because of the

amplification action of biotin. As a result, the spot on the nitrocellulose should be darker than the background color.

The next section is concerned with optimizing the concentration of HRP and R21 to receive the best Signal/Background Noise ratio in order to optimize the opportunity to read the signal.

3.6   Optimization of Detection Antibody and HRP

The following section is split into two parts with each part focusing on the optimization of R21 in combination with HRP. In the first section R21 is immobilized onto the nitrocellulose membrane whereas in the second part the detection antibody is attached to the IαIP forming an ELISA sandwich. Both methods need a separate view regarding the optimization of the concentration.

3.6.1   Directly Immobilized R21

The upper part of the ELISA-sandwich consists of the detection AB R21 labeled with the enzyme biotin. The HRP includes a streptavidin component which is can attach to the HRP. When the HRP is connected to the R21 with the help of the streptavidin component, the DAB induces a color change at the HRP molecule. The problem is to find the optimal concentrations of R21 and HRP. The more R21 on the nitrocellulose the darker the color becomes and consequently the spot becomes more blurred with more HRP.

The top part of the ELISA-sandwich consisting of R21/HRP/DAB is simulated in a lateral flow test. Different dilutions of 0.6µl R21 in PBSx1 (5/10/25/50/100%) are

immobilized onto the nitrocellulose with the same procedure as in section 3.5. In addition to varying dilutions of R21 40μ HRP is used in five different concentrations (40/20/10/5/1 μg/mL). Since the procedure to fabricate the DAB substrate is fixed to certain concentrations, a constant volume of 40μl is pipetted onto each spot.

The exact concentration combinations are displayed in Table 3-2. Each test chip has a set of five dilutions of R21 and one concentrations of HRP.

Table 3-2: R21 and HRP tested concentration	
HRP Concentration [μg/mL]	Dilution of R21 [%]
40	
20	
10	100/50/25/10/1
5	
1	
0 (Negative Control)	

Afterwards the intensity of the color spot is measured where R21 is immobilized and divided by the color intensity of the nitrocellulose's background. The intensity of the R21 spot is lower because the spot is darker and the background is usually lighter which means a higher intensity. Therefore the lower the result the better the signal to noise ratio, this follows vice versa.

3.6.2   R21 in a sandwich ELISA

The detection antibody is released from the conjugate pad as soon as it comes in contact with the analyte with IαIP. The sandwich of capture AB, IαIP and detection AB becomes visible when DAB and HRP (with streptavidin) create a brown color.

In this case, the R21 is not dried onto the nitrocellulose but stored in the conjugate pad. Using the results of section 4.6 six different concentrations of detection antibody in the 20wt. % Sugar Solution are tested to determine which concentration provides the lowest signal to background noise ratio. The concentrations are presented as ratios of the initial solution 1/5/10/25/50/100 µg/mL because the exact concentration of the stock solution was not known.

After the best R21 dilution rate is determined various HRP concentrations are used to lower the background color and to strengthen the intensity of the brown color detection spot.

3.7 Optimization of Conjugate Release

The detection antibody R21 is stored in the conjugate pad. Fridley et. al. [24], Gerbers et. al. [19] and Föllscher et. al. [18] showed different strategies to facilitate the release of stored antibodies in paper e.g. varying pad sizes, materials and sugar concentration as well as several blocking steps. These experiments are conducted using the new detection antibody R21 with biotin.

The lengths of the conjugate pads are varied to 4x5mm and 5x5mm. These two pads are blocked using 10µl of Non-Fat Milk blocker and dried at 37°C on hot plate. The Non-Fat Milk blocker is produced by mixing 1.1g of Non-fat Milk powder in 22g of PBST. Afterwards, they are treated using 10µl of a 20 wt.% sugar solution with trehalose and sucrose in Non-Fat Milk blocker. In the sugar solution the concentration of R21 is kept constant 20vol. % and again dried on a hot plate at 37°C.

Afterwards, 10 µl of 7 µg/mL of HRP is applied onto the conjugate pad so that the HRP can connect to biotin on the R21. The next step is to wash out the HRP and with the R21. Therefore at first 40µl of PBSx1 solution is applied onto pad. Next apply 30µl of PBSx1 after moving the pad to the next spot on the blotting paper. Finally four more additional washing steps are conducted with 20µl of PBSx1. The same procedure is repeated for different materials (glass fiber with binder/without) but regarding blocked pads and pads without blocking the first blocking step is not conducted when a non-blocked pad is tested. To induce the color change 10µl of DAB are pipetted onto each spot where the conjugate pad is washed out. The detailed amounts of fluids used are displayed in Table 3-3

Table 3-3: Detailed Treatment of Conjugate Pads					
Treat	Blocking 10µl	Sugar with R21 10µl	HRP 10µl	PBSx1 1x40µl 1x30µl 4x20µl	DAB 10µl
4x5	x				
5x5	x				
Binder	x				
w/o binder	x	x	x	x	x
Blocked	x				
w/o blocking					

Besides geometry and blocking steps, Fridley et. al. [24] showed that sugar can facilitate the release of antibodies from the conjugate pad. Therefore different sugar concentrations are tested. Trehalose and Sucrose as well as a mixture of these two

reagents are tested. Trehalose and Sucrose are tested in varying wt. % of 1/2/5/10/20 and the mixture of both in 5/10/20 concentrations.

The conjugate pads are also blocked with 10µl of Superblocker and dried at 37°C on a hot plate. Afterwards 10µl of the tested sugar solution is applied on the pad in which 20vol. % of R21 is present and dried once again. The conjugate pad is treated with HRP before it is placed onto the blotting paper. Then it is washed with 120µl of PBSx1 in 10µl steps. Finally 30µl of DAB is applied onto the spot where the antibodies should be washed out.

3.8 Optimization of capture antibodies

In order to enable the highest possible sensitivity the stock solution of capture antibodies were used for preparation of the detection area.

3.9 ELISA standard curve

The final goal is it to produce a standard curve in which the concentration of IαIP is plotted over the intensity of the color spot. Therefore it is important for the test to operate in the range of the natural concentration of IαIP in the blood which is around 400-800 µg/mL and further more at lower concentrations similar to cases when sepsis is present. The limit of detection in the case of a sepsis test is not the first priority, since the concentration of this protein is high compared to other ELISA analytes leaving the LOD to be a less significant factor.

Experiments are performed with varying IαIP concentrations. Since the stock solution has a concentration of 240µg/mL various dilutions will be tested.

3.10 Effects of chemical Valve Reagents in the ELISA Test

As previously discussed the valve technology involves the use of certain chemical reagents like A3CS and FC-72 which are used for the hydrophobic layer and Tween 20 and Ethanol for manufacturing the surfactant paste. Since biological testing is performed on the chips, the effects of these chemicals on the biology need to be evaluated. Therefore concentrations used for the calibration curve are repeated without using of valves. The reagents are applied manually by hand onto the chip. The signal intensity for both cases (using valves/ not using valves) is measured and compared.

4   CHAPTER 4 - FINDINGS

4.1   Influence of the viscosity of the opening times

The results of the experiments on the opening times of the valves with respect to different plasma-buffer concentrations can be seen in Figure 4-1.
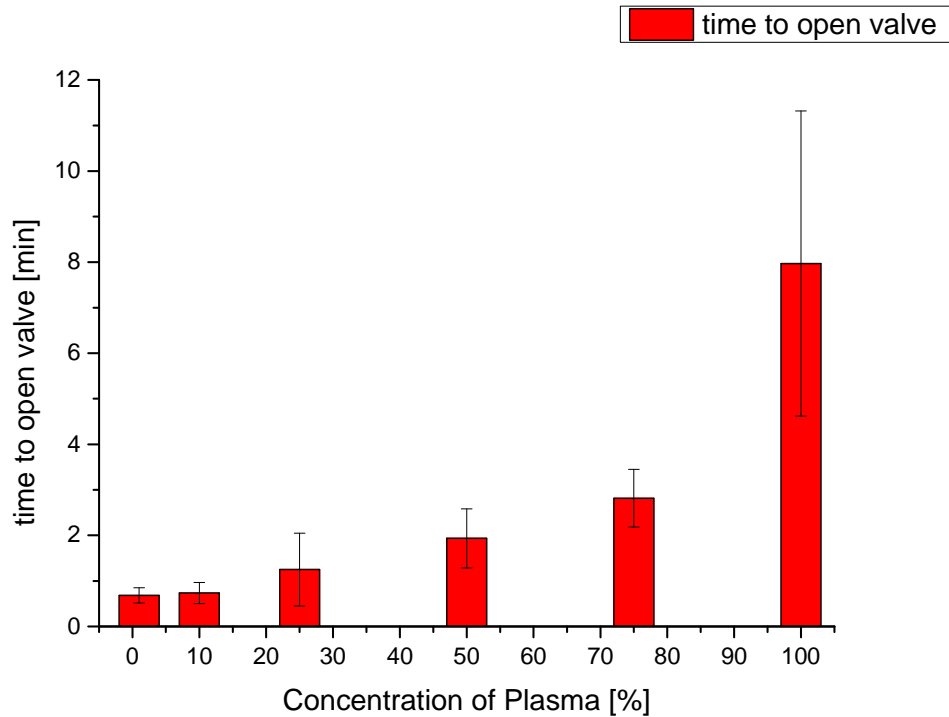
Figure 4-1: Opening Times for various plasma in buffer concentrations

The opening time of the valve changes with respect to the amount of concentration of blood plasma in buffer. The higher the concentration of buffer is correlated with a shorter opening time of the valve. Pure blood plasma needs around 8 min to open the valve whereas diluted blood plasma takes around 2min. The conclusion is that the opening time of the valves is dependent on the concentration of blood plasma in buffer. In other words, the opening time is related to the viscosity

of the solution because pure plasma is not as viscous as diluted plasma. According to Kamke et. al. [64] Blood plasma has a viscosity of 1.8η at 20°C whereas the viscosity of PBS-buffer is much smaller. The theoretical assumption that more PBS-buffer decreases the viscosity and therefore shortens the opening time was confirmed. Further experiments have to show how much blood serum is needed to get a clear color spot in the detection region.

4.2 Trypsin immobilization

The color change was confirmed when putting trypsin and BAPNA together in viles. The results are pictured in Figure 4-2. The left vial contains only trypsin and the right vial is the reacted product.

Figure 4-2: Color change in a vial using trypsin and BAPNA

It can be seen that there is a color change in the right vial. Trypsin changes its color from clear to a bright yellow. This proves that when the two reagents are brought together in solution a color change happens.

70

In Figure 4-3 the immobilization on nitrocellulose and blotting paper is illustrated. The nitrocellulose paper circles are in the upper part of the picture and the blotting paper circles are in the lower part. These circles have a diameter of 5mm.

Figure 4-3: Immobilization of Trypsin on Nitrocellulose (Top) and Blotting Paper (bottom)

It can be seen that there is a slight color change at the outer ring on the nitrocellulose. This phenomenon is known as the coffee ring effect. The solid particles in this case trypsin are left over after the liquid evaporates. They form a ring pattern which is visible after BAPNA gets in contact with trypsin as shown before. The color change is not as strong as it is on the blotting paper where a clear color gradient is visible. This is because of the smaller amount of fluids which are used during testing. Of course the more trypsin that is immobilized on the paper will increase the intensity of the color signal.

Besides immobilizing trypsin onto nitrocellulose and blotting paper Figure 4-4 shows the results of the attempt to immobilize trypsin onto glass fiber membrane filters with and without binder.
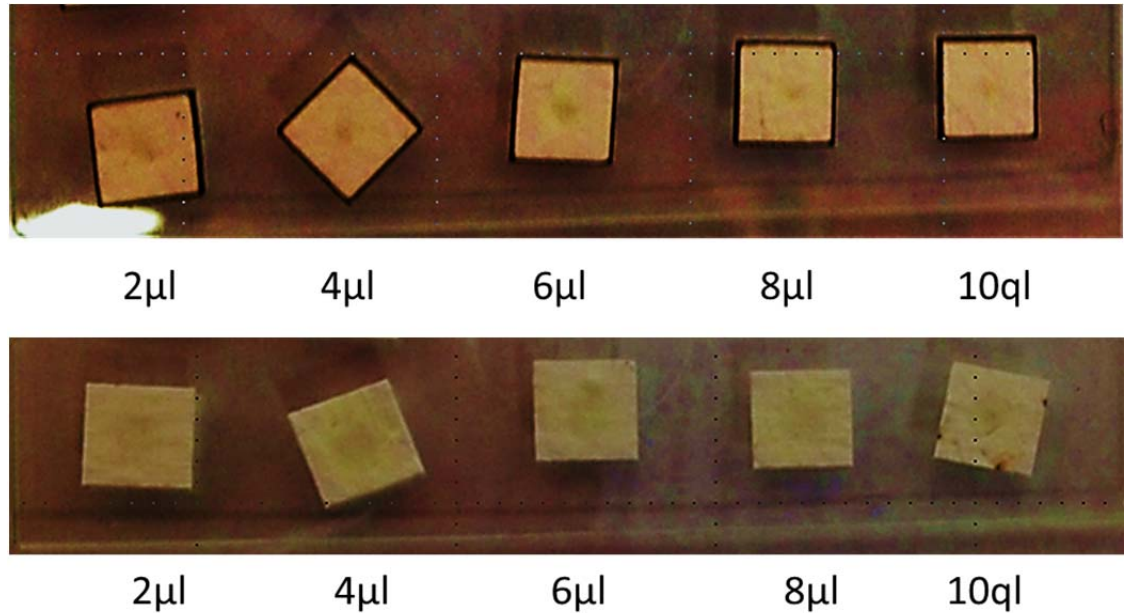
Figure 4-4: Trypsin Immobilization onto Membrane Filter without (top) and with (bottom) Binder

The amount of Trypsin increases from left to right but the volume of BAPNA is kept constant at 12μl. The BAPNA is applied after the spot where trypsin is applied completely dried out. This prevents the reaction from taking place in a wet environment because trypsin is supposed to be dried onto the nitrocellulose membrane.

The Glass Fiber Membrane Filters on which trypsin and BAPNA come together are supposed to have increasing color intensity. More trypsin that is on the membrane will create a stronger signal.

Unfortunately, the color change is not very clear since the light yellow on white paper can barely be seen which makes it hard determine a color change. For this reason, the alternatives of DAB and HRP were investigated.

4.3   Vertical Test DAB

The vertical test is performed to show that the enzymatic reaction of DAB and HRP is possible on paper. The findings are pictured in Figure 4-5 and mathematically analyzed in Figure 4-6.
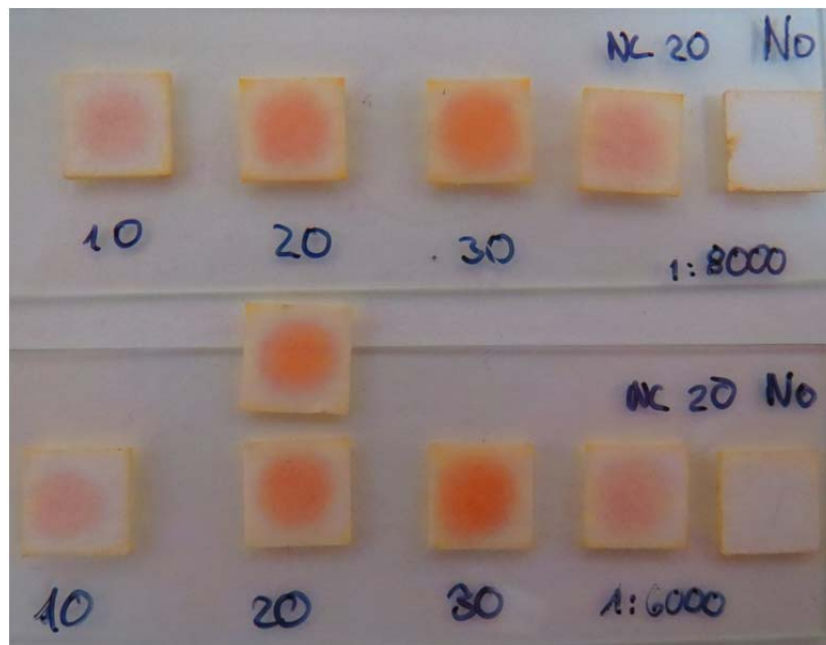

Figure 4-5: DAB Vertical Test

Two concentrations are used for the HRP 1:6000 (bottom) and 1:8000 (top). The color is slightly stronger using the higher concentration of HRP. The negative control without HRP but with 20µl of DAB is lighter than the spot where 20 µl of both reagents are used.

The intensity is measured using ImageJ and compared with the standard white blotting paper to have a reference. The results are plotted in Figure 4-6.
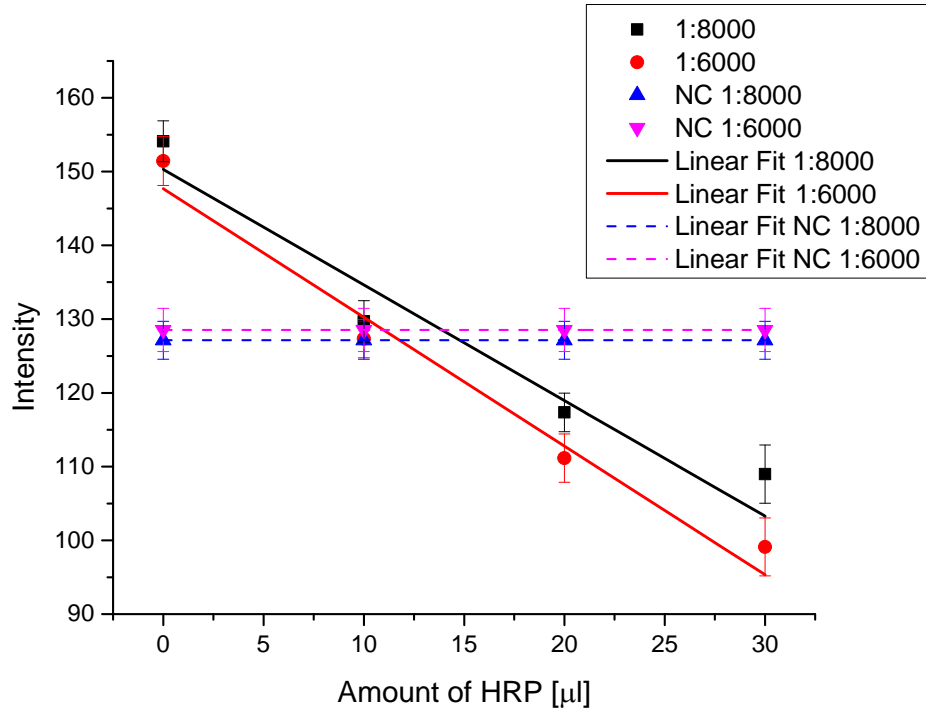
Figure 4-6: Vertical Test DAB 1:6000/8000

It can be seen that the intensity of the color spot is decreasing with an increasing amount of the two reagents. The 1:6000 curve is lower than the 1.8000 curve because a lower intensity corresponds to a darker spot. Since the concentration of HRP is higher in 1:6000 the DAB has more molecules where a color change can happen. The negative control where only DAB is pipetted on the spot is necessary because the DAB substrate itself has a light brown color. Even when there is no HRP the color spot becomes light brown. Due to the enzymatic reaction the color spots gets darker than without the HRP. As one can see the 20µl negative control line has a higher intensity in both cases as compared to the combination of

20µl HRP and 20µl DAB. This proves that there is an enzymatic reaction on the blotting paper.

4.4   Enzymatic Lateral Flow Test

The results of the enzymatic lateral flow test where HRP is immobilized onto nitrocellulose are illustrated in Figure 4-7. A constant volume of 70 µl DAB is pipetted onto each spot.
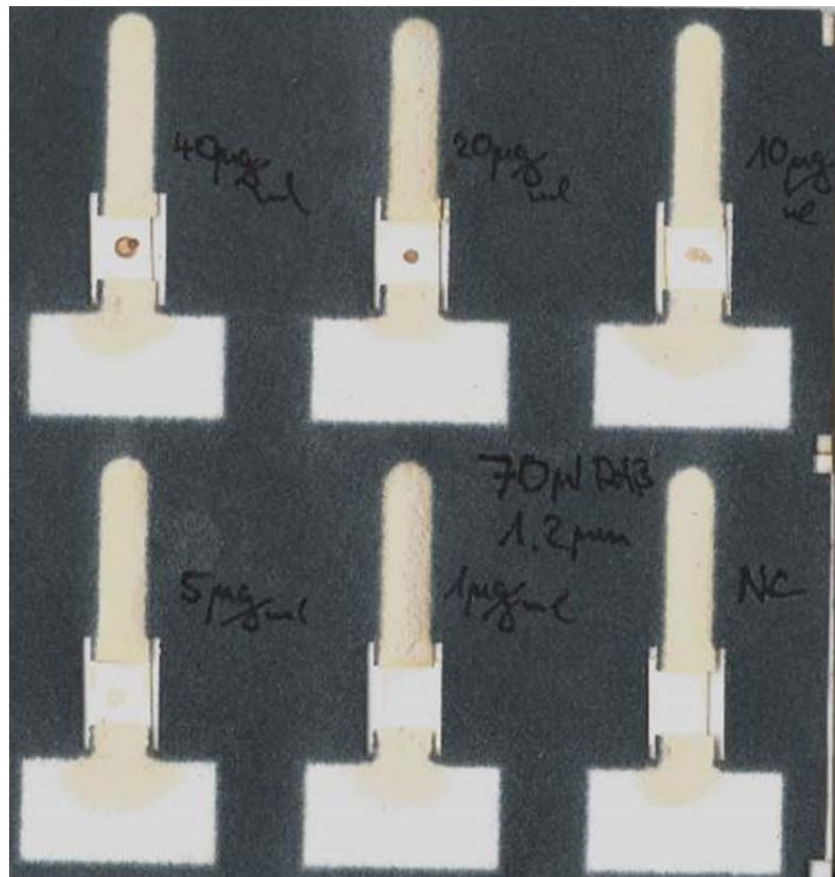
Figure 4-7: Lateral Flow Test Immobilized HRP

The presence of a dark brown color spot proves that it is possible to immobilize HRP onto nitrocellulose. Higher concentrations of HRP result in darker color spot on the nitrocellulose because there is more opportunity for DAB molecules to react with

HRP. The brown color on the channels arises from the substrate DAB which flows down these channels to reach the detection membrane. DAB has a light brown color even when there is no enzymatic reaction.

Besides HRP, R21 with biotin is immobilized onto nitrocellulose. Figure 4-8 shows the results of the lateral flow test.
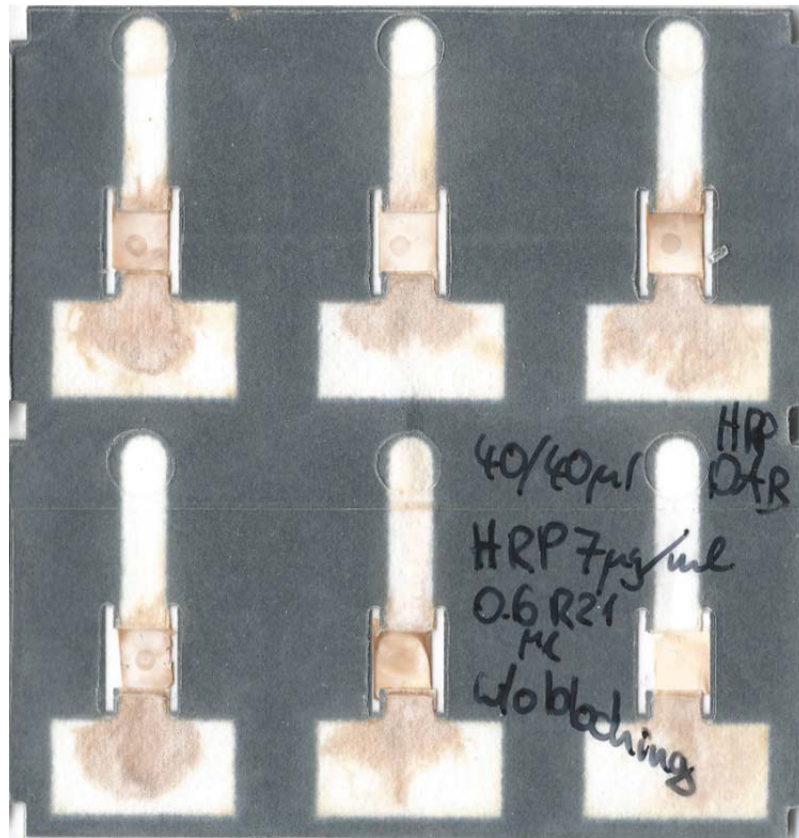
Figure 4-8: Immobilization of R21 onto Nitrocellulose

It is evident that R21 immobilization is successful. The color spot where the ABs are immobilized is darker than the rest of the nitrocellulose. Even though the background color is relatively high compared to the signal itself but it is still visible to the naked eye.

4.5 Optimization of Detection Antibody and amount of HRP

First the optimized concentration of R21 is presented and second the improved concentration of R21 stored in the conjugate pad is presented. Additionally the concentration of HRP is enhanced as well.

4.5.1 Directly Immobilized R21

The color intensity of the signal spot vs. background is measured for all five chips using the software ImageJ. The inverse of Signal/Background is plotted over the concentration of HRP in Figure 4-9.
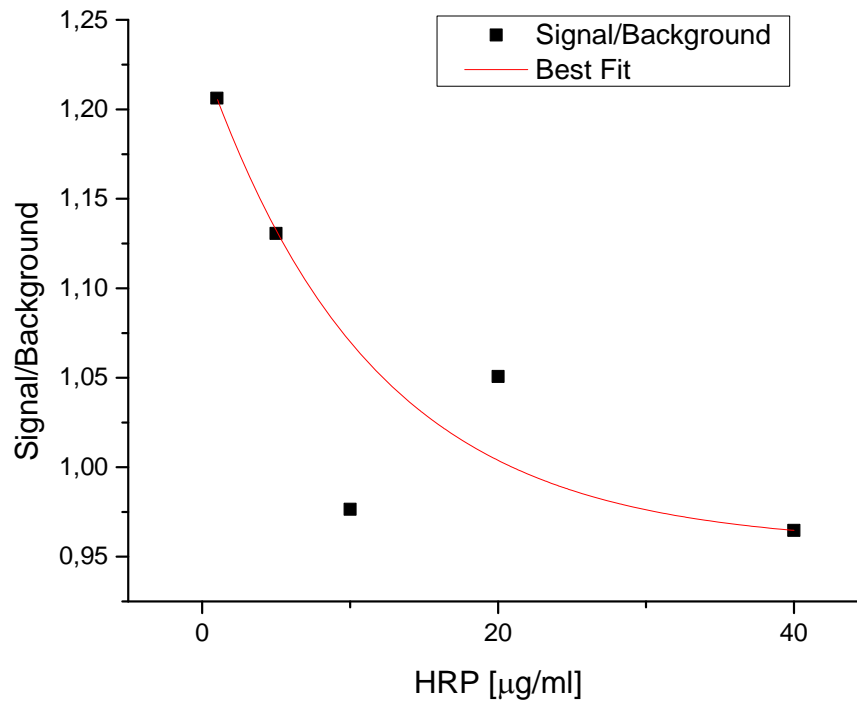
Figure 4-9: Optimization of R21 and HRP Signal/Background curve

The graph shows that the lower concentrations of HRP in PBS result in better Signal to noise ratio on the detection spot. This result is logical since lower amounts of HRP on the background of the nitrocellulose result in less color induced by DAB. However, there comes a point when the amount of HRP is too low to create a strong enough signal on the color spot over that of the background. At this point the curve decreases again. Future studies can optimize this topic. Besides the amount of HRP, the dilution factor of R21 is optimized. Since *ProThera Biologics©* produce the detection AB by tagging the enzyme biotin onto the AB they can't tell the exact concentration anymore. Therefore a dilution is more suitable than trying to determine the concentration. Only one vial with detection antibody is used otherwise there also might have been variation in the concentration in a batch of R21. In Figure 4-10 the Inverse of Signal to noise is plotted over different dilution factors of R21 in PBSx1.
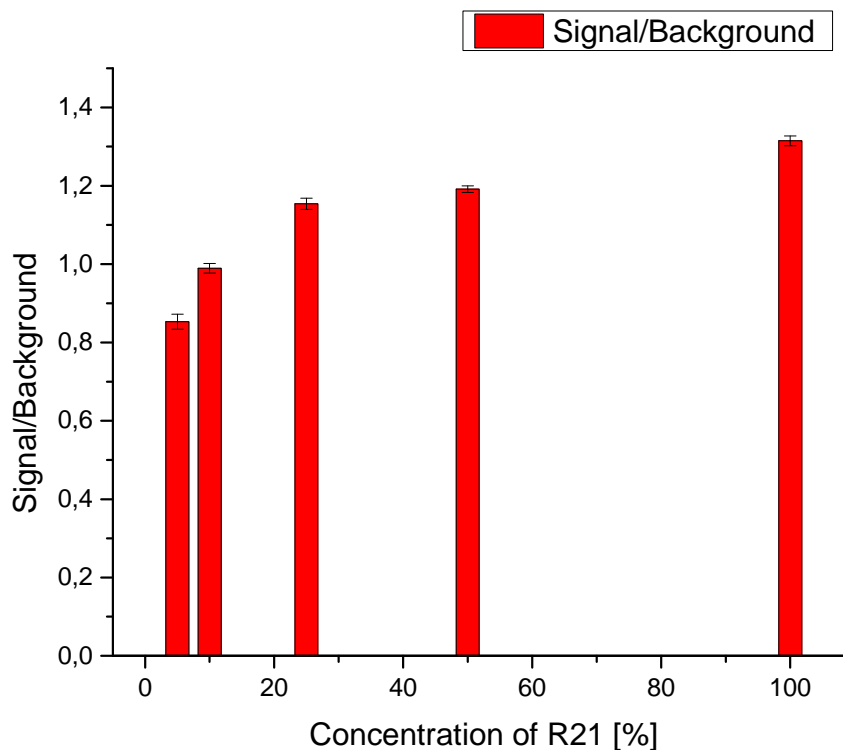
Figure 4-10: Optimization of detection antibody

The graph shows that the lower the concentration of R21 in PBSx1 has a better signal to noise ratio as the graph is slightly increasing. However, it cannot be determined if the optimal concentration of R21 is the non-diluted detection AB itself or if the signal can be improved later on by producing a higher concentrated detection AB.

4.5.2 R21 in a sandwich ELISA

Five different concentrations of HRP are tested to evaluate which is the most effective dilution for the ELISA test. The proportion of Signal to Background is plotted in Figure 4-11 over the concentration.
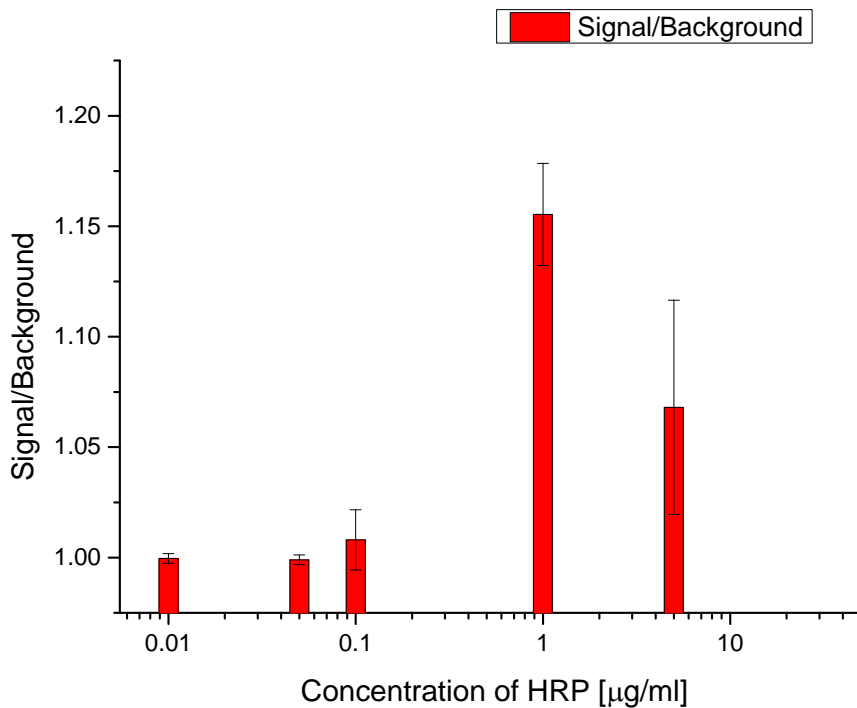
Figure 4-11: Optimization of HRP complete ELISA

The concentration of 1µg/mL has the best signal to noise ratio whereas the two results of the of the lowest concentration correlate to a spot which is almost invisible due the dark background.

Various amounts of detection antibodies diluted in the sugar solution are stored in the conjugate pad to be washed out from the analyte which is IαIP in PBSx1. The results regarding the optimal signal to background proportion are displayed in Figure 4-12.
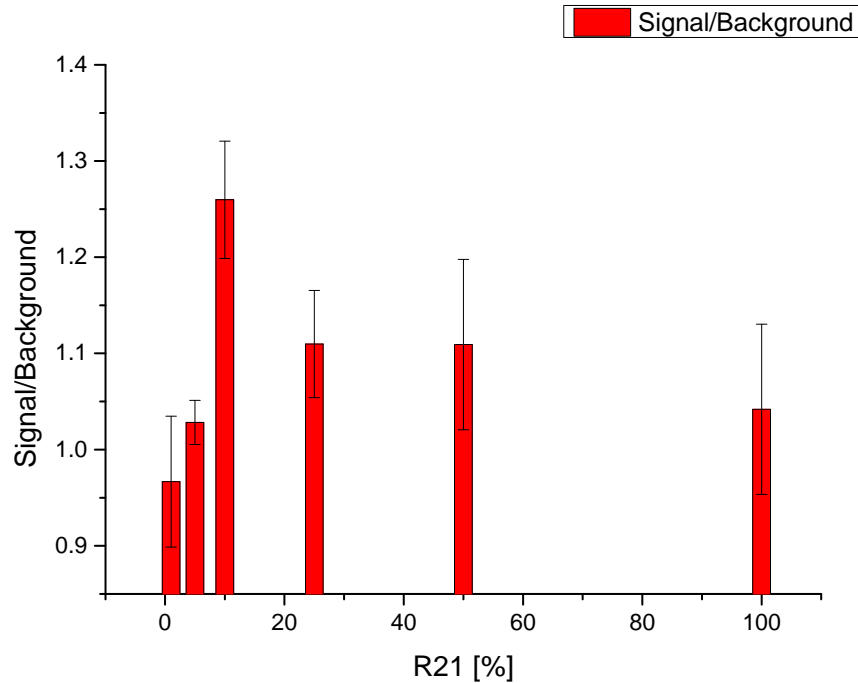
Figure 4-12: Optimization of R21 in the conjugate pad

It can be recognized that the optimal concentration of R21 in the sugar solution is 10µg/mL. This dilution provides the best Signal to Background proportion which means that the intensity of the signal is strong but the background intensity is low in comparison.

4.6 Optimization of Conjugate Release

The results of the conjugate pad release optimization are displayed in Figure 4-13 to Figure 4-16. Different materials, sizes and chemical treatments as well as sugar blocking are tested in order to find the best design and pre-treatment of the conjugate pad used in the PBV.

In Figure 4-13 the findings of two different pad sizes are illustrated. It can be clearly seen that the 4x5mm conjugate pad releases the R21 detection antibody

faster than a 5x5mm pad. The amount of fluid to wash out the antibodies is around

90µl for the small pad and around 150µl for the larger conjugate pad.

Size	40µl	30µl	20µl	20µl	20µl	20µl
4x5						
5x5						
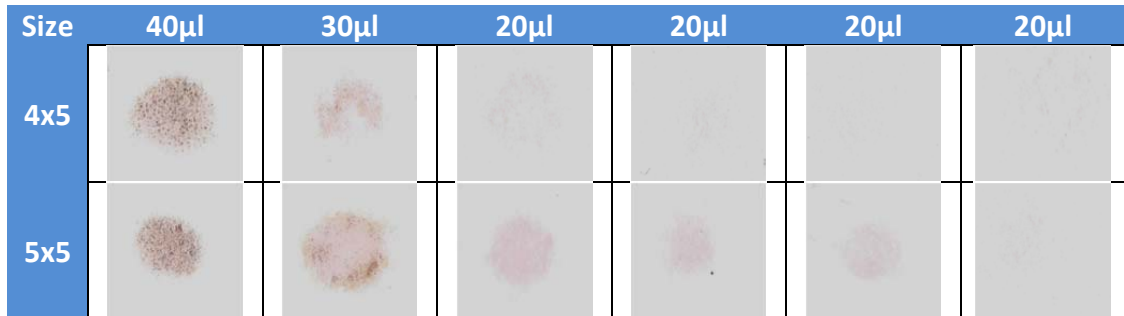
Figure 4-13: Different sizes of Conjugate Pads

One explanation for a better release of a smaller pad is the lower amount of

non-specific binding of the detection antibody because the surface area is smaller in

comparison to a larger conjugate pad. The R21 cannot connect to as many paper

fibers as in the 5x5mm pad. Furthermore, the geometry of a quadratic conjugate pad

may affect the fluid flow more than just a rectangular shaped pad. The

miniaturization of a conjugate pad is limited because a smaller pad is more difficult to

handle in the assembly process. Therefore the chip is fabricated with a 4x5mm

conjugate pad.

Figure 4-14 shows the impact of a blocking step before applying the 20 wt.%

sugar solution with detection antibody on the conjugate. The figure shows that the

detection antibody is released much quicker from the blocked pad than from the one

without a blocking step.

Treated	40µl	30µl	20µl	20µl	20µl	20µl
w/o blocking						
blocked						
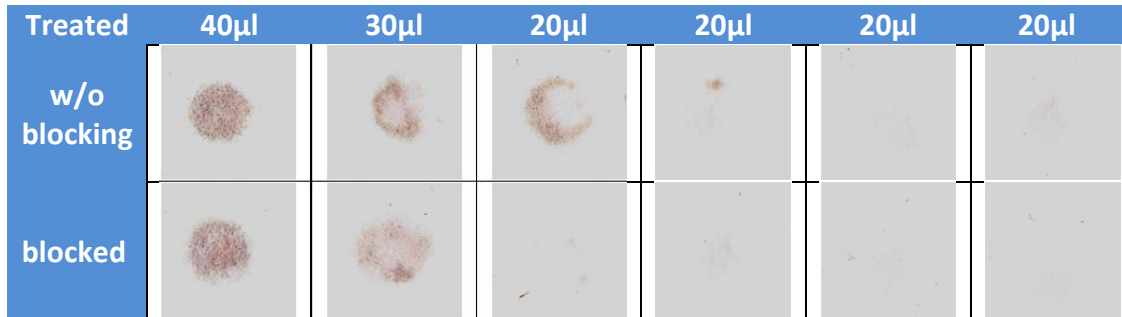
Figure 4-14: Different blocking of Conjugate Pads

The blocking step prevents antibodies from binding to a surface which improves the signal to noise ratio as well as the release of antibodies. No interaction with the conjugate surface facilitates their release.

The next test is performed using conjugate pads with and without binders (Figure 4-15). The paper with binder releases the detection antibody much better than the paper without binder. The prevention of non-specific binding in the conjugate seems to be an appropriate way to facilitate antibodies release.

Treated	40µl	30µl	20µl	20µl	20µl	20µl
w/o binder						
With binder						

Figure 4-15: Different Conjugate Pad Materials

The use of sugar e.g. trehalose and sucrose facilitates the release in conjugate pads enormously. Therefore, five different concentrations and three different mixtures are tested. The results are displayed in Figure 4-16.

Wt. %	Trehalose		Sucrose		Mix	
1						
2						
5						
10						
20						
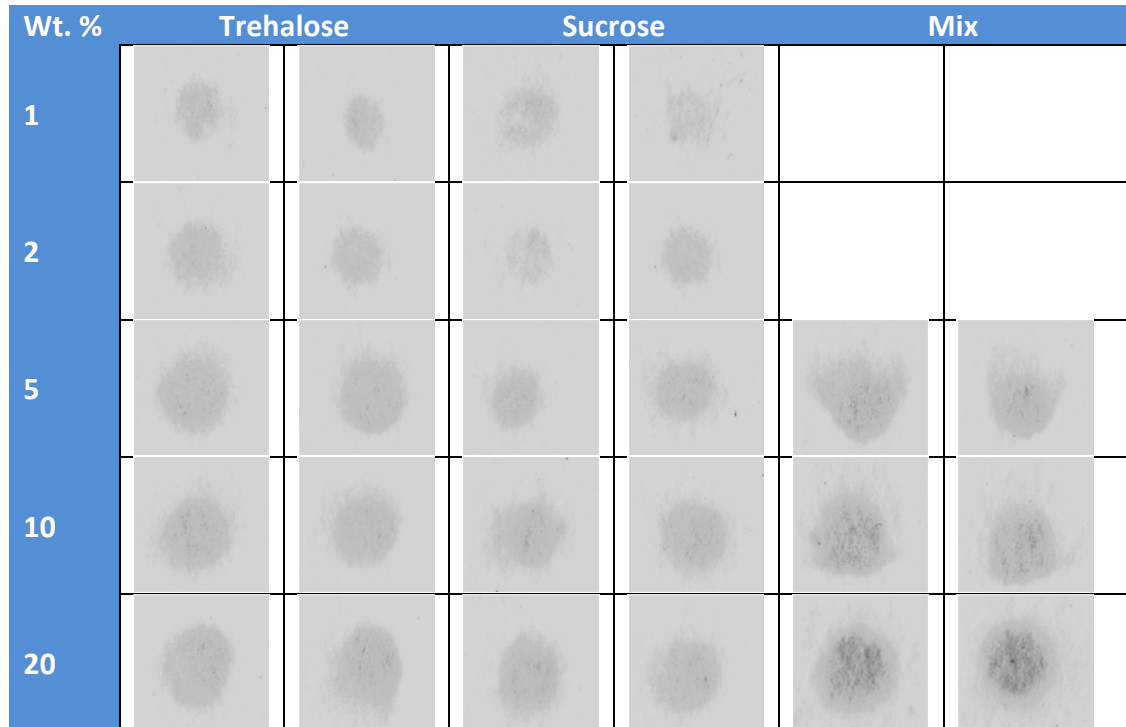
Figure 4-16: Conjugate release using varying sugar concentrations

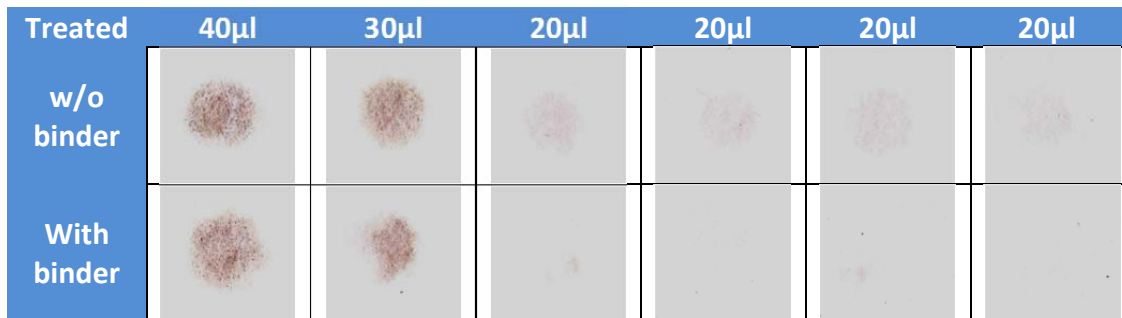The 20wt. % mixture of the two sugar components seems to have the best improvement regarding the color intensity of the spot. This means a good release of the antibodies. Nevertheless the intensity of the color spots is very low which let to use a greyscale picture in order to determine the best result more easily.

Stevens et. al. [48] remarked that trehalose and sucrose molecules substitute for the water hydroxyl groups which are lost after drying. When fluid runs over the dried proteins hydroxyl group re-substitute for the sugar again allowing for a higher yield in releasing the proteins.

ImageJ is used to determine the mean intensities of the color spots. The intensities are plotted over the sugar concentrations in Figure 4-17. Additionally curves are calculated to the fit in the best way.
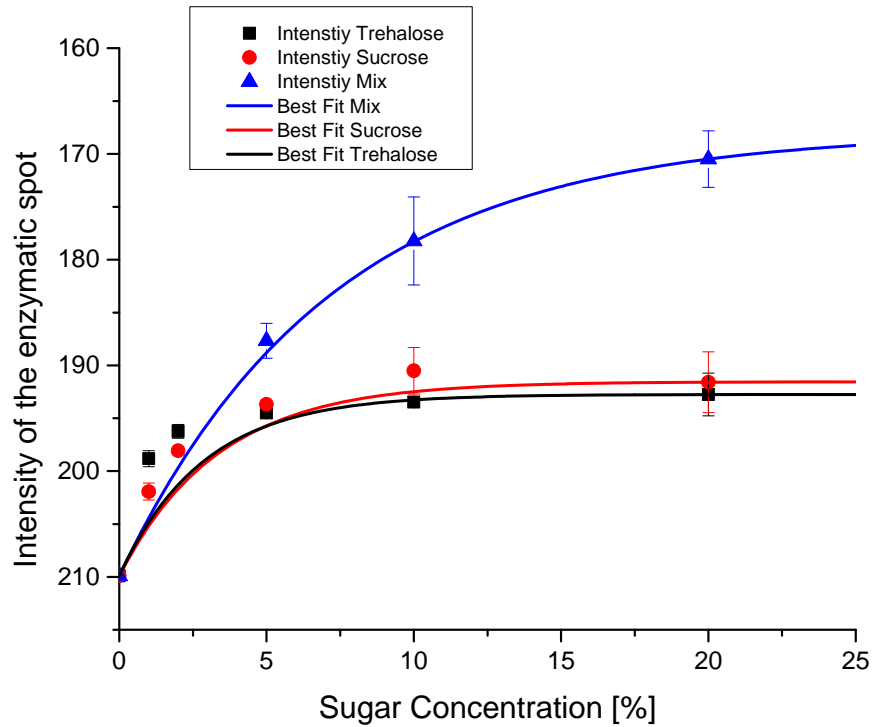
Figure 4-17: Optimization of varying sugar concentrations

The non-linear fit for the trehalose/ sucrose mix is illustrated in equation (4).

$$y = 41.98 \, e^{\left(\frac{-x}{7.15}\right)} + 167.92 \tag{4}$$

This equation is used to calculate the intensity for a theoretical optimal sugar concentration. At the point of the optimal concentration, the x-value becomes 100 assuming that the pure sugar mixture is used. This value is compared to the value of a 20wt. % sugar solution. The improvement is around 1.5%.

X=20	X=100	Improvement [%]
170.487	167.926	1.502

The sugar solution is restricted to amounts higher than 20wt. % otherwise the fluid is very viscous which makes it hard to handle this solution which led to the decision to use a 20wt. % sugar solution.

4.7 Proof of Concept

To prove the concept of a fluidic circuit which is capable of loading fluids sequentially, a chip is run with food color. The picture sequence in Figure 4-18 proves that two fluids are sequentially loaded.

| T=0s | T=30s | T=60s | T=300s | T=310s | T=600s |
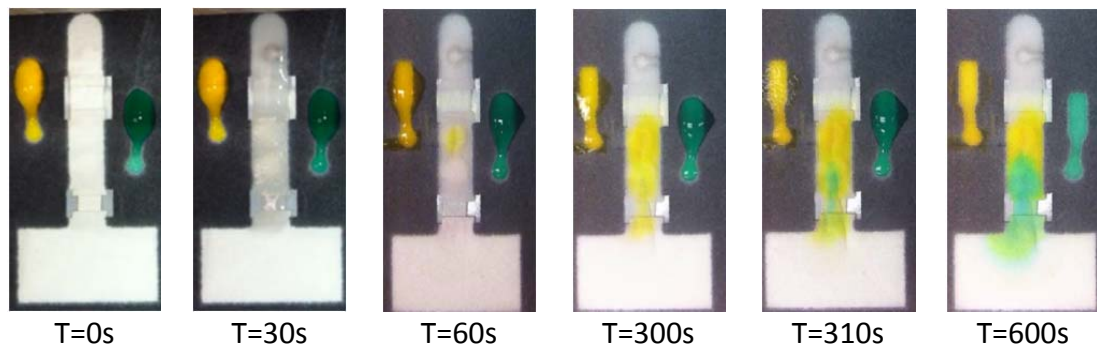
Figure 4-18: Sequential Loading of the Fluids

The two reagents (yellow and green food colored water) which need to be triggered are stored in the two inlets beside the main channel. The valves hold the reagents back until the surfactant is dissolved. Next, the sample is applied on the main spot. It runs down the main channel as well as into the second layer. Dissolving the surfactant the yellow reagent comes up first to the main channel and runs down to the absorption area and second, the green reagent is triggered in the same way. It can be seen that the fluids are triggered in the correct sequence. This ensures that later on the whole amount of reagent can react with the test spot.

4.8   Complete ELISA test

Figure 4-19 shows that the ELISA test is working because a brown dot is visible on the detection membrane. The bottom right corner of every batch of six chips is the negative control where no capture antibodies are immobilized onto the nitrocellulose membrane. No color spot is visible.
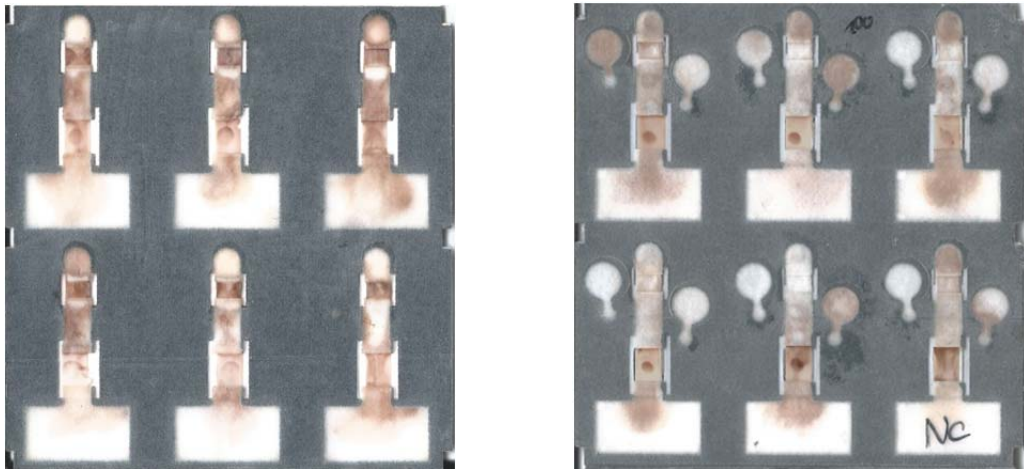
Figure 4-19: ELISA test

In case of the left chip the reagents are pipetted manually onto the chip whereas the right chip is run without any interaction after the reagents were applied onto the chip. The next step is to use varying concentrations of IαIP to create a standard curve.

4.9   ELISA standard curve

In Figure 4-20 the Signal Background proportion is plotted over different concentrations of IαIP. The lower the concentration of IαIP is the lower is proportion of Signal to Background.
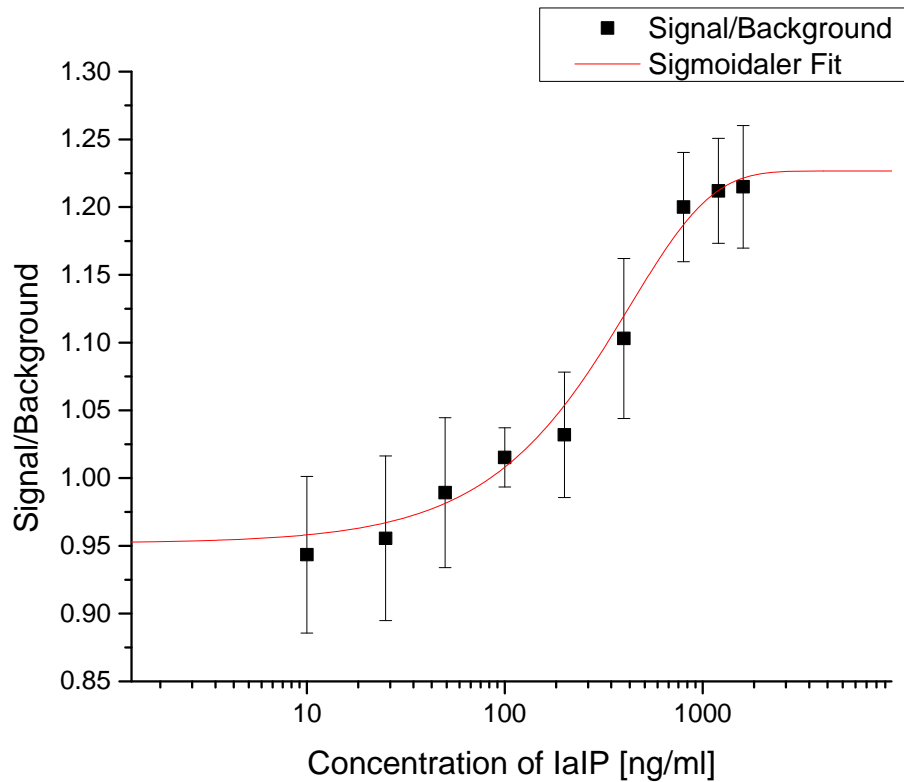
Figure 4-20: IαIP Standard Curve

This curve makes it possible to run a paper based ELISA with IαIP. After estimating the intensity of the detection spot and the background the curve makes it possible to find the concentration of the analyte. The concentrations which are used to create the standard curve are in a range of 800 to 25 ng/mL, but in the human body the concentration is around 800 to 200 μg/mL. In this study of IαIP LOD is not the primary goal to find because the concentration of the test analyte is three orders of magnitude lower than the actual concentration of IαIP in human blood.

Table 4-1 show the decreasing intensity of the ELISA sandwich spots (brown dot). An ELISA sandwich cannot be formed without IαIPs which means a lower

concentration results in a less intensive color spot because unbound detection antibodies are washed away. The detection antibody itself cannot bind directly to the capture antibody 69.26. The products of the enzymatic reaction are rinsed into the absorption area.

Table 4-1: Detection Spots						
	800	400	200	100	50	25
c(IαIP) ng/mL						

4.10 Effects of chemical Valve Reagents in the ELISA Test

The proposed standard curve is produced with the paper chip with its fluidic valve technology which autonomously triggers the reagents when they are needed. All of the reagents are applied manually on the chip at the right time. The obtained results are the same.

5   CHAPTER 5 – CONCLUSION

The experiments show the development of a paper-based device which is able to perform an ELISA autonomously after the reagents needed are applied onto the device. The transfer from a microtiter-plate ELISA onto paper is proved. All criteria of POC device e.g. low cost, low fluid volumes, sustainable and rapid testing are met. The overall test time for microtiter-plates which is around several hours is reduced to minutes disregarding the assembly process of the device itself.

Research is conducted regarding LOD, optimal assay concentrations as well as reproducibility. Starting from simple spot test with two different approaches (BAPNA and trypsin or HRP and DAB) the more promising HRP and DAB enzymatic reaction was chosen. The ELISA is split up into single parts which are conducted successfully on their own. The conjugate release is optimized using different materials, sizes as well as a sugar solution which facilitates the release of the detection AB. Afterwards all parts were put together to perform a complete ELISA on paper.

The final result is a standard curve where the intensity of the ELISA result in form of a color spot is plotted over the concentration of IαIP in a buffer sample..

5.1   Recommendation and Future Work

In the following abstract future directions of research are discussed to improve the usage of paper based microfluidic devices in biological testing. So far microtiter plates still have a lower limit of detection. The goal is to produce a paper chip which has the same LOD as a 96-well ELISA. Besides improvements regarding parts of the

chip a different method to detect the concentration of IαIP is presented. In the case not an ELISA but an enzymatic test is conducted. The advantages are that the color difference of two detection areas is measured to determine the amount of IαIP by referring the concentration to the color intensity difference.

5.1.1   Two Way Circuit

Besides the presented ELISA test further experiments should be conducted using trypsin and BAPNA to perform not an ELISA but an enzymatic assay. In Figure 5-1 the schematic of the enzymatic assay reaction is illustrated. The reaction takes place on the nitrocellulose of the chip. In the first step trypsin (blue tile) which represents the capture antibody is immobilized on the nitrocellulose membrane (gray-shaded area).
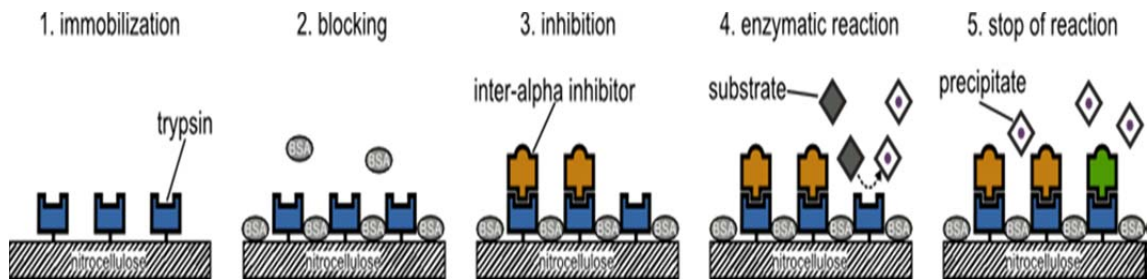
Figure 5-1: Schematic of the enzymatic assay for the detection of IαIP's

Due to the electrostatic forces of the membrane trypsin can easily be bonded onto the surface. Trypsin is only applied in the center of the detection spot so that most of the membrane is not covered with trypsin and is still active. These areas have to be blocked with the blocking reagent bovine serum albumin (BSA) (grey circles) to inactivate them in the second step. After that other proteins cannot bind to other

91

regions but can connect to the trypsin. As previously discussed antibodies or antigens can only bind to the specific counterpart of themselves with respect to the key-lock principle. In the third step the sample runs over the detection area and IαIP's (brown tiles) can bind only to the immobilized trypsin. In the next step, a chromogenic substrate (BAPNA) runs over the membrane (grey hash). This causes a color change of the detection spot to yellow. The more IαIP's connects to the trypsin the lower the color intensity of the spot becomes because less substrate can bind to free trypsin particles. Finally a stop solution such as Basic Pancreatic Trypsin inhibitor (BPTI) flows over the test spot (white dotted hash) and deactivates the remaining enzymes and quenches further development of the color change. This step can be left out since the chip stop its reaction when all fluid ran over the detection spot.

The developed two way circuit has two ways and in total three nitrocellulose spots: Two detection membranes and one filter membrane. The detection membranes work as discussed before. The filter membrane is different because it has monoclonal antibodies 69.26/69.31 instead of trypsin immobilized on the nitrocellulose to capture only IαIP's. The two detection areas should develop altering intensities because on one side no IαIPs are presented anymore since they are filtered on the monoclonal antibody nitrocellulose. Figure 5-2 illustrates the proposed two way fluidic circuit which is able to compare two samples.
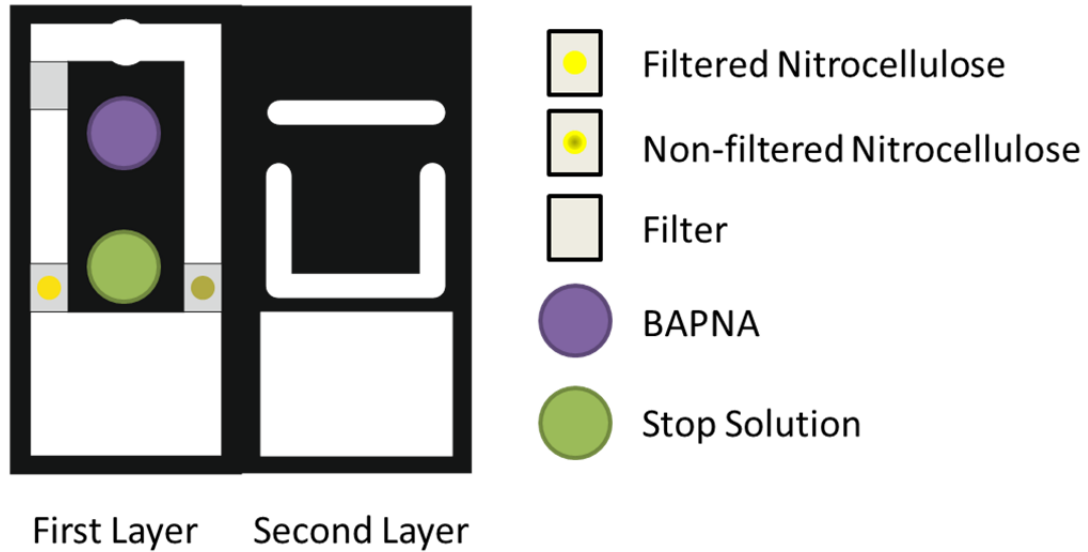
Figure 5-2: Two Way Circuit using Trypsin and BAPNA

The solution with IαIPs is applied on the top spot of the chip. It divides its flow-One part of the solutions runs over the Filter and later on to the Detection Area. The other flows down directly to the Nitrocellulose. Meanwhile the surfactant part of the valves which are positioned under the two fluid storage area are reached. The fluid opens the valves as soon as the complete solution runs over the chip. BAPNA connects to the remaining immobilized trypsin particles and induces a color change. The more IαIPs are present on the nitrocellulose the less intensive is the signal. Therefore the yellow on the filtered spot should be brighter than on the unfiltered spot. Optional is the stop solution which ends the enzymatic reaction but this step might be eligible to be left out. Instead a wash step could be added to produce a clearer signal. The detailed flow of the fluids is shown in Figure 5-3. Due to the symmetry of the chip the fluid flow is displayed on only one side of the chip.
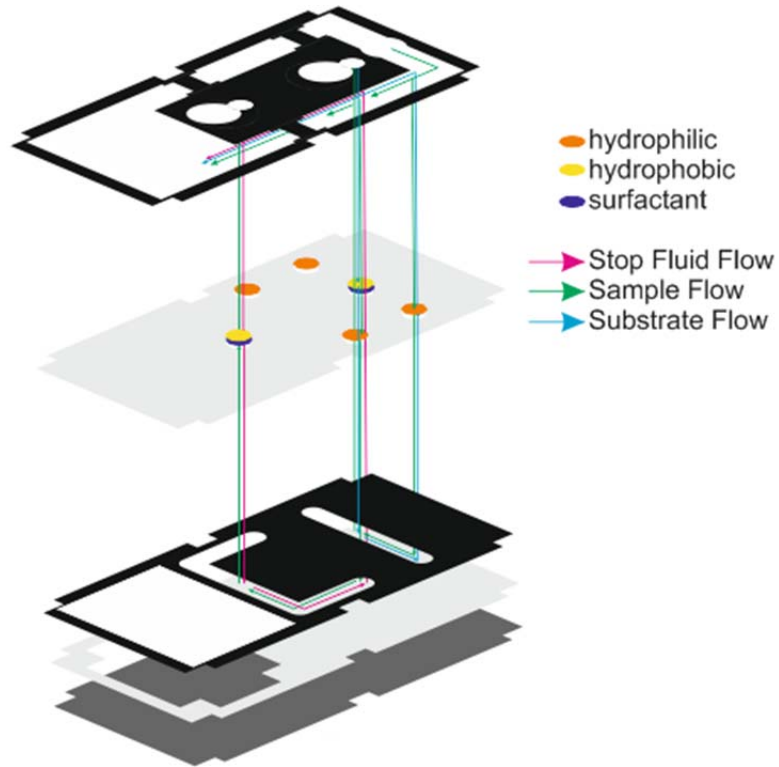
Figure 5-3: Two Way Circuit Detailed Flow

Gerbers et. al. [19] and Föllscher et. al. [18] figured out that the yield of the chips is increased when they are placed in a housing. Connections between different materials of the chip are facilitated. Figure 5-4 displays the housing of the two way circuit where the left picture is the top of the housing and the right figure sows the bottom of the housing.
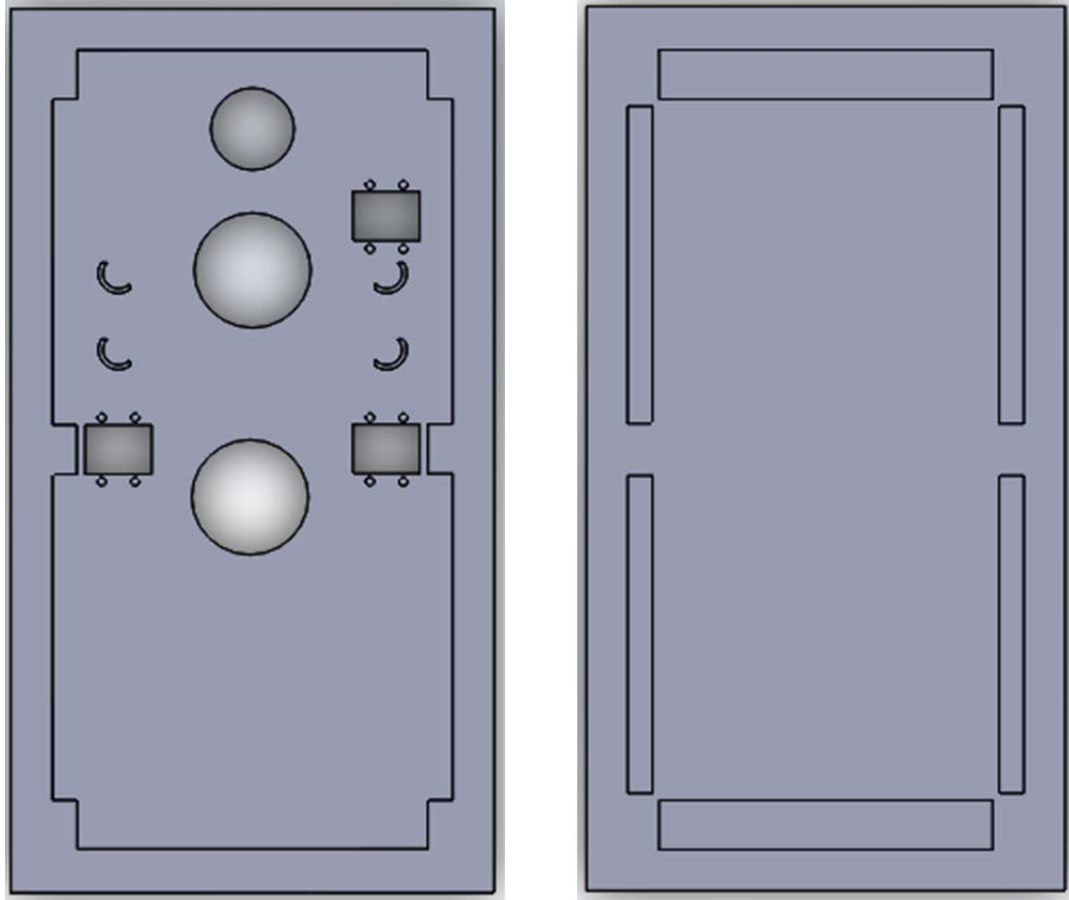
Figure 5-4: Housing for the Two Way Circuit

Three cutouts are made for the fluid storage in the center of the chip and three more for the detection areas of the chip as well as the proposed filter for IαIP. Right before and after these areas little pins ensure the connection between the wax paper channel and the nitrocellulose paper. The half-moon extrusions are placed in the housing to eliminate the possibilities of an air gap between the different layers of the valve. The bottom part of the housing acts as a base which presses the chip together.

5.2 Optimization of Valve components

The valve mentioned in the thesis is proposed as a unique part of the PBD which makes it possible to sequentially load the fluids at the right time. This valve is the most important part because having a valve which opens too early the order of the ELISA is not correct anymore. As a result no or a worse result can be obtained. Spreading the hydrophilic and surfactant paste into the holes of the tape by hand causes different amounts of paste every time. This affects the opening time of the valves as well as the time fluid needs to bridge the layers. Developing a better way to spread a constant volume of paste in the holes of the chip is the key to a higher yield performing tests with PBD. Pre-producing the paste as a pellet which is afterwards placing in the hole would ensure a constant amount of reagents needed to form a paper valve. Another possibility is to mix the paste in a syringe and to inject a certain amount of wet paste which is afterwards formed to a circular pellet.

6   LIST OF REFERENCES

[1]. Baudouin, Simon. *Sepsis.* London : Springer, 2008.

[2]. Jarman B, Aylin P, Bottle A. Trends in admissions and deaths in English NHS hospitals. *BMJ.* 2004, pp. 328-855.

[3]. Glueck, Thomas MD. NEJM Journal watch. [Online] 05 13, 2009. [Cited: 03 15, 2014.] http://www.jwatch.org/id200905130000004/2009/05/13/evaluation-piro-classification-system-sepsis.

[4]. Calandra T, Cohen J. The international sepsis forum consensus conference on definitions of infection in the intensive care unit. *Critical Care Medicine.* 2005, pp. 1538-1548.

[5]. Borchard-Tuch, Claudia. Pharmazeutische Zeitung online. [Online] April 2012. [Cited: April 1, 2014.] http://www.pharmazeutische-zeitung.de/?id=40662.

[6]. Müller-Werdan, U., Buerke, M., Werdan, K. Fortschritte in der Therapie der Sepsis. *Internist.* 2003, pp. 1531-1540.

[7]. Chemotherapie, Österreichische Gesellschaft für Antimikrobielle. Sepsis. [Online] 2011. [Cited: April 01, 2014.] http://www.infektionsnetz.at/InfektionenSepsis.phtml.

[8]. Lisheng Zhuo, Vincent C. Hascall and Koji Kimata. Inter-α-trypsin inhibitor a covalent protein-glycosaminoglycan-protein complex. *The journal of Biological Chemistry.* May 2004, pp. 38079-38082.

[9]. Kaczmarczyk, Aneta and Fries, Erik. Inter-a-inhibitor, hyaluronan and inflammation. *Acta Biochimica Polonica.* 2003, pp. 735-742.

[10]. Bost, F., M. Diarra-Mehrpour, and J. Martin. Inter-alpha-trypsin inhibitor proteoglycan family; a group of proteins binding and stabilizing the extracellular matrix. *Eur. J. Biochem.* 1998, pp. 339–346.

[11]. Kultar Singh, Ling Xiu Zhang, Kreso Bendelja, Ryan Heath, Shaun Murphy, Surendra Sharma, James F. Padbury, and Yow-Pin Lim. Inter-Alpha Inhibitor Protein (IAIP) Administration Improves Survival From Neonatal Sepsis In Mice. *PMC.* 09 01, 2011, pp. 242–247.

[12]. Hala Chaaban, MD, Kultar Singh, MD, Juliza Huang, Ed Sirayporn, Yow-Pin-Lim, MD, PHD, and James F. Padbury, MD. The Role of Inter-Alpha Inhibitor Proteins in the Diagnosis of Neonatal Sepsis. *The Journal of Pediatrics.* April 2009, pp. 620-623.

[13]. Zhuo, Lisheng and Kimata, Koji. Structure and Function of Inter-α-Trypsin Inhibitor Heavy Chains. *informa healthcare.* 2008, pp. 311-320.

[14]. Yow-Pin Lim, Kresimir Bendelja, Steven M. Opal, Edward Siryaporn, Douglas C. Hixson, and John E. Palardy. Correlation between Mortality and the Levels of Inter-Alpha Inhibitors in the Plasma of Patients with Severe Sepsis. *The Journal of Infectious Diseases.* 08 26, 2003, pp. 919-926.

[15]. Steven M. Opal, Andrew W. Artenstein, Patricia A. Cristofaro, Jhung W. Jhung, John E. Palardy, Nicholas A. Parejo and Yow-Pin Lim. Inter-Alpha-Inhibitor

Proteins Are Endogenous Furin Inhibitors and Provide Protection against Experimental Anthrax Intoxication. *INFECTION AND IMMUNITY.* 2005, pp. 5101-5105.

[16]. Camenisch, TD, et al. Disruption of hyaluronan synthase-2 abrogates normal cardiac morphogenesis and hyaluronan-mediated transformation of epithelium to mesenchyme. *Journal of Clinical Investigation.* 2000, pp. 349-360.

[17]. Michele, Turner. Dictionary.com. [Online] 2014. [Cited: 02 18, 2014.] http://dictionary.reference.com/browse/immunoadsorbent.

[18]. Föllscher, Wilke. *Development of a Platform for Lateral Flow Test Devices with the Capability of using Multiple Fluids.* Kingston University of Rhode Island : s.n., 2013.

[19]. Gerbers, Roman. *Development of enhanced lateral flow test devices for point-of-care diagnostics.* Kingston University of Rhode Island : s.n., 2013.

[20]. Murdock, Richard, et al. Optimization of a Paper-Based ELISA for a Human Performance Biomarker. *Analytical Chemistry.* 2013, pp. 11634-11642.

[21]. Elain Fu, Stephen A. Ramseyb, Peter Kauffmana, Barry Lutza, and Paul Yagera. Transport in two-dimensional paper networks. *Microfluid Nanofluidics.* 01 2011, pp. 29-35.

[22]. Paul Yager, Gonzalo J. Domingo, and John Gerdes. Point-of-Care Diagnostics for Global Health. *The Annual Review of Biomedical Engineering.* 03 20, 2008, pp. 107-144.

[23]. Jie Hu, ShuQiWang,1, LinWang, FeiLi, BelindaPingguan-Murphy, Tian JianLu, FengXu. Advances in paper-based point-of-care diagnostics. *Biosensors andBioelectronics.* 2014, pp. 585-597.

[24]. Gina E. Fridley, Huy Q. Le, Elain Fu and Paul Yager. Controlled release of dry reagents in porous media for tunable temporal and spatial distribution upon rehydration. *Lab on a Chip.* 12 2012, pp. 4321-4327.

[25]. Helka Juvonen, Anni Maattanen, Patrick Lauren, Petri Ihalainen, Arto Urtti, Mario Yliperttula, Jouko Peltonen. Biocompatibility of printed paper-based arrays for 2-D cell cultures. *Acta Biomaterialia.* 02 04, 2013, pp. 6704-6710.

[26]. Barry R. Lutz, Philip Trinh, Cameron Ball, Elain Fu and Paul Yager. Two-dimensional paper networks: programmable fluidic disconnects for multi-step processes in shaped paper. *Lab on a Chip.* 2011, pp. 4274-4278.

[27]. GmbH, Wiley Information Services. Chemgaroo, ChemgaPedia. [Online] 2013. [Cited: 04 02, 2014.] http://www.chemgapedia.de/vsengine/vlu/vsc/de/ch/8/bc/vlu/biotoxine/antibi otika.vlu/Page/vsc/de/ch/8/bc/biotoxine/ab_resistenz.vscml.html.

[28]. Reinhart, K., et al. Diagnose und Therapie der Sepsis: S2-Leitlinien der Deutschen Sepsisgesellschaft e.V. (DSG) und der Deutschen Interdisziplinären Vereinigung für Intensiv- und Notfallmedizin (DIVI). *Internist .* 2006, pp. 356-373.

[29]. Engel, C., et al. Epidemiology of sepsis in Germany: Results from a national prospective multicenter study. *Intensive Care Med.* 2007, pp. 606-618.

[30]. Brunkhorst, F. M., Reinhart, K. Diagnose und kausale Therapie der Sepsis. *Internist .* 2009, pp. 810-816.

[31]. Biosystems, T2. Business Wire. [Online] 04 07, 2011. [Cited: 04 28, 2014.] http://www.businesswire.com/news/home/20110407005350/en/T2-Biosystems-Demonstrates-First-Ever-Ability-Accurately-Rapidly#.U4X40ChArMg.

[32]. Zheng, C., et al. Rapid detection of fish major allergen parvalbumin using superparamagnetic nanoparticle-based lateral flow immunoassay. *Food Control.* 2012, pp. 446-452.

[33]. Healthcare, General Electric Life Sciences. Lateral Flow Assays. [Online] 05 01, 2014. [Cited: 01 04, 2014.] https://promo.gelifesciences.com/na/K13080/lateral.asp.

[34]. Chao-Min Cheng, Andres W. Martinez, Jinlong Gong, Charles R. Mace, Scott T. Phillips, Emanuel Carrilho, Katherine A. Mirica, and George M. Whitesides. Paper-Based ELISA. *Angewandte Chemie.* 2010, pp. 4881-4884.

[35]. Peng, Bai, et al. Study on Enzyme Linked Immunosorbent Assay Using Paper-based Micro-zone Plates. *Chines Journal of Analytical Chemistry.* 01 01, 2013, pp. 20-24.

[36]. Per A. Larsson, Sushma G. Puttaswamaiah, Christine Ly, Alois Vanerek, J. Christopher Hall, Francois Droleta. Filtration, adsorption and immunodetection of virus using polyelectrolyte multilayer-modified paper. *Colloids and Surfaces B: Biointerfaces.* 06 05, 2012, pp. 205-209.

[37]. Österberg, E., Bergström, K., Holmberg, K., Schuman, T. P., Riggs, J. A., Burns, N. L., Van Alstine, J. M. and Harris, J. M. Protein-rejecting ability of surface-bound dextran in end-on and side-on configurations: Comparison to PEG. *Biomed. Mater. Res.* 1995, pp. 741-747.

[38]. Steinitz, M. Quantitation of the blocking effect of Tween 20 and bovine serum albumin in ELISA microwells. *Anal. Biochem.* 2000, pp. 232-238.

[39]. Bai Peng, Luo Yan, LI Ying, YU Xiao-Dong, CHEN Hong-Yuan. Study on Enzyme Linked Immunosorbent Assay Using Paper-based Micro-zone Plates. *Chines Journal of Analytical Chemistry.* 01 01, 2013, pp. 20-24.

[40]. Wang, S., et al. Paper-based chemiluminescence ELISA: Lab-on-paper based on chitosan modified paper device and wax-screen-printing. *Biosensors and Bioelectronics.* 2012, pp. 212-218.

[41]. Ashori, A. and Raverty, W.D. Printability of sized kenaf (Hibiscus cannabinus) paper. *Polymer-Plastics Technology and Engineering.* 2007, pp. 683-687.

[42]. Andersson, Caisa. New ways to enhance the functionality of paperboard by surface treatment – a review. *Packaging Technology and Science.* 10 2008, pp. 339-373.

[43]. Elain Fu, Tinny Liang, Jared Houghtaling, Sujatha Ramachandran, Stephen A. Ramsey, Barry Lutz, and Paul Yager. Enhanced Sensitivity of Lateral Flow Tests Using a Two-Dimensional Paper Network Format. *analytical chemistry.* 09 21, 2011, pp. 7941-7946.

[44]. *Gold-based autometallography.* Hainfeld, J. F. et al. Berlin : Springer-Verlag, 1999. Proceedings of the Fifty-Seventh Annual Meeting. Microscopy Society of America.

[45]. Washburn, E. W. The Dynamics of Capillary Flow. *Phys. Rev. 17.* 1921, pp. 273-283.

[46]. Darcy, H. *Les fontaines pupliques de la ville Dijon.* Paris : s.n., 1856.

[47]. Stevens, D.Y., et al. Enabling a microfluidic immunoassay for the developing world by integration of on-card dry reagent storage. *Lab on a Chip.* 2008,, pp. 2038–2045.

[48]. Martinez, A. W., et al. Programmable diagnostic devices made from paper and tape. *Lab Chip.* 2010, pp. 2499-2504.

[49]. Chen, Hong, Microfluidic Polymer- and Paper-Based Devices for in-vitro diagnostics. *Dissertation.* University of Rhode Island : s.n., 2012.

[50]. Elain Fu, Tinny Liang, Paolo Spicar-Mihalic, Jared Houghtaling, Sujatha Ramachandran, and Paul Yager. Two-Dimensional Paper Network Format That Enables Simple Multistep Assays for Use in Low-Resource Settings in the Context of Malaria Antigen Detection. *Analytical Chemistry.* 2012, p. 4574–4579.

[51]. Elain Fu, Barry Lutz, Peter Kauffman and Paul Yager. Controlled reagent transport in disposable 2D paper networks. *Lab on a Chip.* 01 15, 2010, pp. 918-920.

[52]. Zimmermann, Martin, et al. Modeling and Optimization of High-Sensitivity, Low-Volume Microfluidic-Based Surface Immunoassays. *Biomedical Microdevices.* 2005, pp. 99-110.

[53]. Elain Fu, Kjell E. Nelson, Stephen A. Ramsey,Jennifer O. Foley, Kristen Helton, and Paul Yager. Modeling of a Competitive Microfluidic Heterogeneous Immunoassay: Sensitivity of the Assay Response to Varying System Parameters. *Analytical Chemistry.* 05 1, 2009, pp. 3407-3413.

[54]. Temsiri Songjaroen, Wijitar Dungchai, Orawon Chailapakul, Wanida Laiwattanapaisale. Novel, simple and low-cost alternative method for fabrication of paper-based microfluidics by wax dipping. *Talanta.* 08 17, 2011, pp. 2587-2593.

[55]. Martinez, Andres W., et al. Patterned Paper as a Platform for Inexpensive, Low-Volume, Portable Bioassays. *Angew.Chem. Int.* 2007, pp. 1318-1320.

[56]. Bruzewicz, Derek A., Reches, Meital and Whitesides, George M. Low-Cost Printing of Poly(dimethylsiloxane) Barriers To Define Microchannels in Paper. *Anal. Chem.* 2008, pp. 3387-3392.

[57]. Abe, Koji, Suzuki, Koji and Citterio, Daniel. Inkjet-Printed Microfluidic Multianalyte Chemical Sensing Paper. *Analytical Chemistry.* 2008, pp. 6928-6934.

[58]. Martinez, Andres W., Phillips, Scott T. and Whitesides, George M. Diagnostics for the Developing World: Microfluidic Paper-Based Analytical Devices. *Analytical Chemistry.* 2010, pp. 3-10.

[59]. Carrilho, E., Martinez, A. W. and Whitesides, G. M. Understanding wax printing: a simple micropatterning process for paper-based microfluidics. *Analytical Chemistry.* 2009, pp. 7091-7095.

[60]. Phillips, Hyeran Noh and Scott T. Metering the Capillary-Driven Flow of Fluids in Paper-Based Microfluidic Devices. *Analytical Chemistry.* 05 15, 2010, pp. 4181-4187.

[61]. Lewis, Gregory G., et al. High throughput method for prototyping three-dimensional, paper-based microfluidic devices. *Lab on a Chip.* 05 15, 2012, pp. 2630-2633.

[62]. IHC-WOLRD. IHCWorld Life Science Products & Services. [Online] 05 30, 2014. [Cited: 03 12, 2014.] http://www.ihcworld.com/_protocols/chromogen_substrates/POD_DAB_brown.htm.

[63]. Kamke, Detlef and Walcher, Wilhelm. *Physik für Mediziner 2.Edition.* s.l. : Vieweg und Teubner, 1994.

[64]. Ana C. Glavan, Ramses V. Martinez, E. Jane Maxwell, Anand, Bala Subramaniam, Rui M. D. Nunes, Siowling Soha and George M. Whitesides. Rapid fabrication of pressure-driven open-channel microfluidic devices in omniphobic RF paper3. *Lab on a Chip.* 2013, pp. 2922–2930.

[65]. Kevin M. Schilling, Daisy Jauregui and Andres W. Martinez. Paper and toner three-dimensional fluidic devices: programming fluid flow to improve point-of-care diagnostics. *Lab on a Chip.* 2013, pp. 628-631.

[66]. Wei Liu, Juan Kou,Huizhong Xing, Baox in Li. Paper-based chromatographic chemiluminescence chip for the detection of dichlorvos in vegetables. *Biosensors and Bioelectronics.* 2014, pp. 76-81.

[67]. Nira R. Pollock, Donn Colby, and Jason P. Rolland. A Point-of-Care Paper-based Fingerstick Transaminase Test: Toward Low-cost "Lab-on-a-Chip" Technology for the Developing World. *ADVANCES IN TRANSLATIONAL SCIENCE.* 2013, pp. 478-482.

[68]. Dong Sun, Yong-Il Cho, Patrick Comyn, Kyoung-Jin Yoon. Use of blood collected onto and dried on filter paper for diagnosing pregnancy in cattle. *The Veterinary Journal.* 09 11, 2013, pp. 494-497.

[69]. Guillermo Ortiz-Ruiz, Marco A. Perafán, Eugen Faist, Carmelo Dueñas Castell. *Sepsis Second Edition.* New York : Springer, 2006.

[70]. Helka Juvonen, Anni Määttänen, Patrick Laurén, Petri Ihalainen, Arto Urtti, Marjo Yliperttula, Jouko Peltonen. Biocompatibility of printed paper-based arrays for 2-D cell cultures. *Acta Biomaterialia.* 2013, pp. 6704-6710.

[71]. Corporation, Worthingotn Biochemical. Worthington Biochemical. [Online] 2014. [Cited: 04 07, 2014.] http://www.worthington-biochem.com/TRY/.

[72]. Millipore, EMD. Rapid Lateral Flow Test Strips. Considerations for Product Development. [Online] 2013. [Cited: 02 17, 2014.] http://www.millipore.com/techpublications/tech1/tb500en00.
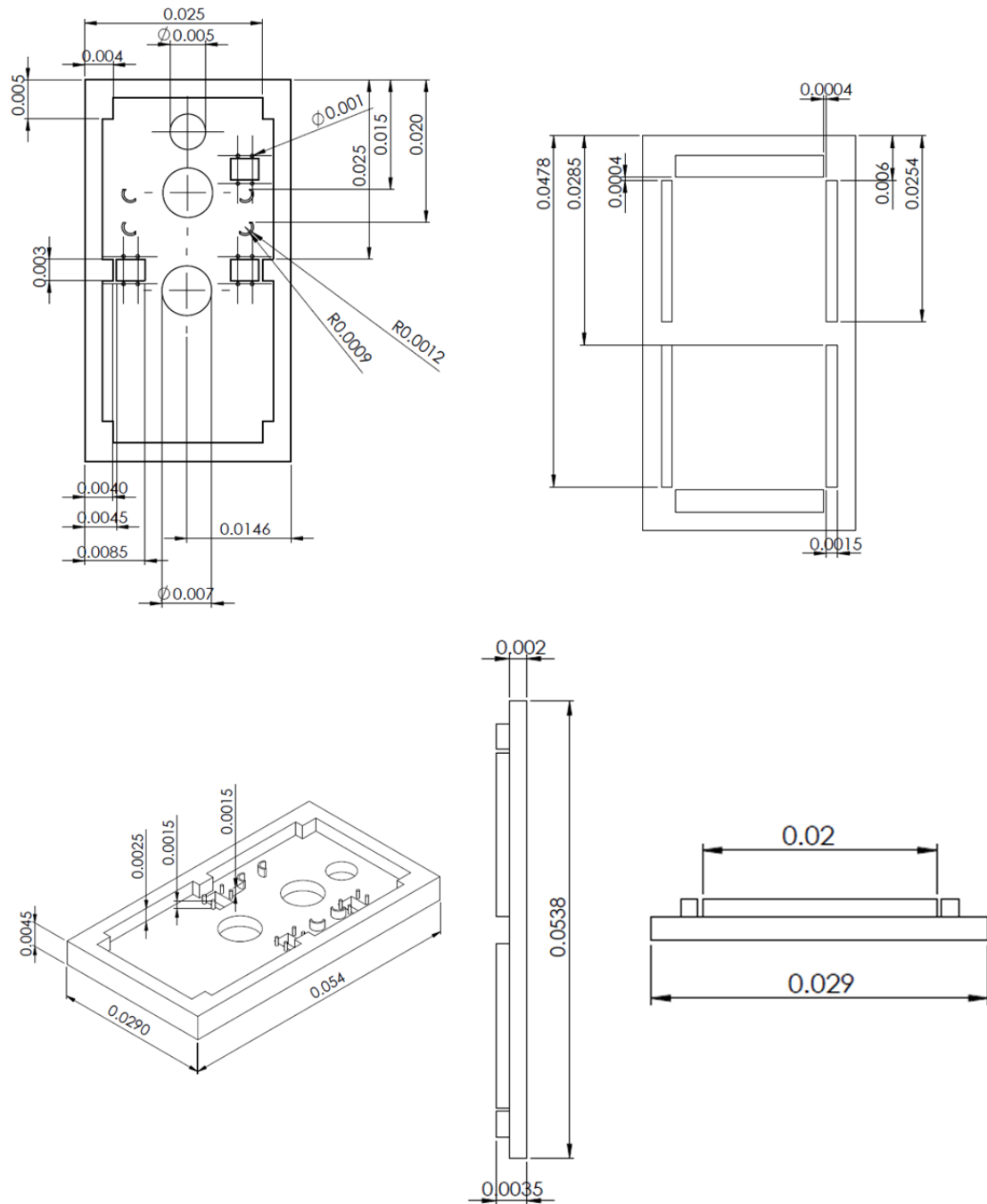
7   APPENDICES

Figure 7-1: Dimensions of the Housing

8   BIBLIOGRAPHY

Abe, K., Suzuki, K., & Citterio, D. (2008). Inkjet-Printed Microfluidic Multianalyte Chemical Sensing Paper. *Analytical Chemistry*, S. 6928-6934.

Ana C. Glavan, R. V. (2013). Rapid fabrication of pressure-driven open-channel microfluidic devices in omniphobic RF paper3. *Lab on a Chip*, pp. 2922–2930.

Andersson, C. (10 2008). New ways to enhance the functionality of paperboard by surface treatment – a review. *Packaging Technology and Science*, S. 339-373.

Ashori, A., & Raverty, W. (2007). Printability of sized kenaf (Hibiscus cannabinus) paper. *Polymer-Plastics Technology and Engineering*, S. 683-687.

Bai Peng, L. Y.-D.-Y. (2013, 01 01). Study on Enzyme Linked Immunosorbent Assay Using Paper-based Micro-zone Plates. *Chines Journal of Analytical Chemistry*, pp. 20-24.

Barry R. Lutz, P. T. (2011). Two-dimensional paper networks: programmable fluidic disconnects for multi-step processes in shaped paper. *Lab on a Chip*, pp. 4274-4278.

Baudouin, S. (2008). *Sepsis.* London: Springer.

Biosystems, T. (2011, 04 07). *Business Wire*. Retrieved 04 28, 2014, from http://www.businesswire.com/news/home/20110407005350/en/T2-Biosystems-Demonstrates-First-Ever-Ability-Accurately-Rapidly#.U4X40ChArMg

Borchard-Tuch, C. (2012, April). *Pharmazeutische Zeitung online*. Retrieved April 1, 2014, from http://www.pharmazeutische-zeitung.de/?id=40662

Bost, F. M.-M. (1998). Inter-alpha-trypsin inhibitor proteoglycan family; a group of proteins binding and stabilizing the extracellular matrix. *Eur. J. Biochem*, S. 339–346.

Brunkhorst, F. M. (2009). Diagnose und kausale Therapie der Sepsis. *Internist* , S. 810-816.

Bruzewicz, D. A., Reches, M., & Whitesides, G. M. (2008). Low-Cost Printing of Poly(dimethylsiloxane) Barriers To Define Microchannels in Paper. *Anal. Chem.*, pp. 3387-3392.

Calandra T, C. J. (2005). The international sepsis forum consensus conference on definitions of infection in the intensive care unit. *Critical Care Medicine*, S. 1538-1548.

Camenisch, T., Spicer, A., Brehm-Gibson, T., Biesterfeldt, J., Augustine, M., Calabro, A. J., . . . McDonald, J. (2000). Disruption of hyaluronan synthase-2 abrogates normal cardiac morphogenesis and hyaluronan-mediated transformation of epithelium to mesenchyme. *Journal of Clinical Investigation*, pp. 349-360.

Carrilho, E. M. (2009). Understanding wax printing: a simple micropatterning process for paper-based microfluidics. *Analytical Chemistry*, S. 7091-7095.

Chao-Min Cheng, A. W. (2010). Paper-Based ELISA. *Angewandte Chemie*, pp. 4881-4884.

Chemotherapie, Ö. G. (2011). *Sepsis*. Retrieved April 01, 2014, from
http://www.infektionsnetz.at/InfektionenSepsis.phtml

Chen, H. D. (2012). Microfluidic Polymer- and Paper-Based Devices for in-vitro
diagnostics. *Dissertation*. University of Rhode Island.

Corporation, W. B. (2014). *Worthington Biochemical*. Retrieved 04 07, 2014, from
http://www.worthington-biochem.com/TRY/

Darcy, H. (1856). In *Les fontaines pupliques de la ville Dijon.* Paris.

Dong Sun, Y.-I. C.-J. (2013, 09 11). Use of blood collected onto and dried on filter
paper for diagnosing pregnancy in cattle. *The Veterinary Journal*, pp. 494-497.

Elain Fu, B. L. (2010, 01 15). Controlled reagent transport in disposable 2D paper
networks. *Lab on a Chip*, pp. 918-920.

Elain Fu, K. E. (2009, 05 1). Modeling of a Competitive Microfluidic Heterogeneous
Immunoassay: Sensitivity of the Assay Response to Varying System
Parameters. *Analytical Chemistry*, pp. 3407-3413.

Elain Fu, T. L. (2011, 09 21). Enhanced Sensitivity of Lateral Flow Tests Using a Two-
Dimensional Paper Network Format. *analytical chemistry*, pp. 7941-7946.

Elain Fu, T. L.-M. (2012). Two-Dimensional Paper Network Format That Enables
Simple Multistep Assays for Use in Low-Resource Settings in the Context of
Malaria Antigen Detection. *Analytical Chemistry*, p. 4574–4579.

Elain Fu, S. A. (2011, 01). Transport in two-dimensional paper networks. *Microfluid
Nanofluidics*, pp. 29-35.

Engel, C. e. (2007). Epidemiology of sepsis in Germany: Results from a national prospective multicenter study. *Intensive Care Med*, S. 606-618.

Föllscher, W. (2013). *Development of a Platform for Lateral Flow Test Devices with the Capability of using Multiple Fluids.* Kingston University of Rhode Island.

Gerbers, R. (2013). *Development of enhanced lateral flow test devices for point-of-care diagnostics.* Kingston University of Rhode Island.

Gina E. Fridley, H. Q. (2012, 12). Controlled release of dry reagents in porous media for tunable temporal and spatial distribution upon rehydration. *Lab on a Chip*, pp. 4321-4327.

Glueck, T. M. (2009, 05 13). *NEJM Journal watch*. Retrieved 03 15, 2014, from http://www.jwatch.org/id200905130000004/2009/05/13/evaluation-piro-classification-system-sepsis

GmbH, W. I. (2013). *Chemgaroo, ChemgaPedia*. Retrieved 04 02, 2014, from http://www.chemgapedia.de/vsengine/vlu/vsc/de/ch/8/bc/vlu/biotoxine/antibiotika.vlu/Page/vsc/de/ch/8/bc/biotoxine/ab_resistenz.vscml.html

Guillermo Ortiz-Ruiz, M. A. (2006). *Sepsis Second Edition.* New York: Springer.

Hainfeld, J. F. (1999). Gold-based autometallography. *Proceedings of the Fifty-Seventh Annual Meeting. Microscopy Society of America.* Berlin: Springer-Verlag.

Hala Chaaban, M. K.-P.-L. (April 2009). The Role of Inter-Alpha Inhibitor Proteins in the Diagnosis of Neonatal Sepsis. *The Journal of Pediatrics*, S. 620-623.

Healthcare, G. E. (01. 05 2014). *Lateral Flow Assays*. Abgerufen am 04. 01 2014 von

https://promo.gelifesciences.com/na/K13080/lateral.asp

Helka Juvonen, A. M. (2013, 02 04). Biocompatibility of printed paper-based arrays

for 2-D cell cultures. *Acta Biomaterialia*, pp. 6704-6710.

Helka Juvonen, A. M. (2013). Biocompatibility of printed paper-based arrays for 2-D

cell cultures. *Acta Biomaterialia*, S. 6704-6710.

IHC-WOLRD. (30. 05 2014). *IHCWorld Life Science Products & Services*. Abgerufen am

12. 03 2014 von

http://www.ihcworld.com/_protocols/chromogen_substrates/POD_DAB_bro

wn.htm

Jarman B, A. P. (2004). Trends in admissions and deaths in English NHS hospitals.

BMJ, S. 328-855.

Jie Hu, S. L.-M. (2014). Advances in paper-based point-of-care diagnostics. *Biosensors*

andBioelectronics, pp. 585-597.

Kaczmarczyk, A., & Fries, E. (2003). Inter-a-inhibitor, hyaluronan and inflammation.

Acta Biochimica Polonica, S. 735-742.

Kamke, D., & Walcher, W. (1994). *Physik für Mediziner 2.Edition.* Vieweg und

Teubner.

Kevin M. Schilling, D. J. (2013). Paper and toner three-dimensional fluidic devices:

programming fluid flow to improve point-of-care diagnostics. *Lab on a Chip*,

pp. 628-631.

Kultar Singh, L. X.-P. (2011, 09 01). Inter-Alpha Inhibitor Protein (IAIP) Administration Improves Survival From Neonatal Sepsis In Mice. *PMC*, pp. 242–247.

Lewis, G. G., DiTucci, M. J., Baker, M. S., & Phillips, S. T. (2012, 05 15). High throughput method for prototyping three-dimensional, paper-based microfluidic devices. *Lab on a Chip*, pp. 2630-2633.

Lisheng Zhuo, V. C. (May 2004). Inter-α-trypsin inhibitor a covalent protein-glycosaminoglycan-protein complex. *The journal of Biological Chemistry*, S. 38079-38082.

Martinez, A. W., Phillips, S. T., & Whitesides, G. M. (2010). Diagnostics for the Developing World: Microfluidic Paper-Based Analytical Devices. *Analytical Chemistry*, S. 3-10.

Martinez, A. W., Phillips, S. T., Butte, M. J., & Whitesides, G. M. (2007). Patterned Paper as a Platform for Inexpensive, Low-Volume, Portable Bioassays. *Angew.Chem. Int.*, pp. 1318-1320.

Martinez, A. W., Phillips, S. T., Nie, Z. C.-M., Carrilho, E., Wiley, B. J., & Whitesides, G. M. (2010). Programmable diagnostic devices made from paper and tape. *Lab Chip*, pp. 2499-2504.

Michele, T. (2014). *Dictionary.com*. Retrieved 02 18, 2014, from http://dictionary.reference.com/browse/immunoadsorbent

Millipore, E. (2013). *Rapid Lateral Flow Test Strips. Considerations for Product Development.* Abgerufen am 17. 02 2014 von http://www.millipore.com/techpublications/tech1/tb500en00

Müller-Werdan, U. B. (2003). Fortschritte in der Therapie der Sepsis. *Internist*, pp. 1531-1540.

Murdock, R., Shen, L., Kelley-Loughnane, N. P., & Hagen, J. (2013). Optimization of a Paper-Based ELISA for a Human Performance Biomarker. *Analytical Chemistry*, pp. 11634-11642.

Nira R. Pollock, D. C. (2013). A Point-of-Care Paper-based Fingerstick Transaminase Test: Toward Low-cost "Lab-on-a-Chip" Technology for the Developing World. *ADVANCES IN TRANSLATIONAL SCIENCE*, pp. 478-482.

Österberg, E. B. (1995). Protein-rejecting ability of surface-bound dextran in end-on and side-on configurations: Comparison to PEG. *Biomed. Mater. Res.*, S. 741-747.

Paul Yager, G. J. (2008, 03 20). Point-of-Care Diagnostics for Global Health. *The Annual Review of Biomedical Engineering*, pp. 107-144.

Peng, B., Yan, L., Ying, L., Xiao-Dong, Y., & Hong-Yuan, C. (2013, 01 01). Study on Enzyme Linked Immunosorbent Assay Using Paper-based Micro-zone Plates. *Chines Journal of Analytical Chemistry*, pp. 20-24.

Per A. Larsson, S. G. (2012, 06 05). Filtration, adsorption and immunodetection of virus using polyelectrolyte multilayer-modified paper. *Colloids and Surfaces B: Biointerfaces*, pp. 205-209.

Phillips, H. N. (2010, 05 15). Metering the Capillary-Driven Flow of Fluids in Paper-Based Microfluidic Devices. *Analytical Chemistry*, pp. 4181-4187.

Reinhart, K. e. (2006). Diagnose und Therapie der Sepsis: S2-Leitlinien der Deutschen Sepsisgesellschaft e.V. (DSG) und der Deutschen Interdisziplinären Vereinigung für Intensiv- und Notfallmedizin (DIVI). *Internist*, pp. 356-373.

Steinitz, M. (2000). Quantitation of the blocking effect of Tween 20 and bovine serum albumin in ELISA microwells. *Anal. Biochem.*, S. 232-238.

Steven M. Opal, A. W.-P. (2005). Inter-Alpha-Inhibitor Proteins Are Endogenous Furin Inhibitors and Provide Protection against Experimental Anthrax Intoxication. *INFECTION AND IMMUNITY*, pp. 5101-5105.

Stevens, D., Petri, C. R., Osborn, J. L., Spicar-Mihalic, P., McKenzie, K., & Yager, P. (2008,). Enabling a microfluidic immunoassay for the developing world by integration of on-card dry reagent storage. *Lab on a Chip*, pp. 2038–2045.

Temsiri Songjaroen, W. D. (2011, 08 17). Novel, simple and low-cost alternative method for fabrication of paper-based microfluidics by wax dipping. *Talanta*, pp. 2587-2593.

Wang, S., Ge, L., Song, X., J., Y., Ge, S., Huang, J., & Zeng, F. (2012). Paper-based chemiluminescence ELISA: Lab-on-paper based on chitosan modified paper device and wax-screen-printing. *Biosensors and Bioelectronics*, pp. 212-218.

Washburn, E. W. (1921). The Dynamics of Capillary Flow. In *Phys. Rev. 17* (S. 273-283).

Wei Liu, J. K. (2014). Paper-based chromatographic chemiluminescence chip for the detection of dichlorvos in vegetables. *Biosensors and Bioelectronics*, pp. 76-81.

Yow-Pin Lim, K. B. (2003, 08 26). Correlation between Mortality and the Levels of Inter-Alpha Inhibitors in the Plasma of Patients with Severe Sepsis. *The Journal of Infectious Diseases*, pp. 919-926.

Zheng, C., Wang, X., Lu, Y., & Liu, Y. (2012). Rapid detection of fish major allergen parvalbumin using superparamagnetic nanoparticle-based lateral flow immunoassay. *Food Control*, S. 446-452.

Zhuo, L., & Kimata, K. (2008). Structure and Function of Inter-α-Trypsin Inhibitor Heavy Chains. *informa healthcare*, S. 311-320.

Zimmermann, M., Delamarche, E., Wolf, M., & Hunziker, P. (2005). Modeling and Optimization of High-Sensitivity, Low-Volume Microfluidic-Based Surface Immunoassays. *Biomedical Microdevices*, pp. 99-110.